

Relativistic one-boson-exchange model for the nucleon-nucleon interaction

Franz Gross

*College of William and Mary, Williamsburg, Virginia 23185
and Continuous Electron Beam Accelerator Facility,
12000 Jefferson Avenue, Newport News, Virginia 23606*

J. W. Van Orden

*Department of Physics, Old Dominion University, Norfolk, Virginia 23529
and Continuous Electron Beam Accelerator Facility,
12000 Jefferson Avenue, Newport News, Virginia 23606*

Karl Holinde

*Institut für Kernphysik, Kernforschungsanlage Jülich,
D-5170 Jülich, Federal Republic of Germany*

(Received 9 August 1991)

Nucleon-nucleon data below 300-MeV laboratory energy are described by a manifestly covariant wave equation in which one of the intermediate nucleons is restricted to its mass shell. Antisymmetrization of the kernel yields an equation in which the two nucleons are treated in an *exactly* symmetric manner, and in which all amplitudes satisfy the Pauli principle *exactly*. The kernel is modeled by the sum of one boson exchanges, and four models, all of which fit the data very well ($\chi^2 \cong 3$ per data point) are discussed. Two models require the exchange of *only* the π , σ , ρ , and ω , but also require an admixture of γ^5 coupling for the pion, while two other models restrict the pion coupling to pure $\gamma^5\gamma^\mu$, but require the exchange of *six* mesons, including the η , and a light scalar-isovector meson referred to as σ_1 . Deuteron wave functions resulting from these models are obtained. The singularities and relativistic effects which are a part of this approach are discussed, and a complete development of the theory is presented.

PACS number(s): 21.30.+y, 13.75.Cs

I. OVERVIEW, RESULTS, AND CONCLUSIONS

A. Introduction

With the discovery of quarks, and the construction of powerful new facilities, such as the Continuous Electron Beam Accelerator Facility (CEBAF), we have the opportunity to study and understand the structure of strongly interacting matter at short distances (or high momentum transfers). One goal of such studies is the development of an effective theory of strongly interacting particles, tied to the underlying theory of quarks and gluons (QCD), but including effective variables and degrees of freedom which are efficient to describe strongly interacting matter at momentum transfers of a few GeV/c. We do not at this time know what these effective degrees of freedom will be. They may be the quarks and gluons themselves, or it may be that the mesons and nucleons observed at low momentum transfers will continue to be the correct variables to use at a few GeV. To compare these two pictures, or to test either one, it is necessary to have simple, dynamical models which can be applied consistently to a large variety of interactions.

Models which are to be used to study processes involving momentum transfers of a few GeV should be relativistic. This means not only that the energies of all particles must satisfy the relativistic energy relation, but

also that it must be possible to transform all amplitudes and wave functions from one Lorentz frame to another. This feature is essential if we wish to eliminate all ambiguities which arise from frame dependent choices, and treat recoil, spin orbit, and other significant effects correctly.

Relativistic covariance can be achieved either by (1) finding a way to boost amplitudes calculated in one special frame to an arbitrary frame or by (2) using a dynamical theory which is covariant at every stage of the calculation. The former method, which we will refer to as relativistic Hamiltonian dynamics [1], has been developed by Coester, Keister, Polyzou, and their collaborators, and has been recently applied to the calculation of the deuteron form factors [2]. The use of light front variables seems to be a key to the success of this method. The latter method, which will be referred to as manifestly covariant dynamics, has been developed by Tjon and collaborators [3], who have used the Bethe-Salpeter [4] and the Blankenbecler-Sugar [5] equation, and by one of us (F.G.) using the spectator equation [6]. The advantage of relativistic Hamiltonian dynamics is that the issue of Lorentz covariance is separated from the dynamics, so that any phenomenological, nonrelativistic, or semi-relativistic calculation can be made covariant. A disadvantage, from our point of view, is that no connection is made to an underlying field theory which is assumed to

describe the physics. One consequence of this is that field theory cannot be used to develop the connection between the electromagnetic current operator and the strong interaction physics, reducing the predictive power of such calculations.

The work presented in this paper is an example of manifestly covariant dynamics. The low energy nucleon-nucleon scattering amplitude is calculated using a relativistic equation in which one particle is restricted to its mass shell, which we refer to as the spectator equation. This equation was first introduced [7] in 1969, and studied on several occasions since then [8, 9], but this is the first time the equation has been properly symmetrized for NN scattering, and solved exactly. (A short account of the present work can be found in Ref. [10].) We believe that all of the theoretical problems associated with the application of this equation to elastic NN scattering have now been solved, and one of the principle purposes of this paper is to present a careful and detailed treatment of the theory in rather general terms. This is the main thrust of Part II. A brief review of work leading up to the present paper is given in Sec. IB below, which also discusses how this paper relates to other work in this field.

A second principal purpose of this paper is to demonstrate that the relativistic spectator equation can serve as basis of a successful relativistic phenomenology of low energy NN scattering. We chose to describe the dynamics with a one-boson-exchange (OBE) model, primarily because the exchange of the lightest bosons is associated with the longest range, peripheral part of the interaction, which is the only part of the interaction we can hope to describe with such an approach. All shorter range effects are assumed to be accounted for by form factors, which are treated purely phenomenologically. Our choice of the OBE model is also consistent with our use of the spectator equation, which we believe has a structure which tends to minimize the contributions from higher order irreducible kernels (a fact which can be proved for scalar theories). Other advantages of the OBE model are that OBE parameters have a clear physical meaning, the dynamics is closely coupled to a field theory (permitting the model to be extended consistently to other processes), and OBE models have enjoyed considerable success in the past. A fit which requires only a few bosons may be better than one which requires many; since the boson couplings are treated as free parameters, extra bosons can always be added if there is a reason. Because of this possibility, we were especially pleased to find that a very nice fit to all the data below 300 MeV can be found using only four bosons: π , σ , ρ , and ω . These four have long been regarded as playing a central role in NN scattering, and it is hard to imagine any reasonable OBE description without all of them, but to our knowledge this is the first time a quantitatively accurate fit has been achieved using *only* these four. This is because the off-shell contributions which arise from our relativistic treatment are large, and necessary to the fit, and this is the first time these off-shell contributions have been carefully evaluated.

The fits to data, the OBE parameters, χ^2 and other numerical results are presented in Sec. IC, while Sec. ID

includes a discussion of important off-shell and relativistic effects. In these sections, four models are presented and discussed. Models IA and B are examples of the four boson case mentioned above, while Models IIA and B are ones with six bosons (the four of Models I plus the η and ϵ_1 , a spin-zero, isospin-one meson) chosen to keep off-shell effects small. (The Models previously described in Ref. [10] are the same as the A versions given in this paper.) We find that all of these models work very well, giving a very nice fit to the data and phase parameters below 200 MeV, and a satisfactory fit over the entire range up to 300 MeV. This brings us to the third principle purpose of this paper, which is to find models which all agree with the on-shell NN data, but have significantly different off-shell extrapolations. These can be used to study the sensitivity of electromagnetic or hadronic probes to off-shell effects and to determine which measurements will most improve our understanding. In electron scattering experiments, such a program will have the greatest impact when the current operator is strongly constrained by the strong interaction dynamics. Recently, we have learned how to construct this current operator in a way which insures the conservation of current [11], and calculations of the deuteron form factors and deuteron electrodisintegration are underway. The connection to the underlying field theory has also been a useful guide toward developing a consistent relativistic multiple scattering theory [12], and calculations [13] of \vec{p} ^{40}Ca scattering observables based on these ideas and the specific nucleon-nucleon scattering amplitudes described in this paper are in good agreement with data.

This paper is organized into three major parts. This part (I) includes a full introduction, presentation of numerical results, discussion and conclusions. An attempt has been made to write this in a self-contained manner, so that all the results can be understood without referring to the other parts. Part II, General Theory, presents relativistic formalism applicable to any choice of relativistic kernel (potential), while Part III discusses the detail of the construction and treatment of the relativistic OBE kernel. Three appendices include more detailed discussion of technical points.

B. Background and overview

Manifestly covariant dynamics (as defined in this paper) can be said to have started with the introduction of the Bethe-Salpeter (BS) equation [4] in 1951. Some people refer to *any* relativistic equation for the scattering amplitude M which is of the linear form

$$M = V + \int VGM \quad (1.1)$$

(where V is the relativistic kernel and G the propagator) as a BS equation. When we refer to the BS equation we will mean (a) that the propagator G describes the propagation of two *off-shell* nucleons, and (b) that the integral operator includes the integration over all four components of the relative momentum $p = \frac{1}{2}(p_1 - p_2)$, the total four-momentum $P = p_1 + p_2$ being fixed by energy-

momentum conservation. For two spin zero particles with masses m_1 and m_2 , the BS propagator is therefore [in the c.m. where $P = (W, 0)$]

$$\begin{aligned} G_{\text{BS}} &= \frac{-i}{[m_1^2 - (\frac{1}{2}P + p)^2 - i\epsilon][m_2^2 - (\frac{1}{2}P - p)^2 - i\epsilon]} \\ &= \frac{-i}{[E_1^2 - (\frac{1}{2}W + p_o)^2 - i\epsilon][E_2^2 - (\frac{1}{2}W - p_o)^2 - i\epsilon]} \end{aligned} \quad (1.2)$$

where $E_i = \sqrt{m_i^2 + \mathbf{p}^2}$.

If the kernel V includes all Feynman diagrams which are two-body irreducible, then the solution to (1.1) gives the exact result for the M matrix. In this sense, the role of the BS equation is to reduce the number of diagrams which must be summed in perturbation theory, but since the two-body irreducible diagrams are still infinite in number, the method may not converge in theories where the elementary couplings are large. Only when the series of irreducible diagrams can be shown to converge more rapidly than the full Feynman series is the introduction of (1.1) an advantage.

One case where this is true is the study of bound states in quantum electrodynamics (QED), or in any weak coupling theory. A bound state pole can only be generated by an infinite number of diagrams, since each individual diagram has no such pole. In a weak coupling theory, a first approximation to the sum of irreducible diagrams can be obtained from the lowest order diagrams, which are the one-boson-exchange (OBE) diagrams. The bound state then emerges because the *reducible* diagrams generated from OBE (the so-called ladder diagrams) are all of comparable size near the bound state energy where the propagator G is large. In strong coupling theories, the ladder sum can still generate a bound state, but it is now less clear that this is a good approximation to the actual problem because V may not be well approximated by OBE diagrams.

The BS equation was originally applied to QED systems. In 1966, Blankenbecler and Sugar [5] introduced an equation (referred to here as the BBS equation) more suitable to theories where the coupling constant is large. They argued that, to a good approximation, the two-body propagator (1.2) could be replaced (for spin-zero particles) by

$$\begin{aligned} G_{\text{BBS}} &= \pi \int ds \frac{\delta_+(m_1^2 - (\frac{1}{2}\bar{P} + p)^2)\delta_+(m_2^2 - (\frac{1}{2}\bar{P} - p)^2)}{s - P^2 - i\epsilon} \\ &= \pi \frac{(E_1 + E_2)}{E_1 E_2} \frac{\delta(\frac{1}{2}\frac{m_1^2 - m_2^2}{E_1 + E_2} - p_o)}{[(E_1 + E_2)^2 - W^2 - i\epsilon]} \end{aligned} \quad (1.3)$$

where $\bar{P} = (\sqrt{s + \mathbf{P}^2}, \mathbf{P})$ is the total four-momentum of the two particles if they are both on their mass shell, $\delta_+(m^2 - p^2) = \delta(m^2 - p^2)\theta(p_o)$, and the second result in (1.3) is specialized for the c.m. system. This propagator is still covariant, but now depends on only three continuous variables, the fourth variable (the relative energy p_o) being constrained by the mass-shell requirement. Blankenbecler and Sugar were led to the simpler propagator (1.3) from the observation that both (1.2) and (1.3)

have the same elastic (unitarity) cut, and since the large contributions from reducible diagrams owe their origin to this cut, they reasoned that (1.3) should be sufficient to give a good description of low energy scattering and bound states.

Independently, it was observed [7] that when the kernel V is constructed so that all ladder and crossed ladder diagrams are to be summed by the integral equation, using a propagator which restricts one particle to its mass-shell significantly improves the convergence of the resulting series for V . In the notation of this section, this propagator (for particle 1 on-shell) is

$$\begin{aligned} G_S &= \frac{2\pi\delta_+(m_1^2 - (\frac{1}{2}P + p)^2)}{m_2^2 - (\frac{1}{2}P - p)^2 - i\epsilon} \\ &= \frac{2\pi\delta(E_1 - \frac{1}{2}W - p_o)}{2E_1[E_2^2 - (W - E_1)^2 - i\epsilon]}. \end{aligned} \quad (1.4)$$

Note that this propagator also constrains the fourth variable (p_o) so that the resulting integral equation, while covariant, depends only on the relative three-momentum. This relativistic equation, which will be referred to as the spectator equation, is the one used in this paper.

Subsequent study has revealed more about the relationship between these equations. It was pointed out [14] that (1.3) and (1.4) are only special cases of an infinite family of equations, all of which are covariant and three dimensional. One continuous family of such equations [9] can be described by the propagator

$$G_\alpha = \frac{2\pi\delta_+(\frac{1+\alpha}{2}A_1 - (\frac{1-\alpha}{2}A_2))}{A_1 + A_2} \quad (1.5)$$

where α is a parameter which can be varied continuously from -1 to 1 , and

$$A_1 = m_1^2 - \left(\frac{1}{2}P + p\right)^2, \quad (1.6)$$

$$A_2 = m_2^2 - \left(\frac{1}{2}P - p\right)^2.$$

When $\alpha = 1$, the propagator (1.5) is identical to (1.4), and when $\alpha = 0$ the propagator is similar to the BBS propagator (1.3). For scalar theories with neutral particles the following has been shown.

- (i) The fourth-order kernel V , derived from the consideration of box and crossed box diagrams, is of order $\frac{\mu}{m} \times$ (crossed box), where μ is the mass of the exchanged meson and $m = m_1 = m_2$. If the exchanged meson is much lighter than the interacting particles, this means that there is a cancellation between the crossed box and that part of the box *not* included in the first iteration of the OBE diagrams. In short, we have the ironic situation where the use of a simpler equation actually gives a better approximation order by order, to the sum of all ladders and crossed ladders.
- (ii) This cancellation works for any value of the contin-

uous parameter α . However, if $|\alpha|=1$, the adiabatic limit of the fourth-order kernel is local and energy independent. On the other hand, the smallest value of the fourth-order kernel *when evaluated at threshold* (initial and final particles at rest) occurs when $\alpha = 0$ [15].

- (iii) If one of the masses, say m_1 , becomes very large, the cancellation described above works to *all* orders, and leads naturally to a relativistic one body equation, with $\alpha=1$, for the lighter particle (m_2 in this case) moving in a potential “created” by heavier particle. (This potential becomes instantaneous as $m_1 \rightarrow \infty$.)

Unfortunately, these results do not generalize to the case of particles with spin exchanging charged mesons. However, in the realistic case of spin- $\frac{1}{2}$ nucleons exchanging charged pions which satisfy a chirally covariant interaction, the cancellation does occur [9] in the fourth-order kernel associated with the spectator equation (1.4).

Furthermore, putting one particle (the spectator) on shell does seem to have some conceptual advantages. When this approach is extended to the three-body system [16], relativistic Faddeev equations emerge which can be reduced to coupled two-dimensional integral equations in the usual manner. These equations satisfy the requirement of cluster separability; when one particle is removed to infinity, the two remaining ones interact as if the third were not present. Namyslowski has shown [17] that the three-body BBS equation does not have this desirable property. Finally, in the study of electron scattering [18], or nucleon-nucleus scattering [12], it is natural to treat some of the nucleons as spectators, and this approach to the two-body problem is well suited for extension to these other, more complex problems. In fact, the idea of putting the spectator on its mass shell originated from the study of electromagnetic form factors [18].

Two studies of the application of the spectator equation to the two nucleon problem have been carried out. The nonrelativistic limit of the equations have been studied [8], and the parameters of an OBE model have been determined approximately by fitting the nonrelativistic limit of the kernel to the Reid potential [19]. In the nonrelativistic limit, the equations have a simple form [cf. Eq. (2.80) and Sec. II G]

$$\begin{aligned} \left(\frac{\nabla^2}{m} - \epsilon\right) \psi^+(r) &= V^{++}(r)\psi^+(r) + V^{+-}(r)\psi^-(r) \\ 2m\psi^-(r) &= V^{-+}(r)\psi^+(r) + V^{--}(r)\psi^-(r) \end{aligned} \quad (1.7)$$

corresponding to coupled equations for two channels (+ and -) describing propagation of the off-shell nucleon in its positive (+) or negative (-) energy state. (The other nucleon is on-shell, and hence is always in a positive energy state; the index which could describe this is suppressed.) The asymptotic solution for $\psi^-(r)$ is therefore zero as expected; the (-) channel is closed. Hence all binding energies and phase shifts are determined by the asymptotic solutions for $\psi^+(r)$, which approximately satisfies the equation

$$\left(\frac{\nabla^2}{m} - \epsilon\right) \psi^+(r) = \left(V^{++}(r) + \frac{|V^{+-}|^2}{2m}\right) \psi^+(r) \quad (1.8)$$

obtained by neglecting V^{--} and eliminating $\psi^{(-)}$. [Note that $V^{-+} = (V^{+-})^\dagger$.] One interesting feature of the effective potential in Eq. (1.8) is that the quadratic term, $|V^{+-}|^2/2m$, is always repulsive, and dominates V^{++} at short range because of its more singular structure. The fits to the Reid potential showed that this term could indeed account for the repulsive core for practical (fitted) choices of the OBE parameters. Another feature of the quadratic potential, not fully appreciated at the time, was that it makes very important spin and isospin dependent contributions, which can be helpful in phenomenological fits.

In order to produce a successful phenomenology with a OBE model with only the four basic mesons ($\pi, \sigma, \rho, \omega$), it was necessary to introduce a mixed coupling for the pion of the form [cf. Eq. (3.3)]

$$g_\pi \left[\lambda_\pi \gamma^5 + (1 - \lambda_\pi) \frac{(\not{p} - \not{p}')}{2m} \gamma^5 \right] \quad (1.9)$$

where p and p' are the four-momenta of the final and initial nucleon, respectively. Note that (1.9) is independent of λ_π if both initial and final nucleons are on-shell, and hence is sensitive only to off-shell contributions. The value $\lambda_\pi = 0.41$ emerged from the nonrelativistic fits in Ref. [8]. The complete relativistic fits (Models IA and B) presented here give $\lambda_\pi \approx 0.22$.

In a second study [20], the equations were solved exactly for a family of relativistic deuteron wave functions. One focus of this study was to see the effect of varying λ_π on deuteron properties. The relativistic deuteron wave functions have four components; in addition to the familiar S and D states, there are two small P state components which play a role similar to the small lower components of the Dirac wave function of the hydrogen atom (for example). It was found that the small, relativistic P state components were very sensitive to λ_π , as expected. When $\lambda_\pi=1$, there is strong coupling to negative energy states through the off-diagonal γ^5 matrix, and the P states, a measure of the (-) channel strength, increase linearly with λ_π . It was also found that the exact solutions were insensitive to V^{--} . However, since this study was limited to the deuteron only, the wave functions determined were not constrained by other NN data.

This paper extends the work of Ref. [20] to all partial waves. We present fits obtained by solving the spectator equation exactly for all NN scattering parameters below 300 MeV. (A brief account of some of this work has already been presented in Ref. [10].) The new deuteron wave functions we determine are therefore constrained by all the low energy NN data. Furthermore, the fits are quantitatively good, and the helicity amplitudes which result can be used to predict the results of other processes [13].

Before turning to the results of this paper, we conclude

this section with a discussion of some of the objections which have been raised to using the spectator equation for the NN problem. There seem to be two principle objections, both of which are dealt with fully in this paper. These are the following:

- (i) The spectator equation puts one nucleon on shell, and therefore seems to treat the two nucleons differently. How can this be consistent with the Pauli principle?
- (ii) The kernel has spurious singularities which appear to violate the requirement of Hermiticity [21].

The first objection can be eliminated completely and is discussed fully in Sec. II A. The equations can be written in two equivalent forms. In the first form, the propagator is taken to be an average of a term in which particle 1 is on-shell and one in which particle 2 is on-shell. Hence each particle is on-shell for an equal fraction of the propagation, and the equation in this form is manifestly symmetric. It is then shown how to *transform* the equation into a form in which only one particle is on-shell. The resulting equation has a kernel which is explicitly antisymmetrized, and this is the key. If the kernel is explicitly

antisymmetrized, the propagator need not be. Unfortunately, this point was not discussed correctly in Ref. [8], and a considerable part of the effort in the preparation of this paper went into clarifying all of these issues. The final result is that *all* of the amplitudes and equations used can be shown to be *exactly* consistent with the Pauli principle.

The resolution of the second objection is less satisfying. It can be shown that the spurious singularities in the kernels of one order are canceled by spurious singularities in kernels of higher order [9], and hence would automatically be cancelled if the kernel could be calculated to *all* orders. This means that one is justified in dropping the singularities order by order to the extent this is possible. The imaginary parts can be dropped by taking the principal value of all singularities, and this solves the problem of Hermiticity in a simple way. However, we have not yet found a way to eliminate the real parts of the singularities without a major restructuring of the equations, which would spoil their simplicity. Hence, after much consideration, we have decided to treat the singularities numerically. One can see that the half off-shell solutions have no singularities and that all observables are also singularity free, so that the net result is that one must live with the nuisance of doing principle

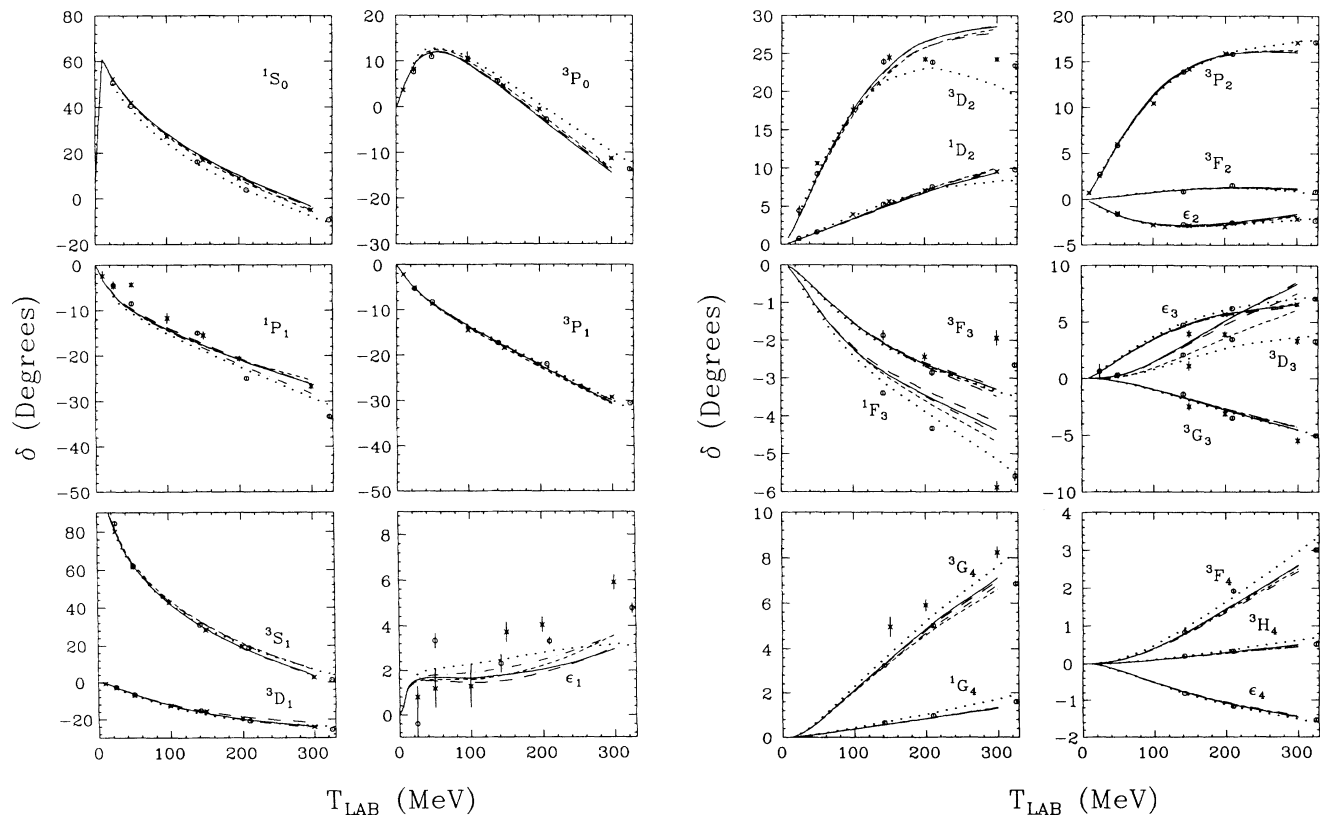


FIG. 1. Nucleon - nucleon np bar phase shifts. The curves are for Models IA (solid), IB (dash-dotted), IIA (long dashes), IIB (short dashes), and the Bonn [22] (dots). The crosses and circles (both with error bars) are the SF89 solutions of Arndt and Roper [23] and Bugg [24], respectively. All phase parameters are in degrees, and the horizontal scale is the laboratory kinetic energy of the incoming nucleon, in MeV.

value integrals over moving singularities. The quantitative effect of these singular principal value contributions can be inferred from the differences between the models designated A and those designated B. The A models (previously described in Ref. [10]) have the singularities removed using the “mixed” prescription described in Sec. III C and Appendix B, while the B models retain the principle value of the singularities, as discussed above. We emphasize that the most straightforward treatment of the equations, and hence the preferred approach, is to retain the singularities as a principle value, and hence the B versions of the two models are preferred; the A versions previously published are presented for comparison only. These issues and techniques are discussed in considerable detail in Sec III C, and in Appendix B. We find that the singularities do not produce large numerical effects, but that there is some sensitivity.

We now present the principle numerical results of this paper.

C. Numerical results

Fits to the low energy nucleon-nucleon phase shifts obtained for Models I and II are shown in Fig. 1. Our fits are compared with the full Bonn potential [22] (which includes boxes and crossed boxes), and energy independent phase parameters obtained from the Arndt-Roper SP89 [23] fits and from Bugg [24], both shown with error bars. We did not calculate the Coulomb contributions to pp scattering, so our fits to the pp data were based on our np calculations, modified using the semi-phenomenological $\delta(pp) - \delta(np)$ differences in the SAID code. The np phase parameters for Model IIB are tabu-

lated in Table I.

While some differences between our four fits are visible, particularly for ϵ_1 and 3D_3 , the differences are very small, and not significant statistically. We conclude that the four models are essentially indistinguishable on the basis of NN data alone. This view is supported by Table II, which gives χ^2 for the fits to the np data for seven energy bins below 325 MeV, and also for all data in the energy ranges from 8 to 225 and 8 to 325 MeV. Since completing this work, we learned [25] that the semi-phenomenological procedure in the SAID code may not give an accurate estimate of the actual Coulomb corrections, and for this reason we decided not to present, in Table II, the χ^2 for the combined fits to both np and pp data obtained using this procedure. (These combined χ^2 are comparable, but generally slightly larger than those given in the table, except at 300 MeV, where they are significantly smaller. The numbers for the combined energy range from 8 to 325 MeV are 3.41, 3.96, 2.85, and 3.13 for Models IA, IB, IIA, and IIB, respectively, and the total number of np and pp data points is 3377.) Table II also compares the χ^2 for Models I and II with the full Bonn potential [22] and the purely phenomenological Argonne V14 potential [26] (the VPI energy dependent phase shift fit from SP89 is shown for reference). Not only are the χ^2 for the four models very similar (except for Model IB at 300 MeV), but the χ^2 for the fits below 200 MeV compare favorably with the Bonn and Argonne V14 results. We conclude that all of our Models give excellent descriptions of the NN data below 200 MeV, and that the quality of the fit begins to deteriorate only above 200 MeV, where Models IA and B are somewhat less successful than Models IIA and B.

TABLE I. The np phase parameters, in degrees, for Model IIB.

T_{lab} (MeV)	10	25	50	100	150	200	300
1S_0	60.71	52.02	41.76	27.54	17.04	8.436	-5.567
3P_0	4.084	9.182	12.34	10.19	4.780	-1.311	-1.344
1P_1	-3.117	-6.541	-9.984	-14.41	-17.85	-20.81	-25.36
3P_1	-2.207	-5.155	-8.686	-13.92	-18.41	-22.64	-30.73
3S_1	103.3	81.55	63.80	44.10	31.30	21.53	6.625
3D_1	-0.6636	-2.763	-6.407	-12.33	-16.70	-19.95	-24.20
ϵ_1	1.049	1.510	1.588	1.589	1.802	2.227	3.590
1D_2	0.1627	0.6470	1.525	3.391	5.317	7.139	10.07
3D_2	0.8251	3.586	8.621	16.91	22.47	25.84	28.29
3P_2	0.6962	2.543	5.926	11.23	14.26	15.74	16.29
3F_2	0.01318	0.1004	0.3206	0.7554	1.077	1.246	1.044
ϵ_2	-0.2032	-0.8046	-1.710	-2.712	-2.954	-2.773	-1.812
1F_3	-0.06503	-0.4130	-1.116	-2.225	-2.991	-3.591	-4.677
3F_3	-0.03187	-0.2234	-0.6711	-1.504	-2.140	-2.633	-3.395
3D_3	-0.001378	-0.009374	0.1094	0.9244	2.186	3.575	6.071
3G_3	-0.003775	-0.05226	-0.2558	-0.9348	-1.769	-2.635	-4.249
ϵ_3	0.07977	0.5402	1.571	3.410	4.746	5.673	6.683
1G_4	0.003296	0.03744	0.1426	0.3814	0.6135	0.8476	1.346
3G_4	0.01340	0.1659	0.6966	2.060	3.397	4.606	6.628
3F_4	0.001232	0.01809	0.09672	0.4080	0.8603	1.391	2.509
3H_4	0.0001528	0.003713	0.02366	0.09748	0.1886	0.2825	0.4531
ϵ_4	-0.003851	-0.04584	-0.1838	-0.5124	-0.8121	-1.066	-1.450

TABLE II. χ^2 per np data point obtained for the four models, compared with the Argonne V14 (Ref. [26]), the full Bonn results (Ref. [22]), and the Arndt-Roper SP89 fits (Ref. [23]). Numbers are given for each energy bin and for the overall fit from 8 to 225 MeV and from 8 to 325 MeV. The last column is the number of data for which the χ^2 is calculated.

Energy	IA	IB	IIA	IIB	Argonne V14	Bonn	VPIa(SP89)	Data
10	0.95	1.05	0.95	1.09	2.39	1.78	0.98	112
25	1.06	1.21	1.10	1.30	2.63	2.08	0.96	282
50	1.58	1.63	1.64	1.89	1.94	1.91	1.41	307
100	1.41	1.33	1.61	2.44	1.41	1.37	1.45	210
150	1.76	1.59	1.98	2.45	1.91	1.56	1.50	256
200	3.90	4.45	3.20	4.71	3.72	2.51	1.94	299
300	9.93	14.55	7.17	8.08	3.23	7.01	1.70	468
8-225	1.85	1.98	1.82	2.29	2.24	1.88	1.46	1585
8-325	3.62	4.42	2.91	3.40	2.40	2.93	1.48	2264

With the use of the SAID facility, we have looked at how our models fit actual data (in contrast to the phase parameters). These fits are much better than one would naively expect from a look at Fig. 1. This is because the error bars commonly given with phase shifts are diagonal errors which underestimate the true errors. These fits support the conclusion that all the models are, for all practical purposes, indistinguishable, but that there are some differences between our models and the Bonn potential. The fits are excellent at lower energies (as the χ^2 indicate) but begin to give the wrong shape for some observables above 300 MeV. Since we have not included pion production mechanisms, it may not be surprising or unexpected that the quality of the fits should deteriorate

as the pion production threshold (at $E_{\text{lab}} \approx 290$ MeV) is approached.

The parameters of the OBE kernels which produce these results are shown in Table III. Parameters which were varied during the fitting procedure are given in **bold face**; the others were fixed. For precise definitions of all coupling constants, see Eq. (3.3), and for the form factors see Eqs. (3.11) and (3.13). Note that Models I have 10 parameters while Models II have 13. All of the meson coupling constants (including the pion) and $\kappa = \frac{f}{g}$ ratios (for the ρ and ω) were varied in each case. Additional variables were the masses of the σ (and σ_1 for Models II), a form factor mass common to all mesons

TABLE III. OBE parameters for the four models. Numbers in **bold face** were varied during the fitting procedure; others were not. All masses are in MeV, and all parameters are defined precisely in Part III. (The numbers are given to the accuracy necessary to reproduce the deuteron binding energy and other low energy parameters to the precision given in Table IV.)

		Model IA	Model IB	Model IIA	Model IIB
π	$g_\pi^2/4\pi$	13.54403	13.41085	13.35757	13.37758
	λ_π	0.22515	0.21633	0.0	0.0
	m_π	138.0	138.0	138.0	138.0
η	$g_\eta^2/4\pi$			6.40798	5.30321
	λ_η			0.0	0.0
	m_η			548.8	548.8
σ	$g_\sigma^2/4\pi$	5.51070	5.51433	5.04718	4.86870
	m_σ	516.0	523.0	514.0	522.0
σ_1	$g_{\sigma_1}^2/4\pi$			0.32590	0.24372
	m_{σ_1}			573.0	428.0
ω	$g_\omega^2/4\pi$	9.85106	9.02467	9.83054	8.86086
	κ_ω	0.14259	0.20702	0.15050	0.22069
	λ_ω	1.0	1.0	1.0	1.0
	m_ω	782.8	782.8	782.8	782.8
ρ	$g_\rho^2/4\pi$	0.38291	0.26917	0.58686	0.60318
	κ_ρ	7.52525	8.77647	6.14920	5.66983
	λ_ρ	1.0	1.0	0.75218	0.82989
	m_ρ	760.0	760.0	760.0	760.0
	Λ_{nucl}	1610.0	1600.0	1685.0	1675.0
	Λ_{meson}	2135.0	2510.0	1830.0	2185.0

(Λ_m), and a form factor mass for the off-shell nucleon (Λ_N). Finally, off-shell mixing parameters λ_i were introduced for the pion (and η), as defined in Eq. (1.9), and for the vector mesons, Eq. (3.3), but for Models I λ_π was the only such parameter varied, while for Models II only λ_ρ was varied. As previously described, the essential difference between the models I and II is that $\lambda_\pi \approx 0.22$ in Models I, corresponding to an admixture of about 22% γ^5 coupling, while Models II constrain $\lambda_\pi = 0$ (pure $\gamma^5\gamma^\mu$ coupling) and incorporate two extra mesons, the σ_1 and the η , which adds three new parameters. For comparison, the full Bonn potential varies ten parameters. These include the three form factor masses associated with the πNN , ρNN , and $\pi N\Delta$ couplings, the mass of the σ , and the NN couplings of five mesons, the π , σ , ρ , ω , and δ , the latter having a mass of 983 MeV, in agreement with the scalar-isovector resonance observed at this energy.

Our values of $\frac{g_\pi^2}{4\pi}$ are considerably smaller than those obtained in Ref. [22]. All models give numbers in the range of 13.4 – 13.5, compared to the value of 14.28 obtained from older analyses of πN scattering [27]. However, deSwart and collaborators [28] have recently obtained, from a detailed analysis of low energy pp data, a value in the neighborhood of 13.5 for both the neutral and charged pion coupling constants, and Arndt *et al.* [29] recently obtained, from a new analysis of πN scattering data, a value of the charged coupling near 13.3. Our value is consistent with these new results. However, our low value probably partially accounts for somewhat low value of the asymptotic D/S ratio which we obtain [30] (see Table V below). Our value for the ω coupling constant is a factor of two smaller than that used in the Bonn potential [22], a reflection of the fact that the ω , in this model, no longer needs to supply all of the short range repulsion; some of it comes from relativistic effects. Note, however, that it is still considerably larger than predictions derived from the quark model. We mention that the Nijmegen group [31] obtains about the same value as found in this work; in their models a considerable part of the required additional repulsion comes from pomeron exchange. Perhaps the most unusual result we obtain is the small value of the g_ρ for the Model I fits. (The values of f_ρ are similar for all of the models.) We suspect that the small g_ρ values are related, through chiral symmetry, to the presence of the γ^5 coupling, but this effect is still under study.

The fits are very sensitive to the value of λ_π . If only four mesons are considered, and this parameter is allowed to vary, it moves quickly to some value near 0.25, and the fit deteriorates if it is moved significantly away from this value. To get a comparable fit with $\lambda_\pi = 0$, it is necessary to add at least one more meson, the σ_1 , as was done in Models II.

The low energy scattering parameters are shown in Table IV, and properties of the deuteron are shown in Table V. The deuteron binding energy, taken to be exactly 2.2246 MeV, was treated as a constraint to the fits, and attempts were made to also fit the scattering lengths, a , and effective ranges, r . Our values of these quantities agree precisely with the experimental results reported in Ref. [22], except for r_s and (for Models II) r_t which differ by 3 – 4 standard deviations. In view of the overall quality of the low energy fits, we are not concerned by these differences. Arndt has pointed out [32] that these numbers are sensitive to the procedure and range of data used to extract them, and his numbers (also shown in Table IV) are quite different from those quoted in Ref. [22].

The nonrelativistic deuteron magnetic moments agree well with the experimental value, primarily because of our low D state percentage (about 4%), but the quadrupole moment and asymptotic D/S ratio are both too low. The discrepancy between our D/S ratio and the newly reported experimental determination of Rodning and Knutson [33], which is significantly smaller than the value reported in Ref. [22], is only 2 – 5 standard deviations. Nevertheless, these low values, taken together with tendency for ϵ_1 to be too small (as shown in Fig. 1), suggests that our models have too little tensor interaction, and that this should be corrected if the models are to be used for precision studies of the deuteron and its interactions.

The use of nonrelativistic formulas for the calculation of magnetic and quadrupole moments is unjustified if one wishes to make precision comparisons with experimental results. The relativistic corrections to the magnetic moment have been a subject of much discussion for many years [34], but there are also corrections to the quadrupole moment. The relativistic impulse approximation (RIA) to the electromagnetic form factors, when expanded to order $(\frac{v}{c})^2$, yields the following corrections [35]:

TABLE IV. Low energy parameters compared with values reported by Arndt [32] and those experimental values reported in Ref. [22]. Scattering lengths and effective ranges are denoted by a and r , respectively, with the subscript referring to spin singlet (s) and triplet (t).

	Model IA	Model IB	Model IIA	Model IIB	Arndt	Experiment
a_s	-23.748	-23.748	-23.748	-23.748	-24.50	-23.748 ± 0.010
r_s	2.598	2.583	2.612	2.609	2.876	2.75 ± 0.05
a_t	5.423	5.413	5.411	5.382	5.402	5.424 ± 0.004
r_t	1.752	1.738	1.735	1.695	1.876	1.759 ± 0.005

TABLE V. Deuteron properties. The relativistic deuteron wave function has four components, with percentages given. These do not add up to 100%; the additional piece is the size of the $\langle V' \rangle$ term [from Eq. (1.13)] arising from the energy dependence of the kernel. The values of the magnetic and quadrupole moments given in parentheses include the relativistic corrections of Eq. (1.10). The experimental D/S ratio is from Ref. [28].

	Model IA	Model IB	Model IIA	Model IIB	Bonn	Experiment
% S	95.038	94.801	95.284	94.797		
% D	3.969	4.098	4.146	4.538	4.249	
% P_t	0.460	0.468	0.110	0.137		
% P_s	0.007	0.010	0.009	0.006		
Total	99.474	99.377	99.549	99.478		
μ_d	0.8574 (0.8978)	0.8566 (0.9025)	0.8564 (0.8836)	0.8541 (0.8799)	0.8555	0.857406 ± 0.000001
Q_d (fm ²)	0.2665 (0.2702)	0.2596 (0.2634)	0.2626 (0.2647)	0.2604 (0.2627)	0.2807	0.2859 ± 0.0003
A_S (GeV) ^{1/2}	0.4024	0.3985	0.4016	0.3963		
A_D (GeV) ^{1/2}	0.009949	0.009455	0.009714	0.009570		
A_D/A_S	0.0247	0.0237	0.0242	0.0241	0.0267	0.0256 ± 0.0004

$$\Delta\mu_d = \frac{m}{\sqrt{3}} \int_0^\infty r dr \left(u \left[\frac{1}{\sqrt{2}} v_t - v_s \right] - w \left[v_t + \frac{1}{\sqrt{2}} v_s \right] \right),$$

$$\Delta Q_d = \frac{\sqrt{2}}{10m^2} \int_0^\infty r^2 dr \left(\left[\frac{1}{2} (u\hat{w} + w\hat{u}) - \frac{1}{\sqrt{8}} w\hat{w} \right] + \hat{\mu} \frac{3}{2} w \left[\frac{d}{dr} \left(\frac{u}{r} \right) - \frac{1}{\sqrt{2}} \frac{w'}{r} \right] \right. \\ \left. + \hat{\mu} \frac{m}{r} \left[\frac{5}{\sqrt{6}} \left(u \left[v_s + \frac{1}{\sqrt{2}} v_t \right] - w \left[v_t - \frac{1}{\sqrt{2}} v_s \right] \right) - \sqrt{3} w \left[v_s - \frac{1}{\sqrt{2}} v_t \right] \right] \right) \quad (1.10)$$

where

$$\begin{aligned} \hat{w} &= \left(-\frac{d^2}{dr^2} + \frac{6}{r^2} + m\epsilon \right) w, \\ \hat{u} &= \left(-\frac{d^2}{dr^2} + m\epsilon \right) u, \\ w' &= \frac{dw}{dr}, \quad \hat{\mu} = 2\mu_s - 1 \end{aligned} \quad (1.11)$$

and u , w are the familiar S and D state components of the deuteron wave function, v_t , v_s are the two small relativistic P state components defined in Ref. [20] and discussed below, and $\mu_s \cong 0.880$ is the isovector magnetic moment of the nucleon. These corrections have been evaluated for these models, and are

$$\begin{aligned} \Delta\mu_d &= 0.0404 && \text{(Model IA)} \\ &= 0.0459 && \text{(Model IB)} \\ &= 0.0272 && \text{(Model IIA)} \\ &= 0.0258 && \text{(Model IIB)}, \\ \Delta Q_d &= 0.0037 && \text{(Model IA)} \\ &= 0.0038 && \text{(Model IB)} \\ &= 0.0021 && \text{(Model IIA)} \\ &= 0.0023 && \text{(Model IIB)}. \end{aligned} \quad (1.12)$$

Note that all of these are positive; $\Delta\mu_d$ is about 3–6% and ΔQ_d is 1–1½%, and all are many times larger

than the experimental errors in these quantities. The corrected quantities are shown in parentheses in Table V. The correction to Q_d is not nearly large enough to bring it into agreement with experiment, while $\Delta\mu_d$ is much too large and spoils the agreement. However, as the tensor force is increased, μ_d will decrease and Q_d and the D/S ratio will increase, opening the possibility for agreement. Before definitive conclusions can be drawn, a completely consistent calculation of the deuteron moments should be completed. Such a calculation might include contributions not contained in the formulae (1.10), such as contributions from the $\rho\pi\gamma$ exchange current, which is largely independent of the details of the nuclear force model [36].

The asymptotic normalization constants for the S and D state wave functions, A_S and A_D , and the asymptotic D/S ratio, A_D/A_S , are also shown in Table V.

The deuteron wave functions which result from Models I and II are shown in Fig. 2. The relativistic models have wave functions with four components, as mentioned above. The two small P state components v_t and v_s (for spin triplet and singlet) play a role similar to the small components of the Dirac wave function of the hydrogen atom. The definition and normalization of these wave functions is discussed fully in Ref. [20], and generally in Sec. II C. They are normalized according to

$$\int_0^\infty dr [u^2 + w^2 + v_t^2 + v_s^2] + \langle V' \rangle = 1 \quad (1.13)$$

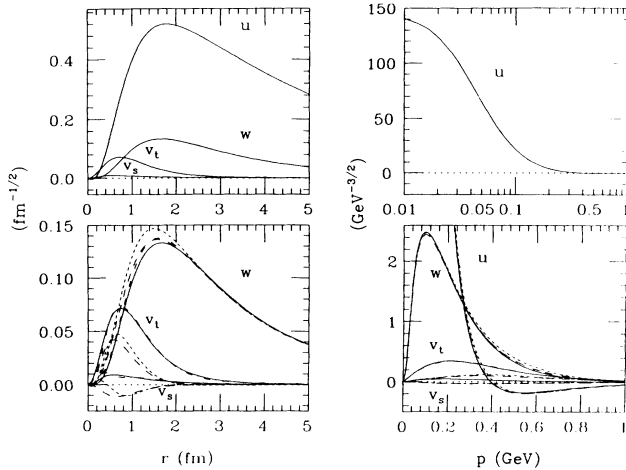


FIG. 2. Deuteron wave functions for Model IA (solid), IB (dash-dotted), IIA (long dashes), IIB (short dashes). The position space wave functions are shown in the two left-hand figures and the momentum space ones in the two right-hand figures. The upper two figures are Model IA only, and show the behavior of the large component u . The lower two figures are drawn so that the comparative sizes of the smaller components, w , v_t , and v_s , can be studied.

where the first term in (1.13) is the reduction of the first term on the right-hand side (RHS) of Eq. (2.50) and $\langle V' \rangle$ is shorthand for the second term on the RHS of that equation. The probabilities of each of the four components of the wave function are given in Table V; the remaining probability (not given) is the contribution of the interesting term $\langle V' \rangle$, which arises from the dependence of the relativistic kernel on the total energy (see Sec. II C), and is about $\frac{1}{2}\%$.

Note that the v_s wave function is negligible for most purposes, and that the size of the v_t wave function is sensitive to λ_π , as discussed in Ref. [20]. Its probability is about $\frac{1}{2}\%$ in Model I and about $\frac{1}{10}\%$ in Model II. While these are very small percentages, the v_t wave function in momentum space is comparable to the others above 500 MeV, and thus may play a role in observables sensitive to such large momentum components.

The OBE parameters were determined by an automatic fitting routine which minimized χ^2 as determined from the error matrix based on the SP89 fit supplied to us by Arndt [32]. Briefly, we minimized the quantity

$$\chi^2 = \sum_{i,j} \rho_{i,j} (\bar{\delta}_i - \delta_i) (\bar{\delta}_j - \delta_j) + \chi_0^2 \quad (1.14)$$

where $\bar{\delta}_i$ are the SP89 phase parameters, δ_i are the calculated phase parameters, $\rho_{i,j}$ is the error matrix, χ_0^2 is the χ^2 of the SP89 fit (given in Table II) and the sum over i and j depends on the energy range and angular momentum states which are included in the fit [37]. The sum (1.14) included phase parameters up to $J = 4$, and used data binned around the seven energies listed in Table II. In each case, the fitting procedure was started by first fitting the phase shifts directly, which is equivalent

to keeping only the diagonal elements of (1.14), and taking $\chi_0^2 = 0$. This always gives a very large χ^2 per data point (values below 15 are almost impossible to achieve, and numbers in the vicinity of 20 indicate a very good fit), but converged quite efficiently to the correct region in parameter space. The fitting was then continued by first adding the deuteron binding energy as a constraint (by adjusting the σ coupling constant to give the exact value for the binding energy) and then minimizing the full expression (1.14), including the correlated errors which come from the off-diagonal terms. This latter procedure is much slower [apparently the surface determined by (1.14) is not smooth], but keeps the minimization from wandering into a region where the fit to the actual data is not as good, which will happen if correlated errors are ignored in the final stages. Unfortunately, the χ^2 obtained from (1.14) is only a quadratic approximation to the true value, and hence is only accurate very near the minimum, so the final χ^2 presented in Table II was calculated directly from the data using the SAID facility [23]. Since our fit was made using (1.14), the values reported in Table II might be improved by doing a complete fit to the actual data, but we expect any such improvements, or any changes in the OBE parameters which would result, to be small.

D. Relativistic effects in NN scattering

In this subsection we will discuss the relativistic effects which arise in our treatment of low energy nucleon-nucleon scattering. These effects arise from four sources: (i) negative energy channels, (ii) retardation in the meson propagators and form factors, (iii) off-shell factors in the meson-nucleon couplings, and (iv) relativistic energy factors in the nucleon propagator.

The importance of contributions from the negative energy channels is easily studied by shutting off the V^{--} and V^{+-} potential terms in the coupled equations. Figure 3 shows how the $J = 0, 1$ phase parameters for Model IA change when V^{--} is set to zero (dotted line), and when both V^{--} and V^{+-} are set to zero (dashed line), leaving only V^{++} . The same results for Model IIA are shown in Fig. 4. Note that in both cases the effects of V^{--} are small, but not completely negligible, while the lowest order effects of the negative energy channel, measured by the sensitivity to V^{+-} , are quite significant. The negative energy channel makes large contributions to the scattering amplitudes in both models.

In view of the discussion following Eq. (1.8), it is not surprising that the negative energy channels are important in Model IA, where λ_π is nonzero, but it was not expected that they would also be important in Model IIA, where λ_π is zero. The explanation for this is suggested by Fig. 5, which shows how these phase parameters vary with λ_π and λ_ρ . Setting λ_π to zero in Model IA produces an effect on most of the phase parameters very similar to setting V^{+-} to zero (except for some of the P waves and ϵ_1 , where the quantitative size of the two effects is somewhat different), showing that the V^{+-} contributions arise, in large part, from the γ_5 coupling of

the pion. However, the figure also shows that the phase parameters in the *singlet* channels are quite sensitive to λ_ρ , and that reducing λ_ρ from 1.0 to 0.8 in these channels produces an effect comparable to changing λ_π from 0.23 to 0, but in the opposite direction. Since both Models II have a value of λ_ρ close to 0.8, the effect of V^{+-} in Models II appears to be due, at least in part, to this off-shell sensitivity of the ρ coupling. (The dotted line in Fig. 5 shows the effect of turning off the $\frac{q^\mu q^\nu}{m_\pi^2}$ term in the vector propagators. Note that this effect is not large.)

In any case, we find that the effect of the negative energy channels is always repulsive, in agreement with Ref. [8], and our discussion following Eq. (1.8). This is in contrast with the results of Fleischer and Tjon [3] and Hippchen and Holinde [38]. Using the Bethe-Salpeter equation, Fleischer and Tjon found that the negative energy states are attractive in the 1S_0 channel (in all other channels the effect is negative, in agreement with our results). Hippchen and Holinde confirmed this by calculating the pair term contributions from box and crossed box diagrams using the Bonn [22] parameters. The differences between these results and ours can be traced to states in which *both* nucleons have negative energy. In our approach, these states are completely suppressed at the level of the OBE approximation, but appear in the two-boson exchange (TBE) (and higher order) kernels, where, as was found in Ref.[9], they are canceled by other TBE

(and higher order) mechanisms which arise from chiral invariance.

The size of the remaining relativistic effects itemized above are shown in Fig. 6, which gives the $J = 0, 1$ phase parameters for Model IA in a sequence of four approximations corresponding to turning off relativistic effects sequentially. The full calculation is the solid curve, and the one to which all other curves should be compared. The long-dashed curve shows the effect of shutting off the retardation factors in the meson propagators and form factors. Specifically, the retardation terms are the energy difference factors of the form $(E_p - E_k)^2$ and $(W - E_p - E_k)^2$ which occur in the meson four-vector momentum transfer, which appears in the denominators $D(z)$ and $\hat{D}(z)$ of the meson propagators given in Eq. (3.14), and also in the meson form factors. Shutting off these terms has a large effect, particularly on the ϵ_1 parameter. Next, the dotted curve shows the effect of shutting off *both* the retardation terms *and* the negative energy channel (by setting V^{+-} and V^{--} equal to zero). Note that retardation and negative energy effects tend to cancel in the S and D states, but in the P waves the effect of the negative energy channel is larger, and is the dominant effect in the 3P_1 channel. Finally, the last curve (the short-dashed line) is the nonrelativistic result, which is obtained when terms proportional to $W - E_p$, $W - E_k$, and $E_p - E_k$ are dropped in the numerator of the V^{++} matrix elements, and when the factor $2E_k - W$ in the g^+ propagator, given in Eq. (2.89), is replaced

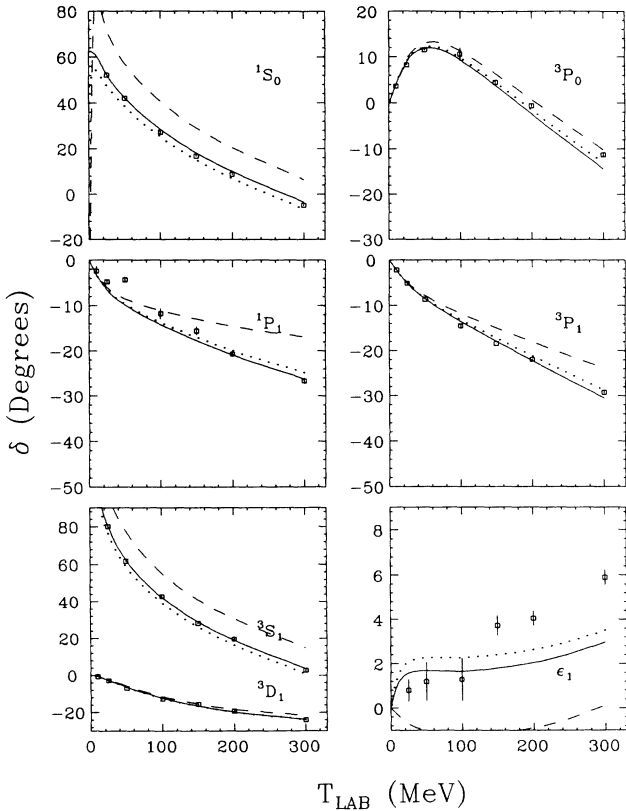


FIG. 3. V^{++} and V^{+-} dependences for Model IA. Full calculation (solid), $V^{--} = 0$ (dots), and $V^{+-} = V^{--} = 0$ (dashes) are shown.

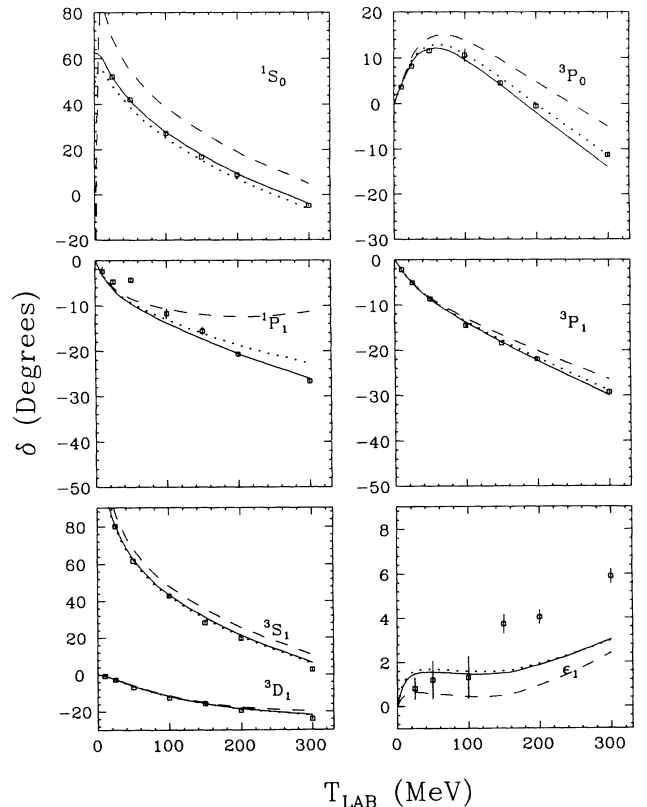


FIG. 4. V^{++} and V^{+-} dependences for Model IIA. Curves are as in Fig. 3.

by $\frac{1}{m}(k^2 - p^2)$. These effects are large in the S and D states, but negligible in the P states. We conclude that all of these relativistic effects are significant, but that they sometimes cancel. In total, our results show that relativistic effects are very significant, even at low energy.

Because nonrelativistic models have been found which also fit low energy nucleon-nucleon scattering, we know that we could compensate for these relativistic effects to some extent by refitting the meson parameters. Thus the difference between relativistic and nonrelativistic models shows up ultimately in the differences between the values of coupling constants and masses required to fit data, in the dynamical degrees of freedom required, and in the applications of any two-nucleon force model to the description of other processes (interactions with external probes, and the three-nucleon problem, for example). In this respect, we have already emphasized that major differences are the (comparatively) small size of the ω coupling constant needed in our fit, and the fact that we find it possible to fit the data with only four mesons. We also expect significant differences to arise when our models are used to describe other physical processes.

We have looked at the sensitivity of our fits to small variations in the parameters. Each of the parameters was changed by 10%, and the effect on the fits examined.

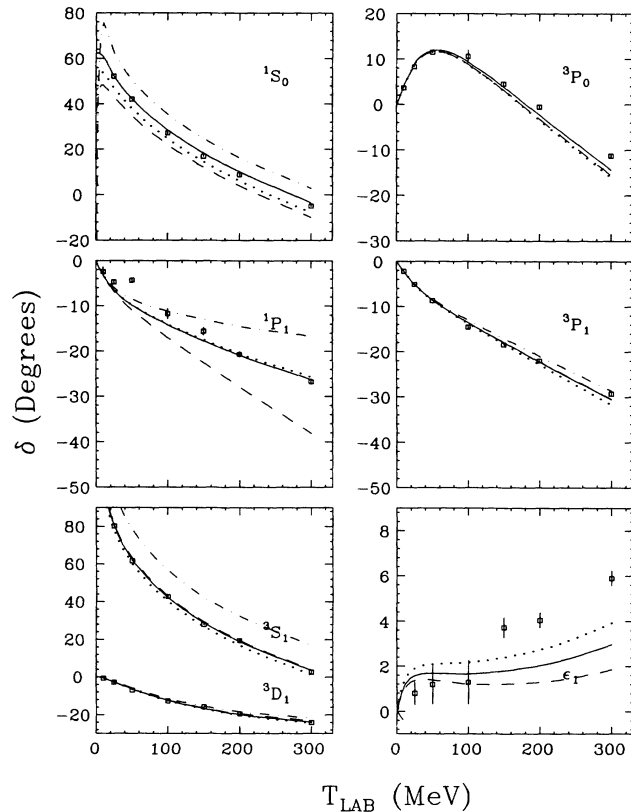


FIG. 5. Dependences on λ_π and λ_ρ for Model IA. Full calculation (solid), $\lambda_\pi = 0$ (dash-dotted), $\lambda_\rho = 0.8$ (dashes), and the result of setting the $q^\mu q^\nu/m_v^2$ terms in the ρ and ω propagators to zero (dots) are shown.

Those parameters which produced the largest change in the χ^2 were Λ_{nucl} , g_π , g_σ , g_ω , κ_ρ , and λ_ρ . Increasing Λ_{nucl} increases the attraction in the S waves, and changes the shape of the 1P_1 phase shift. The shape of the 1P_1 phase shift is also quite sensitive to the value of λ_ρ . The change in g_π had the greatest effect on the $J = 2$ phase shifts, while an increase in g_σ increased the attraction (as expected) particularly in the 1S_0 and 3P_2 channels, and an increase in g_ω had a particularly large repulsive effect on the 3P_0 and 3P_2 channels. The principal effect of an increase in κ_ρ was attractive in the 1S_0 channel and repulsive in the 3P_0 channel. While these changes individually produced a large effect, many of these effects are correlated, so these parameters are not necessarily those most precisely defined by the fit. The pion mixing parameter λ_π was quite well fixed by the Model I fits, but a 10% change in this parameter did not have a large effect on the phase shifts.

The last effect we will discuss is the virtual coupling which occurs in the (formerly) uncoupled channels in which $L = J$. This coupling is discussed in Sec. III. Briefly, when one nucleon is off-shell, the difference in the energies of the two nucleons, p_o , need not be zero, and there exists states which change sign as $p_o \rightarrow -p_o$. Such states are referred to as “odd” states (denoted by a

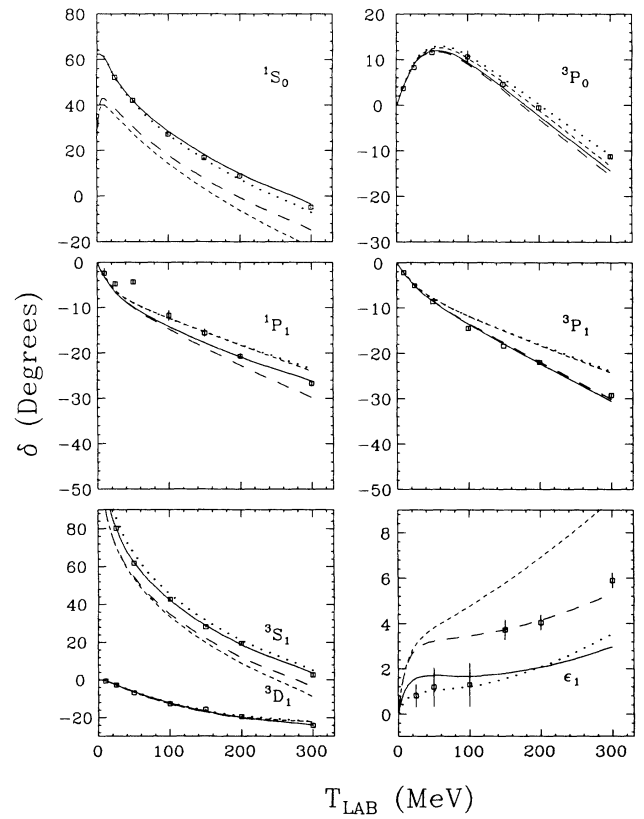


FIG. 6. Relativistic effects (Model IA). Full calculation (solid), without retardation (long dashes), without retardation and the $(-)$ channel (dots), nonrelativistic limit (short dashes). See discussion in the text.

subscript o) and the Pauli principle requires that they be *symmetric* under interchange of all other quantum numbers, the “wrong” symmetry for normal states. Since we assume isospin conservation, and parity conservation fixes L , the only way to construct a “wrong” symmetry state is to assign it a total spin different from the normal assignment. Hence, for example, we find that our isoscalar 1P_1 state is coupled to an “odd” *isoscalar* state with 3P_1 quantum numbers. The odd states go to zero when both particles are on mass-shell (when $p_o = 0$), and hence are closed virtual channels which only couple to the physical states inside the interaction region. In this respect, they play a role similar to the negative energy states, but they are distinct effects not described by the negative energy channel. In fact, each positive energy channel couples to a corresponding negative energy channel, and hence in our relativistic formalism the physical isoscalar 1P_1 state is actually coupled to *four* channels (one is odd and the other two the companion negative energy channels – see Sec. III). The 1S_0 and 3P_0 states are exceptions to this rule, because angular momentum conservation prevents the existence of companion 3S_0 and 1P_0 states, so these states couple to only one other (negative energy) channel. Also, the coupled states with $J \neq L$ do not have companion odd states for a similar reason; it is impossible to construct coupled states with total spin equal to zero. These states there-

fore have four channels: two physical coupled states and two negative energy companion states.

From the above discussion it is clear that the odd states effect only those channels with $J = L > 0$. The effect on these channels of turning off the odd states is shown in Fig. 7. The effect is tiny in all but the $J = 1$ states, where it is small and repulsive.

The next subsection summarizes the major conclusions of this work.

E. Conclusions

The principal conclusions of this paper are summarized as follows.

- (i) The relativistic spectator equations, with an OBE kernel, can be used to describe low energy NN scattering. We obtain very nice fits comparable to the best available.
- (ii) Models with different off-shell behavior have been found which fit the on-shell data equally well. The existence of phase equivalent solutions, embedded in the same formalism, shows (once again) that on-shell data cannot uniquely determine the dynamics, and we plan to look for other phase equivalent solutions. These families of solutions can be used to study the sensitivity of other physical processes to off-shell effects.
- (iii) We find that it is possible to fit the low energy NN data using an OBE model with only four mesons and 10 parameters (Models IA and IB). The existence of such a fit suggests that the low energy NN data cannot alone determine the coupling constants of other mesons which may be present, the role of inelastic processes such as the virtual production of Δ and Roper resonances (which are surely present), or the size of box and crossed box contributions. In particular, we conclude that the η coupling is very poorly determined by such fits (beyond the observation that it is small), and that a successful OBE model can be found which does not require a scalar, *isovector* meson. [Note that, although the $\delta(983)$ surely exists, its coupling to the nucleon is completely unknown.]
- (iv) Our models include contributions from the negative energy states of the propagating nucleons, retardation (energy dependence) in the meson propagators, and off-shell effects in the meson- NN vertex functions, all of which can be considered relativistic effects, and all of which are usually ignored in other calculations. These effects are all individually large, and their combined effect is large, even though they tend to cancel. Perhaps more significantly, they do not appear to be easily described by a single meson, or by a combination of the four basic mesons believed to be essential to any OBE description (the π , σ , ρ , and ω). We believe that this explains our ability to fit the data with only four exchanged mesons. However, because fits with

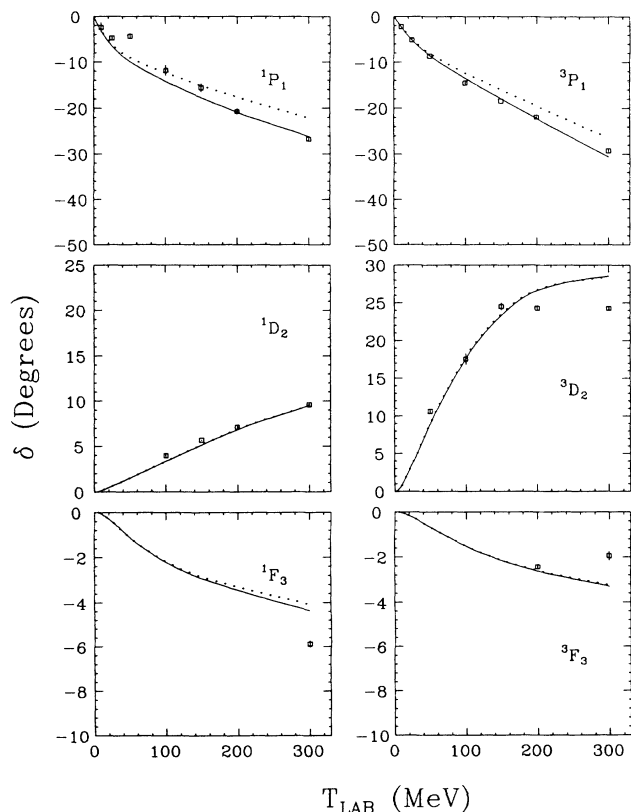


FIG. 7. Dependence of the $J = L > 0$ phase parameters on the virtual “odd” states, as discussed in the text. Full result (solid) and results when odd states are omitted from the coupled equations (dots) are shown.

non-relativistic models are possible, this fact in itself provides only limited evidence for the importance of relativistic effects.

- (v) Two objections to the spectator formalism are addressed in detail. First, it is shown that the equations can be written in a manifestly symmetric form, and that this insures that the Pauli principle is exactly satisfied. Secondly, it is shown how to handle the spurious singularities which arise in the kernel. The differences between versions A and B of the two models show the sensitivity of the results to these singularities. We find that phase equivalent fits can be found, but that some of the coupling constants which emerge from the fits can differ significantly.

This concludes the introduction, overview, and conclusions of Part I. In Part II, the relativistic spectator formalism is described in detail. The discussion applies to any interaction kernel. In Part III, the details of the OBE kernels actually used in this paper are described.

II. GENERAL THEORY

In this part the relativistic wave equations and wave functions are presented and it is proved that the theory is covariant, unitary (below the pion production threshold), and treats the two nucleons symmetrically. Reduction of the equation and amplitudes to a practical form suitable for numerical solution is then described. This reduction involves first separating the 4-component channel which describes propagation of the off-shell nucleon into two 2-component channels in which the off-shell nucleon is either in its positive energy (+) or negative energy (-) state. A partial wave decomposition of the resulting helicity amplitudes is then introduced, and the kernel is block diagonalized into the three independent channels referred to as singlet, triplet, and coupled.

A. Symmetric form of the equations

It is convenient to start with the two-body equations for the scattering amplitude in their fully symmetric 16×16 component form, with initial and final states labeled by two Dirac indices $\{\alpha, \beta\}$. The four-momenta of the two particles are

$$\begin{aligned} p_1 &= \frac{1}{2}P + p, & P &= p_1 + p_2, \\ p_2 &= \frac{1}{2}P - p, & p &= \frac{1}{2}(p_1 - p_2). \end{aligned} \quad (2.1)$$

The symmetric form of the equations will contain amplitudes M in which particle 1 is on-shell in the final state, $p_1^2 = m^2$, and in which particle 2 is on-shell in the final state, $p_2^2 = m^2$. These constraints fix the relative energy p_0 in a covariant manner. To avoid a cumbersome notation, the symbols in (2.1) will refer to the case when $p_1^2 = m^2$, and symbols with the caret, $\hat{p}, \hat{p}_1, \hat{p}_2$, will denote the four-momenta when $p_2^2 = m^2$. In the c.m. system, the following relations therefore hold:

$$\begin{aligned} P &= \hat{P} = (W, \mathbf{0}), \\ p &= \left(E_p - \frac{1}{2}W, \mathbf{p} \right), & \hat{p} &= \left(\frac{1}{2}W - E_p, \mathbf{p} \right) \end{aligned} \quad (2.2)$$

$$\begin{aligned} p_1 &= (E_p, \mathbf{p}), & \hat{p}_1 &= (W - E_p, \mathbf{p}), \\ p_2 &= (W - E_p, -\mathbf{p}), & \hat{p}_2 &= (E_p, -\mathbf{p}), \end{aligned}$$

where $E_p = (m^2 + \mathbf{p}^2)^{\frac{1}{2}}$. Note that changing the sign of \mathbf{p} maps \hat{p} into $-p$.

For simplicity, the equations will be given in the c.m. system, but they are manifestly covariant and the explicit form of the Lorentz transformation of the scattering amplitudes which permits them to be boosted to an arbitrary frame will be given in Sec. IIB below. The symmetric form of the two-body equations for the elastic scattering amplitude M in a channel with isospin I can then be written

$$\begin{aligned} M_{\alpha\alpha',\beta\beta'}(p,p';P) &= \frac{1}{2} \left[V_{\alpha\alpha',\beta\beta'}(p,p';P) + (-1)^I V_{\alpha\beta',\beta\alpha'}(p,-p';P) \right] \\ &\quad - \frac{1}{2} \int \frac{d^3k}{(2\pi)^3} \frac{m}{E_k} V_{\alpha\alpha_1,\beta\beta_1}(p,k;P) G_{\alpha_1\alpha_2,\beta_1\beta_2}(k;P) M_{\alpha_2\alpha',\beta_2\beta'}(k,p';P) \\ &\quad - \frac{1}{2} \int \frac{d^3k}{(2\pi)^3} \frac{m}{E_k} V_{\alpha\alpha_1,\beta\beta_1}(p,\hat{k};P) \hat{G}_{\alpha_1\alpha_2,\beta_1\beta_2}(\hat{k};P) M_{\alpha_2\alpha',\beta_2\beta'}(\hat{k},p';P). \end{aligned} \quad (2.3)$$

A second equation for $M(\hat{p},p';P)$, identical to the above except for the substitution \hat{p} for p , completes the set. The two equations form a coupled set for the amplitudes $M(p,p';P)$ and $M(\hat{p},p';P)$, as illustrated diagrammatically in Fig. 8.

The inhomogeneous term in Eq. (2.3) has been explicitly antisymmetrized with respect to interchange of the two particles in the *initial* state. Note that interchange

of the two particles requires that *all 4 components* of the relative momentum p' change sign; and that the spin and isospin indices also be interchanged. Since isospin indices will be suppressed, their interchange has been represented by an explicit factor of $-(-1)^I$ in Eq. (2.3).

The propagator G is the product of the positive energy projection operator for the on-shell particle 1 and the usual Dirac propagator for the off-shell particle 2:

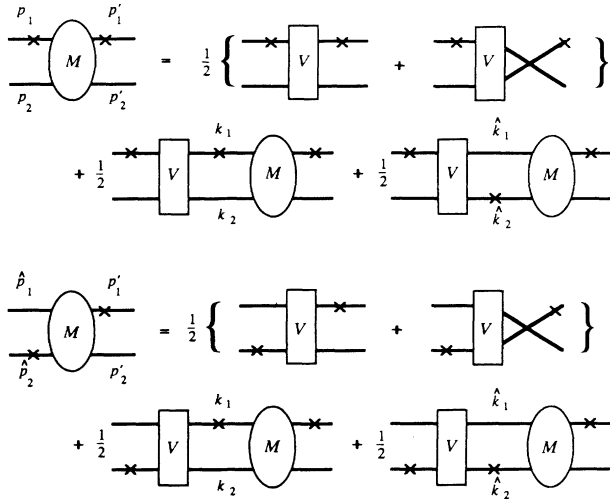


FIG. 8. Diagrammatic representation of the equations (2.3).

$$G_{\alpha_1\alpha_2,\beta_1\beta_2}(k;P) = \Lambda_{\alpha_1\alpha_2}\left(\frac{1}{2}P+k\right)G_{\beta_1\beta_2}\left(\frac{1}{2}P-k\right) \quad (2.4)$$

where, using the subscripts 1,2 to represent $\{\alpha_1, \alpha_2\}$ or $\{\beta_1, \beta_2\}$

$$\begin{aligned} \Lambda_1(k_1) &= \frac{(m + \not{k}_1)_{\alpha_1\alpha_2}}{2m}, \\ G_2(k_2) &= \frac{(m + \not{k}_2)_{\beta_1\beta_2}}{m^2 - k_2^2 - i\epsilon}. \end{aligned} \quad (2.5)$$

The propagator \hat{G} corresponding to propagation in which particle 2 is on-shell is

$$\begin{aligned} \hat{G}_{\alpha_1\alpha_2,\beta_1\beta_2}(\hat{k};P) &= G_{\alpha_1\alpha_2}\left(\frac{1}{2}P+\hat{k}\right)\Lambda_{\beta_1\beta_2}\left(\frac{1}{2}P-\hat{k}\right) \\ &= G_{\beta_1\beta_2,\alpha_1\alpha_2}(-\hat{k};P). \end{aligned} \quad (2.6)$$

The overall effect of dividing the propagation equally between terms in which particle 1 is on-shell and those in which particle 2 is on-shell is to produce a coupled set of equations in which intermediate and final states are antisymmetrized if one starts with an initial state which is properly antisymmetrized.

Before demonstrating this fact explicitly, note that Eq. (2.3) can be formally obtained from the Bethe-Salpeter equation by dividing the k_0 integration into two equal parts, closing one in the upper half plane and retaining only the contribution from the positive energy pole of particle 2, and closing the other in the lower half plane and retaining only the positive energy pole of particle 1. Formally

$$\begin{aligned} G_1(k_1)G_2(k_2) &\rightarrow \frac{1}{2}\Lambda_1(k_1)G_2(k_2)2m\delta_+(m^2 - k_1^2) \\ &\quad + \frac{1}{2}G_1(k_1)\Lambda_2(k_2)2m\delta_+(m^2 - k_2^2). \end{aligned} \quad (2.7)$$

From the antisymmetrization of the inhomogeneous term in Eq. (2.3) with respect to interchange of the two particles in the initial state, it follows immediately that the full scattering amplitude is also antisymmetrized with respect to the initial state

$$M_{\alpha\beta',\beta\alpha'}(p,-p';P) = (-1)^I M_{\alpha\alpha',\beta\beta'}(p,p';P). \quad (2.8)$$

To prove that the final state is also antisymmetric, it is necessary to use the identity

$$V_{\alpha\alpha',\beta\beta'}(p,p';P) = V_{\beta\beta',\alpha\alpha'}(-p,-p';P) \quad (2.9)$$

which is always satisfied by the relativistic kernels (see Part III). Using this property, and relation (2.6), Eq. (2.3) can be written

$$\begin{aligned} M_{\alpha\alpha',\beta\beta'}(p,p';P) &= \frac{1}{2}\left[V_{\alpha\alpha',\beta\beta'}(p,p';P) + (-1)^I V_{\beta\beta',\alpha\alpha'}(-p,p';P)\right] \\ &\quad - \frac{1}{2}\int \frac{d^3k}{(2\pi)^3} \frac{m}{E_k} V_{\alpha\alpha_1,\beta\beta_1}(p,k;P) G_{\alpha_1\alpha_2,\beta_1\beta_2}(k,P) M_{\alpha_2\alpha',\beta_2\beta'}(k,p';P) \\ &\quad - \frac{1}{2}\int \frac{d^3k}{(2\pi)^3} \frac{m}{E_k} V_{\beta\beta_1,\alpha\alpha_1}(-p,k;P) G_{\alpha_1\alpha_2,\beta_1\beta_2}(k,P) M_{\beta_2\alpha',\alpha_2\beta'}(-k,p';P). \end{aligned} \quad (2.10)$$

The second equation is again identical with p replaced by \hat{p} . If, in this second equation, the sign of \mathbf{p} is changed and α and β are interchanged, one obtains an equation for $M_{\beta\beta',\alpha\alpha'}(-p,p';P)$ identical to (2.10) but with the inhomogeneous term multiplied by $(-1)^I$ [and with $M(k,p';P)$ and $M(-k,p';P)$ interchanged]. Hence, since the solutions are unique, it follows that

$$M_{\beta\beta',\alpha\alpha'}(-p,p';P) = (-1)^I M_{\alpha\alpha',\beta\beta'}(p,p';P). \quad (2.11)$$

Hence the final state is also antisymmetric. Using (2.11), Eq. (2.10) can be written in a compact form:

$$M_{\alpha\alpha',\beta\beta'}(p,p';P) = \bar{V}_{\alpha\alpha',\beta\beta'}(p,p';P) - \int \frac{d^3k}{(2\pi)^3} \frac{m}{E_k} \bar{V}_{\alpha\alpha_1,\beta\beta_1}(p,k;P) G_{\alpha_1\alpha_2,\beta_1\beta_2}(k,P) M_{\alpha_2\alpha',\beta_2\beta'}(k,p';P) \quad (2.12)$$

where

$$\bar{V}_{\alpha\alpha',\beta\beta'}(p,p';P) = \frac{1}{2} \left[V_{\alpha\alpha',\beta\beta'}(p,p';P) + (-1)^J V_{\beta\beta',\alpha\alpha'}(-p,p';P) \right]. \quad (2.13)$$

This symmetrized potential is shown diagrammatically in Fig. 9. The form (2.12) of the equations will be used throughout the remainder of this paper. While it appears to be asymmetric in the treatment of the two particles because it contains the propagator G only, the antisymmetrization of the potential (2.13) insures that the Pauli principle is satisfied and that the particles are, in fact, treated identically. The reader can easily confirm that the steps leading from (2.3) to (2.12) can be reversed, permitting the recovery of the manifestly symmetric form (2.3) from (2.12).

B. Reduction of the on-shell particle

The next step is to simplify Eq. (2.12) by exploiting the fact that particle 1 is on-shell. Use the expansion

$$\Lambda_1(k_1) = \sum_{\lambda_1} u(\mathbf{k}, \lambda_1) \bar{u}(\mathbf{k}, \lambda_1) \quad (2.14)$$

where the sum is over the two possible helicities $\lambda_1 = \pm \frac{1}{2}$, and introduce the matrix elements

$$\mathbf{M}_{\lambda_1\lambda'_1,\beta\beta'}(p,p';P) = \bar{u}_\alpha(\mathbf{p}, \lambda_1) M_{\alpha\alpha',\beta\beta'}(p,p';P) u_{\alpha'}(\mathbf{p}', \lambda'_1), \quad (2.15)$$

$$\mathbf{V}_{\lambda_1\lambda'_1,\beta\beta'}(p,p';P) = \bar{u}_\alpha(\mathbf{p}, \lambda_1) \bar{V}_{\alpha\alpha',\beta\beta'}(p,p';P) u_{\alpha'}(\mathbf{p}', \lambda'_1).$$

This gives

$$\mathbf{M}_{\lambda_1\lambda'_1,\beta\beta'}(p,p';P) = \mathbf{V}_{\lambda_1\lambda'_1,\beta\beta'}(p,p';P) - \int \frac{d^3k}{(2\pi)^3} \frac{m}{E_k} \mathbf{V}_{\lambda_1\lambda,\beta\beta_1}(p,k,P) G_{\beta_1\beta_2}(k_2) \mathbf{M}_{\lambda\lambda'_1,\beta_2\beta'}(k,p';P). \quad (2.16)$$

Note that the quantum numbers of the on-shell particle have been completely removed from the propagator, which describes the propagation of the off-shell particle 2 only, and that the particle states are now described by only $2 \times 4 = 8$ components. The behavior of the amplitudes \mathbf{M} and \mathbf{V} under Lorentz transformations follows from the corresponding behavior of M and \bar{V} introduced in the last section. Introducing the operators $S(\Lambda)$, which represent the Lorentz transformations Λ on the Dirac subspace and satisfy

$$S^{-1}(\Lambda) \gamma^\mu S(\Lambda) = \Lambda^\mu{}_\nu \gamma^\nu \quad (2.17)$$

it follows that M and \bar{V} satisfy the transformation law

$$\begin{aligned} S_{\alpha\alpha_1}(\Lambda) S_{\beta\beta_1}(\Lambda) M_{\alpha_1\alpha_2,\beta_1\beta_2}(p,p';P) S_{\alpha_2\alpha'}^{-1}(\Lambda) S_{\beta_2\beta'}^{-1}(\Lambda) \\ = M_{\alpha\alpha',\beta\beta'}(\Lambda p, \Lambda p'; \Lambda P). \end{aligned} \quad (2.18)$$

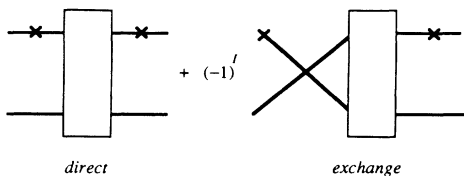


FIG. 9. Antisymmetrized potential (2.13), with direct and exchange terms.

In applications, this can be used to boost the M matrix to its c.m. frame, so that it is sufficient to carry out all numerical computations of M in the c.m. frame. The u spinors also have relatively simple transformation properties [35]

$$\begin{aligned} S(\Lambda) u(p'_1, \lambda) &= u(\Lambda p'_1, \lambda') D_{\lambda',\lambda}(R'_\Lambda), \\ \bar{u}(p_1, \lambda) S^{-1}(\Lambda) &= D_{\lambda,\lambda'}^\dagger(R_\Lambda) \bar{u}(\Lambda p_1, \lambda') \end{aligned} \quad (2.19)$$

where D are the representations of the rotations on the spin- $\frac{1}{2}$ space, λ and λ' are helicities, summed over when indices are repeated, and R_Λ and R'_Λ are the Wigner rotations, which depend on the four momenta p_1 (and p'_1) and transformation Λ , as follows:

$$R_\Lambda = H_{\Lambda p_1}^{-1} \Lambda H_{p_1}, \quad (2.20)$$

$$R'_\Lambda = H_{\Lambda p'_1}^{-1} \Lambda H_{p'_1}$$

Here H_{p_1} is the pure boost in the \hat{z} direction, following a rotation to the \hat{p}_1 direction which carries the four-vector $(m, \mathbf{0})$ into (E_{p_1}, \mathbf{p}_1) (see Appendix A). Using these relations, the transformation law for the \mathbf{M} and \mathbf{V} amplitudes is

$$\begin{aligned} S_{\beta\beta_1}(\Lambda) \mathbf{M}_{\lambda\lambda',\beta_1\beta_2}(p,p';P) S_{\beta_2\beta'}^{-1}(\Lambda) \\ = D_{\lambda\lambda_1}^\dagger(R_\Lambda) \mathbf{M}_{\lambda_1\lambda_2,\beta\beta'}(\Lambda p, \Lambda p'; \Lambda P) D_{\lambda_2\lambda'}(R'_\Lambda). \end{aligned} \quad (2.21)$$

The unitarity of the D matrices

$$D_{\lambda\lambda_1}(R_\Lambda) D_{\lambda'\lambda_1}^*(R_\Lambda) = \delta_{\lambda\lambda'} \quad (2.22)$$

and the covariance of the volume integration

$$\int \frac{d^3k}{2E_k} = \int d^4k \delta_+(m^2 - k^2) \quad (2.23)$$

ensure that Eq. (2.16) is covariant.

C. Relativistic wave functions

It is sometimes convenient to use relativistic wave functions instead of scattering amplitudes. Wave functions satisfy a homogeneous wave equation. In this paper, the relativistic *scattering* wave function will be defined only when the initial state is on shell, and only in the c.m. system in which case $E_{p'} = W/2$, and

$$\begin{aligned} \psi_{\lambda\beta}(p, p'; P) &= \frac{E_p}{m} (2\pi)^3 \delta^3(p - p') u_\beta(\mathbf{p}'_2, \lambda'_2) \delta_{\lambda\lambda'_1} \\ &\quad - G_{\beta\beta'}(p_2) \mathbf{M}_{\lambda\lambda'_1, \beta'\beta''}(p, p'; P) u_{\beta''}(\mathbf{p}'_2, \lambda'_2). \end{aligned} \quad (2.24)$$

Note that reference to the helicities of the initial on-shell particles (λ'_1 and λ'_2) has been suppressed in ψ . It is easy to see that ψ satisfies the homogeneous equation

$$\begin{aligned} G_{\beta\beta'}^{-1}(p_2) \psi_{\lambda\beta'}(p, p'; P) \\ = - \int \frac{d^3k}{(2\pi)^3} \frac{m}{E_k} \mathbf{V}_{\lambda\lambda', \beta\beta'}(p, k; P) \psi_{\lambda'\beta'}(k, p'; P). \end{aligned} \quad (2.25)$$

The relativistic deuteron wave function has been defined previously [20]; discussion of it will be included here

$$O_{\lambda_1\beta}^\mu(p, \overset{\circ}{P}) \xi_\mu(\lambda) = - \int \frac{d^3k}{(2\pi)^3} \frac{m}{E_k} \mathbf{V}_{\lambda_1\lambda, \beta\beta_1}(p, k; \overset{\circ}{P}) G_{\beta_1\beta_2}(k_2) O_{\lambda_2\beta_2}^\mu(k, \overset{\circ}{P}) \xi_\mu(\lambda) \quad (2.31)$$

where $\overset{\circ}{P} = (M_d, \mathbf{0})$ in the c.m. system. The relativistic deuteron wave function is defined to be

$$\psi_{\lambda_1\beta, \lambda}(p, \overset{\circ}{P}) = N G_{\beta, \beta'}(p_2) O_{\lambda_1\beta'}^\mu(p; P) \xi_\mu(\lambda) \quad (2.32)$$

and it satisfies Eq. (2.25), the same equation satisfied by the scattering wave function. The choice of normalization constant N will be discussed in the next section.

D. Unitarity and normalization

The unitarity relation for \mathbf{M} and the normalization of the bound state wave function (2.32) can be obtained directly from the fundamental equation (2.16). To this end it is convenient to suppress indices and write (2.16) in the compact form

$$\mathbf{M} = \mathbf{V} - \int \mathbf{V} G \mathbf{M}. \quad (2.33)$$

for completeness. It is assumed that the scattering amplitude \mathbf{M} develops a spin 1 pole at $P^2 = M_d^2$, so that it can be written

$$\begin{aligned} \mathbf{M}_{\lambda_1\lambda'_1, \beta\beta'}(p, p'; P) &= -O_{\lambda_1\beta}^\mu(p, P) \Delta_{\mu\nu}(P) O_{\lambda'_1\beta'}^{\nu\dagger}(p', P) \\ &\quad + R_{\lambda_1\lambda'_1, \beta\beta'}(p, p'; P) \end{aligned} \quad (2.26)$$

where $\Delta_{\mu\nu}$ is the deuteron propagator, which has a pole at $P^2 = M_d^2$, R is a remainder function nonsingular at the pole, and the deuteron vertex functions are

$$O_{\lambda_1\beta}^\mu(p, P) = \left[\Gamma^\mu(p, P) C \right]_{\beta\beta'} \bar{u}_{\beta'}^T(\mathbf{p}_1, \lambda_1) \quad (2.27)$$

with [20]

$$\Gamma^\mu(p, P) = F\gamma^\mu + \frac{G}{m} p^\mu - \frac{(m - \not{p}_2)}{m} \left(H\gamma^\mu + \frac{I}{m} p^\mu \right). \quad (2.28)$$

The four invariant functions F , G , H , and I are functions of p^2 and P^2 , but are uniquely defined only at the pole, where $P^2 = M_d^2$, and they become functions of p^2 only. The deuteron propagator is

$$\Delta_{\mu\nu}(P) = \left(g_{\mu\nu} - \frac{P_\mu P_\nu}{M_d^2} \right) \frac{1}{M_d^2 - P^2}. \quad (2.29)$$

At the deuteron pole, the projection operator reduces to a sum over the three helicity states of the deuteron.

$$\sum_\lambda \xi_\mu(\lambda) \xi_\nu^*(\lambda) = g_{\mu\nu} - \frac{P_\mu P_\nu}{M_d^2}. \quad (2.30)$$

Hence, substituting (2.26) into (2.16), and going to the pole gives a homogeneous equation for the deuteron vertex function

Equivalently, taking the Dirac conjugate of this equation gives

$$\bar{\mathbf{M}} = \mathbf{V} - \int \bar{\mathbf{M}} \bar{G} \mathbf{V} \quad (2.34)$$

where

$$\bar{\mathbf{M}}_{\lambda_1\lambda'_1, \beta\beta'}(p, p'; P) = \gamma^\circ_{\beta\beta_1} \mathbf{M}_{\lambda_1\lambda'_1, \beta_1\beta_2}^\dagger(p, p'; P) \gamma^\circ_{\beta_2\beta'}. \quad (2.35)$$

This operation has the effect of complex conjugating all of the invariant functions of which \mathbf{M} is constructed, but does not otherwise alter the structure of \mathbf{M} . For example, note that \bar{G}

$$\bar{G}(k_2) = \gamma^\circ \left[m + \not{k}_2^\dagger \right] \gamma^\circ = \frac{m + \not{k}_2}{m^2 - k_2^2 + i\epsilon} \quad (2.36)$$

differs from G only in the sign of the $i\epsilon$ prescription. It is assumed that the relativistic kernel is real so that $\bar{\mathbf{V}} = \mathbf{V}$.

Use (2.34) to eliminate \mathbf{V} under the integral in (2.33) and (2.33) to eliminate \mathbf{V} under the integral in (2.34). This gives the following two equations:

$$\mathbf{M} = \mathbf{V} - \int \bar{\mathbf{M}} G \mathbf{M} - \int \int \bar{\mathbf{M}} \bar{G} \mathbf{V} G \mathbf{M}, \quad (2.37)$$

$$\bar{\mathbf{M}} = \mathbf{V} - \int \bar{\mathbf{M}} \bar{G} \mathbf{M} - \int \int \bar{\mathbf{M}} \bar{G} \mathbf{V} G \mathbf{M}; \quad (2.38)$$

taking the difference of these two equations gives the unitarity relation

$$\bar{\mathbf{M}} - \mathbf{M} = - \int \bar{\mathbf{M}} \left[\bar{G} - G \right] \mathbf{M} = 2i \int \bar{\mathbf{M}} \Delta G \mathbf{M} \quad (2.39)$$

where

$$\bar{G} - G = -2i \Delta G = -2\pi i \delta(m^2 - k_2^2) 2m \Lambda(k_2). \quad (2.40)$$

Restoring the indicies and integrations gives explicitly

$$\bar{\mathbf{M}}_{\lambda_1 \lambda'_1, \beta \beta'}(p, p'; P) - \mathbf{M}_{\lambda_1 \lambda'_1, \beta \beta'}(p, p'; P)$$

$$= i \sqrt{\frac{W^2 - 4m^2}{4W^2}} m^2 \int \frac{d\Omega_{\mathbf{k}}}{(2\pi)^2} \bar{\mathbf{M}}_{\lambda_1 \lambda, \beta \beta_1}(p, \mathring{\mathbf{k}}; P) \Lambda_{\beta_1 \beta_2}(k_2) \mathbf{M}_{\lambda \lambda'_1, \beta_2 \beta'}(\mathring{\mathbf{k}}, p; P) \quad (2.41)$$

where the superscript \circ on relative four-momenta specifies that both particles are on shell, so that in the c.m. system

$$\mathring{\mathbf{k}} = (0, \mathbf{k}). \quad (2.42)$$

The normalization condition for the bound state wave function can also be obtained from the nonlinear Eq. (2.37). Substituting (2.26) into (2.37) gives terms which contain double poles at $P^2 = M_d^2$, and terms which contain single poles. The double pole terms all cancel because of the bound state Eq. (2.31). Similarly, the terms involving single poles and the terms in \mathbf{M} not singular at the pole also cancel. (These terms include contributions from the smooth remainder term R and derivatives of O with respect to P at $P^2 = M_d^2$.) However, cancellation of all single pole terms imposes a new condition on the vertex function O which depends on the propagator and the energy dependence of the kernel.

This condition arises from the requirement that the residue of the single pole on the left-hand-side (LHS) Eq. (2.37) must equal the residue of the pole on the right-hand side (RHS). Terms which contribute to the residue on the RHS come from the energy dependence of the propagator G and the potential \mathbf{V} near the pole. Expanding these around $P^2 = M_d^2$ gives

$$G(P) = G(\mathring{P}) + G'(\mathring{P})(P^2 - M_d^2) + \dots, \quad (2.43)$$

$$\mathbf{V}(P) = \mathbf{V}(\mathring{P}) + \mathbf{V}'(\mathring{P})(P^2 - M_d^2) + \dots$$

where

$$G'(\mathring{P}) = \left. \frac{P^\mu}{2P^2} \frac{\partial G}{\partial P_\mu} \right|_{P=\mathring{P}} \quad (2.44)$$

and similarly for \mathbf{V} . Substituting these expansions into (2.37) and equating residues gives

$$\begin{aligned} -1 &= \int \bar{\Gamma} G'(\mathring{P}) \Gamma + \int \int \bar{\Gamma} G'(\mathring{P}) \mathbf{V} G \Gamma \\ &+ \int \int \bar{\Gamma} G \mathbf{V}'(\mathring{P}) G \Gamma + \int \int \bar{\Gamma} G \mathbf{V} G'(\mathring{P}) \Gamma \end{aligned} \quad (2.45)$$

where Γ [not to be confused with the Γ of Eq. (2.28)] is a short representation for the deuteron vertex function (2.27)

$$\Gamma_{\lambda_1 \beta}^\lambda = O_{\lambda_1 \beta}^\mu \xi_\mu(\lambda), \quad (2.46)$$

$$\bar{\Gamma}_{\lambda_1 \beta}^\lambda = \xi_\mu^*(\lambda) O_{\lambda_1 \beta}^{\mu \dagger}$$

and, in this notation Eqs. (2.26) and (2.31) are

$$\mathbf{M} = - \frac{\Gamma \bar{\Gamma}}{M_d^2 - P^2} + R, \quad (2.47)$$

$$\Gamma = - \int \mathbf{V} G \Gamma.$$

Using the wave equation for Γ , and

$$G'(\mathring{P}) = G(\mathring{P}) \frac{\mathring{P}}{2M_d^2} G(\mathring{P}). \quad (2.48)$$

Equation (2.45) reduces to

$$1 = \int \bar{\Gamma} G \frac{\mathring{P}}{2M_d^2} G \Gamma - \int \int \bar{\Gamma} G \mathbf{V}'(\mathring{P}) G \Gamma. \quad (2.49)$$

In expanded form, and expressed in terms of the relativistic wave function defined in (2.32), this becomes

$$\begin{aligned} \delta_{\lambda\lambda'} = & \int d^3p \frac{m}{E_p} \bar{\psi}_{\lambda_1\beta\lambda}(p, \overset{\circ}{P}) \frac{\overset{\circ}{\mathbf{R}}_{\beta\beta'}}{M_d} \psi_{\lambda_1\beta'\lambda'}(p, \overset{\circ}{P}) \\ & - 2M_d \int \frac{d^3p d^3p'}{(2\pi)^3} \frac{m^2}{E_p E_{p'}} \bar{\psi}_{\lambda_1\beta\lambda}(p; \overset{\circ}{P}) \mathbf{V}'_{\lambda_1\lambda'_1, \beta\beta'}(p, p'; \overset{\circ}{P}) \psi_{\lambda'_1\beta'\lambda'}(p'; \overset{\circ}{P}) \end{aligned} \quad (2.50)$$

where the normalization constant was chosen to be

$$N = \left[2M_d(2\pi)^3 \right]^{-\frac{1}{2}}. \quad (2.51)$$

Note that the normalization condition (2.50) is covariant, and that it involves the derivative of the potential with respect to P . This condition will be further reduced below.

E. The relativistic \mathbf{R} matrix

For applications to scattering problems it is convenient to introduce a reduced matrix (which will be called \mathbf{R}) which is real. The \mathbf{R} matrix will be defined in such a way that it satisfies the same equation (2.16) satisfied by \mathbf{M} , but with the elastic cut removed. The equation for \mathbf{R} , in the compact notation of Sec. IID, is

$$\mathbf{R} = \mathbf{V} - \mathcal{P} \int \mathbf{V} G \mathbf{R} \quad (2.52)$$

where \mathcal{P} represents the principal value of the integral, so that

$$\int \mathbf{V} G \mathbf{M} = \mathcal{P} \int \mathbf{V} G \mathbf{M} + i \int \mathbf{V} \Delta G \mathbf{M} \quad (2.53)$$

where ΔG was defined in Eq. (2.40). Next, \mathbf{M} is constructed from \mathbf{R} by the operation $O_M(\mathbf{R})$

$$\mathbf{M} = O_M(\mathbf{R}) = \mathbf{R} - i \int \mathbf{R} \Delta G \mathbf{M} \quad (2.54)$$

which is carried out on the variables of the initial state. Applying this operation to Eq. (2.52) gives

$$O_M(\mathbf{R}) = O_M(\mathbf{V}) - \mathcal{P} \int \mathbf{V} G O_M(\mathbf{R}) \quad (2.55)$$

or, using (2.53)

$$\begin{aligned} \mathbf{M} &= \mathbf{V} - i \int \mathbf{V} \Delta G \mathbf{M} - \mathcal{P} \int \mathbf{V} G \mathbf{M} \\ &= \mathbf{V} - \int \mathbf{V} G \mathbf{M}. \end{aligned} \quad (2.56)$$

Since the solution of the (2.16) is unique, this procedure of constructing \mathbf{M} from \mathbf{R} which solves (2.52) necessarily gives the correct scattering matrix.

Furthermore, it can be confirmed that \mathbf{M} determined

$$M_{\lambda_1\lambda'_1, \lambda_2\lambda'_2}^{\rho\rho'}(p, p'; P) = V_{\lambda_1\lambda'_1, \lambda_2\lambda'_2}^{\rho\rho'}(p, p'; P) - \int \frac{d^3k}{(2\pi)^3} \left\{ V_{\lambda_1\mu_1, \lambda_2\mu_2}^{\rho\rho''}(p, k; P) G^{\rho''}(k) M_{\mu_1\lambda'_1, \mu_2\lambda'_2}^{\rho''\rho'}(k, p'; P) \right\} \quad (2.60)$$

where summation on the RHS is over repeated indicies and ρ, ρ' , and ρ'' take on the values $+$ or $-$ corresponding to

from (2.54) satisfies the unitarity relation provided only that \mathbf{R} is real ($\mathbf{R}=\bar{\mathbf{R}}$). To prove this result, first observe that $\bar{\mathbf{M}}$ is also given by \mathbf{R}

$$\bar{\mathbf{M}} = \mathbf{R} + i \int \bar{\mathbf{M}} \Delta G \mathbf{R}. \quad (2.57)$$

Substituting (2.57) into (2.54), and (2.54) into (2.57) gives

$$\mathbf{M} = \mathbf{R} - i \int \bar{\mathbf{M}} \Delta G \mathbf{M} - \int \int \bar{\mathbf{M}} \Delta G \mathbf{R} \Delta G \mathbf{M}, \quad (2.58)$$

$$\bar{\mathbf{M}} = \mathbf{R} + i \int \bar{\mathbf{M}} \Delta G \mathbf{M} - \int \int \bar{\mathbf{M}} \Delta G \mathbf{R} \Delta G \mathbf{M}.$$

Subtracting the two equations yields the unitarity relation (2.39).

The relation between \mathbf{R} and \mathbf{M} can be simplified after the partial wave expansions have been introduced. However, the full relation (2.54) may be useful in applications.

F. Separation of channels

It is now time to separate the four degrees of freedom of the off-shell particle (which will be particle 2) into two channels, each with only two degrees of freedom. The means of carrying out this separation is through use of the familiar identity for the nucleon propagator, which in the c.m. frame of the pair becomes

$$G_2(k_2) = \frac{m}{E_k} \sum_{\lambda_2} \left\{ \frac{u(-\mathbf{k}, \lambda_2) \bar{u}(-k, \lambda_2)}{(2E_k - W)} - \frac{v(\mathbf{k}, \lambda_2) \bar{v}(k, \lambda_2)}{W} \right\} \quad (2.59)$$

where k_2 and W are as defined in Eq. (2.2). Note that this decomposition breaks the manifest covariance of the theory; the mixing between u and v spinors defined in (2.59) is frame dependent. Because of this, most of the expressions obtained in the rest of this part will not be manifestly Lorentz invariant, and it is for this reason that separation into channels is delayed as long as possible. All separations will be carried out in the c.m. frame of the pair, where the expressions are simplest.

Channels involving u (v) spinor degrees of freedom of the off-shell particle will be referred to as $+$ ($-$) channels. Using (2.59), Eq. (2.16) reduces to two coupled equations

the two channels involved. These are directly related to the ρ spin indicies introduced originally by Kubis [39], except that in Eq. (2.60) an index is needed *only* for the off-shell particle; the on-shell particle is always in the + state. The λ 's and μ 's refer to helicity states; the Kubis convention will be used here, and is described in Appendix A. The propagators for each ρ spin channel are

$$G^+(k) = \frac{1}{2E_k - W - i\epsilon}, \quad G^-(k) = -\frac{1}{W}. \quad (2.61)$$

These M and V amplitudes (not to be confused with the M and V amplitudes introduced in Sec. II A above) are related to the relativistic amplitudes \mathbf{M} and \mathbf{V} defined in (2.15) by

$$V_{\lambda_1 \lambda'_1 \lambda_2 \lambda'_2}^{++}(p, p'; P) = \left(\frac{m^2}{E_p E'_p} \right) \bar{u}_\beta(-p, \lambda_2) \mathbf{V}_{\lambda_1 \lambda'_1, \beta \beta'}(p_1 p'; P) u_{\beta'}(-p', \lambda'_2), \quad (2.62)$$

$$V_{\lambda_1 \lambda'_1 \lambda_2 \lambda'_2}^{-+}(p, p'; P) = \left(\frac{m^2}{E_p E'_p} \right) \bar{v}_\beta(p, \lambda_2) \mathbf{V}_{\lambda_1 \lambda'_1, \beta \beta'}(p, p'; P) u_{\beta'}(-p', \lambda'_2)$$

and similarly for V^{+-} and V^{--} in cases where the initial channel involves a $v(p', \lambda'_2)$ spinor.

Note that the equations (2.60) have a form similar to nonrelativistic equations except for the presence of the relativistic energy E_k in the propagator G^+ and for the presence of the extra (-) channel, which arises from the coupling to the v spinors required by relativity. Otherwise, the equations are identical to what would arise in a nonrelativistic limit of (2.60), and this will be discussed in Sec. II G below.

The relativistic wave functions, unitarity relation, and normalization condition all take on simple forms when re-expressed in terms of the coupled (+, -) channels. The relativistic scattering wave functions become, in the c.m. system,

$$\psi_{\lambda\beta}(p, p'; P) = \frac{W}{2m} \left[\psi_{\lambda\lambda'}^+(p, p'; P) u_\beta(-\mathbf{p}, \lambda') + \psi_{\lambda\lambda'}^-(p, p'; P) v_\beta(\mathbf{p}, \lambda') \right] \quad (2.63)$$

where

$$\psi_{\lambda\lambda'}^+(p, p'; P) = (2\pi)^3 \delta^3(p - p') \delta_{\lambda\lambda'} \delta_{\lambda'\lambda'_2} - \frac{M_{\lambda\lambda'_1, \lambda'\lambda'_2}^{++}(p, p'; P)}{(2E_p - W - i\epsilon)}, \quad (2.64)$$

$$\psi_{\lambda\lambda'}^-(p, p'; P) = \frac{1}{W} M_{\lambda\lambda'_1, \lambda'\lambda'_2}^{-+}(p, p'; P).$$

The homogeneous equations satisfied by these wave functions are

$$(2E_p - W) \psi_{\lambda\lambda'}^+(p, p'; P) = - \int \frac{d^3k}{(2\pi)^3} V_{\lambda\lambda'_1, \lambda'\lambda'_2}^{+\rho}(p, k; P) \psi_{\lambda_1 \lambda_2}^\rho(k, p'; P), \quad (2.65)$$

$$-W \psi_{\lambda\lambda'}^-(p, p'; P) = - \int \frac{d^3k}{(2\pi)^3} V_{\lambda\lambda'_1, \lambda'\lambda'_2}^{-\rho}(p, k; P) \psi_{\lambda_1 \lambda_2}^\rho(k, p'; P).$$

Similarly, the bound state wave function is

$$\psi_{\lambda_1 \beta, \lambda}(p, \mathring{P}) = \psi_{\lambda_1 \lambda_2, \lambda}^+(p, \mathring{P}) u_\beta(-\mathbf{p}, \lambda_2) + \psi_{\lambda_1 \lambda_2, \lambda}^-(p, \mathring{P}) v_\beta(\mathbf{p}, \lambda_2) \quad (2.66)$$

where summation over λ_2 is implied, and using the normalization constant Eq. (2.51)

$$\psi_{\lambda_1 \lambda_2, \lambda}^+(p, \mathring{P}) = \frac{m}{\sqrt{(2\pi)^3 2M_d}} \frac{\bar{u}_\beta(-\mathbf{p}, \lambda_2) O_{\lambda_1 \beta}^\mu(p, \mathring{P}) \xi_\mu(\lambda)}{E_p (2E_p - M_d)}, \quad (2.67)$$

$$\psi_{\lambda_1 \lambda_2, \lambda}^-(p, \mathring{P}) = - \frac{m}{\sqrt{(2\pi)^3 2M_d}} \frac{\bar{v}_\beta(\mathbf{p}, \lambda_2) O_{\lambda_1 \beta}^\mu(p, \mathring{P}) \xi_\mu(\lambda)}{E_p M_d}.$$

This definition is identical to that previously used in Buck and Gross [20], and these wave functions satisfy the same coupled equations (2.65).

The unitarity relation, expressed in terms of the \pm amplitudes, becomes

$$\text{Im } M_{\lambda_1 \lambda'_1, \lambda_2 \lambda'_2}^{++}(p, p'; P) = -\kappa \int \frac{d\Omega_k}{(2\pi)^2} M_{\lambda_1 \lambda, \lambda_2 \lambda'}^{++*}(p, k; P) M_{\lambda \lambda'_1, \lambda' \lambda'_2}^{++}(k, p'; P), \quad (2.68)$$

$$\text{Im } M_{\lambda_1 \lambda'_1, \lambda_2 \lambda'_2}^{-+}(p, p'; P) = -\kappa \int \frac{d\Omega_k}{(2\pi)^2} M_{\lambda_1 \lambda, \lambda_2 \lambda'}^{-+*}(p, k; P) M_{\lambda \lambda'_1, \lambda' \lambda'_2}^{-+}(k, p'; P)$$

where

$$\kappa = \frac{1}{16} \sqrt{W^2(W^2 - 4m^2)}. \quad (2.69)$$

Note that the phase of M^{-+} is completely determined by M^{++} . This is because M^{-+} does not propagate to infinity (in position space), or have the elastic unitarity cut (in momentum space).

Next, the normalization condition also takes a simple form in the coupled channel representation. Using the relations

$$\bar{u}(-\mathbf{p}, \lambda) \gamma^0 u(-\mathbf{p}, \lambda') = \bar{v}(\mathbf{p}, \lambda) \gamma^0 v(\mathbf{p}, \lambda') = \frac{E_p}{m} \delta_{\lambda \lambda'}, \quad (2.70)$$

$$\bar{u}(-\mathbf{p}, \lambda) \gamma^0 v(\mathbf{p}, \lambda') = \bar{v}(\mathbf{p}, \lambda') \gamma^0 u(-\mathbf{p}, \lambda) = 0,$$

gives

$$\delta_{\lambda \lambda'} = \int d^3 p \psi_{\lambda_1 \lambda_2, \lambda}^{\rho*}(p, \overset{\circ}{P}) \psi_{\lambda_1 \lambda_2, \lambda'}^{\rho}(p, \overset{\circ}{P}) - \int \int \frac{d^3 p d^3 p'}{(2\pi)^3} \psi_{\lambda_1 \lambda_2, \lambda}^{\rho*}(p, \overset{\circ}{P}) \frac{\partial}{\partial M_d} V_{\lambda_1 \lambda'_1, \lambda_2 \lambda'_2}^{\rho \rho'}(p, p'; \overset{\circ}{P}) \psi_{\lambda'_1 \lambda'_2, \lambda'}^{\rho'}(p'; \overset{\circ}{P}) \quad (2.71)$$

where sums over repeated indices are implied. Note that, if the potential is independent of M_d , the ψ^+ and ψ^- wave functions are orthogonal. Finally, the relativistic \mathbf{R} matrix can also be decomposed into (+, -) channels. The $R^{\rho+}$ matrix elements are constructed from \mathbf{R} as in (2.62) and satisfy Eq. (2.60) with the integrals replaced by principal values. The $M^{\rho+}$ matrix is related to $R^{\rho+}$ by

$$M_{\lambda_1 \lambda'_1, \lambda_2 \lambda'_2}^{\rho+}(p, p'; P) = R_{\lambda_1 \lambda'_1, \lambda_2 \lambda'_2}^{\rho+}(p, p'; P) - i\kappa \int \frac{d\Omega_k}{(2\pi)^2} R_{\lambda_1 \lambda, \lambda_2 \lambda'}^{\rho+}(p, k; P) M_{\lambda \lambda'_1, \lambda' \lambda'_2}^{++}(k, p'; P) \quad (2.72)$$

where $\rho = \pm$. This shows that the phase of the half off-shell M matrix is determined by the on-shell M matrix.

G. Nonrelativistic limits

The separation into channels puts the equations into a form ideal for taking nonrelativistic limits. In the extreme nonrelativistic limit, where all terms of order p^2/m^2 are neglected, the coupled equations (2.60) reduce to a single equation for M^{++} only:

$$M^{++} = V^{++} - m \int \frac{d^3 k}{(2\pi)^3} \frac{V^{++} M^{++}}{k^2 - k_o^2 - i\epsilon} \quad (2.73)$$

where

$$k_o^2 = m(2m - W) \quad (2.74)$$

is the square of the nonrelativistic on-shell momentum.

If terms of order p^2/m^2 are retained, but higher order terms ignored, the (-) channel will make a contribution. If all of the potentials V^{++} , V^{+-} , $(V^{-+})^\dagger$, and V^{--} are considered to be of the same order in p^2/m^2 (a debatable assumption), then it follows that

$$M^{-+} \simeq M^{++} \quad (2.75)$$

and the contribution of the M^{-+} term to M^{++} need be included only in leading order. Hence the equations

become

$$M^{++} = V^{++} - \int \frac{d^3 k}{(2\pi)^3} m \left\{ \frac{V^{++} M^{++}}{k^2 - k_o^2 - \frac{k^4}{4m^2} - i\epsilon} - \frac{V^{+-} M^{-+}}{2m^2} \right\}, \quad (2.76)$$

$$M^{-+} = V^{-+} - \int \frac{d^3 k}{(2\pi)^3} m \frac{V^{-+} M^{++}}{k^2 - k_o^2 - i\epsilon}.$$

The second equation can be used to eliminate M^{-+} from the first, giving an equation for M^{++} alone:

$$M^{++} = V_{\text{eff}}^{++} - \int \frac{d^3 k}{(2\pi)^3} m \frac{V_{\text{eff}}^{++} M^{++}}{k^2 - k_o^2 - \frac{k^4}{4m^2} - i\epsilon} \quad (2.77)$$

where

$$V_{\text{eff}}^{++} = V^{++} + \int \frac{d^3 k}{(2\pi)^3} \frac{V^{+-}(V^{-+})^\dagger}{2m}. \quad (2.78)$$

This shows that the V^{+-} terms add, to the diagonal elements of V^{++} , the short range repulsion [8] discussed in Part I.

If position space wave functions and potentials are defined by the relations

$$V(r) = \frac{1}{(2\pi)^3} \int d^3q e^{i\mathbf{q}\cdot\mathbf{r}} V(q), \quad (2.79)$$

$$\psi(r) = \frac{1}{(2\pi)^{3/2}} \int d^3p e^{i\mathbf{p}\cdot\mathbf{r}} \psi(p)$$

where it is assumed that V is local in the nonrelativistic limit, so that $V(p, p'; P) = V(p - p')$, then the equations (2.65) for the wave functions assume a very simple and transparent structure:

$$\left(\frac{\nabla^2}{m} - \epsilon + \frac{\nabla^4}{4m^2} \right) \psi^+(r) = V^{++}(r) \psi^+(r) + V^{+-}(r) \psi^-(r), \quad (2.80)$$

$$(2m + \epsilon) \psi^-(r) = V^{-+}(r) \psi^+(r) + V^{--}(r) \psi^-(r)$$

where $\epsilon \equiv W - 2m$, and the V^{--} potential has been retained for completeness even though it probably should be neglected when working to order p^2/m^2 . To order p^2/m^2 , the solution to this coupled set of equations is

$$\left(\frac{\nabla^2}{m} - \epsilon + \frac{\nabla^4}{4m^2} \right) \psi^+(r) = V_{\text{eff}}(r) \psi^+(r), \quad (2.81)$$

$$\psi^-(r) = \frac{V^{-+}}{2m} \psi^+(r)$$

where

$$V_{\text{eff}}(r) = V^{++}(r) + \frac{V^{+-}(r) V^{-+}(r)}{2m}. \quad (2.82)$$

These equations provide the intuitive interpretation of the role of the V^{+-} , and will be used in subsequent work to interpret results.

H. Partial wave expansions

The equations can be further reduced by introducing partial wave expansions for the helicity amplitudes. The procedure of Jacob and Wick [40] will be followed here, and many details can be found in Appendix A.

One advantage of the separation into \pm channels introduced in Sec. F is that the structure of the partial wave expansion is independent of ρ and ρ' in $V^{\rho\rho'}$. Hence, these ρ spin indices will be suppressed whenever it is convenient to do so.

The partial wave expansion for all amplitudes (V or M) is

$$V_{\lambda_1 \lambda'_1, \lambda_2 \lambda'_2}(p, k; P) = \sum_{J, M} \langle \hat{\mathbf{p}} | JM \lambda_1 \lambda_2 \rangle V_{\lambda_1 \lambda'_1, \lambda_2 \lambda'_2}^J(p, k; P) \langle JM \lambda'_1 \lambda'_2 | \hat{\mathbf{k}} \rangle \quad (2.83)$$

where the partial wave amplitudes V^J depend only on the magnitudes of \mathbf{p} and \mathbf{k} and not on directions. The coupling coefficients are as introduced in Jacob and Wick

$$\langle \hat{\mathbf{p}} | JM \lambda_1 \lambda_2 \rangle = \sqrt{\frac{2J+1}{4\pi}} D_{M\lambda}^{J*}(\phi, \theta, -\phi) = \sqrt{\frac{2J+1}{4\pi}} e^{i(M-\lambda)\phi} d_{M\lambda}^J(\theta) \quad (2.84)$$

where $\lambda = \lambda_1 - \lambda_2$. [The λ dependence of the states $|\hat{\mathbf{p}} \lambda_1 \lambda_2 \rangle$ has been suppressed in (2.84) for convenience.] If the scattering is restricted to the x - z plane, then $\phi = 0$ and

$$V_{\lambda_1 \lambda'_1, \lambda_2 \lambda'_2}(p, k; P) = \frac{1}{4\pi} \sum_J (2J+1) d_{\lambda'_1 \lambda}^J(\theta) V_{\lambda_1 \lambda'_1, \lambda_2 \lambda'_2}^J(p, k; P) \quad (2.85)$$

where use was made of the addition theorem for the d 's:

$$d_{\lambda'_1 \lambda}^J(\theta) = \sum_M D_{M\lambda}^{J*}(\Omega_{\hat{\mathbf{p}}}) D_{M\lambda'}^J(\Omega_{\hat{\mathbf{k}}}) \quad (2.86)$$

and the compact notation $\Omega_{\hat{\mathbf{p}}}$ will sometimes be used for the arguments $(\phi_p, \theta_p, -\phi_p)$ of the D 's. Using both expansions (2.83) and (2.85), the addition theorem (2.86), and the orthogonality relation

$$\int d\Omega_k D_{M'\lambda'}^{J'*}(\Omega_k) D_{M\lambda}^J(\Omega_k) = \frac{4\pi}{2J+1} \delta_{JJ'} \delta_{MM'} \quad (2.87)$$

the coupled equations (2.60) can be separated,

$$M_{\lambda_1 \lambda'_1, \lambda_2 \lambda'_2}^{\rho\rho' J}(p, p'; P) = V_{\lambda_1 \lambda'_1, \lambda_2 \lambda'_2}^{\rho\rho' J} - \int_0^\infty dk V_{\lambda_1 \mu_1, \lambda_2 \mu_2}^{\rho\rho'' J}(p, k; P) g^{\rho''}(k) M_{\mu_1 \lambda'_1, \mu_2 \lambda'_2}^{\rho''\rho' J}(k, p'; P) \quad (2.88)$$

where there is *no* summation over J on the RHS, and the reduced propagators are

$$g^+(k) = \frac{1}{(2\pi)^3} \left(\frac{k^2}{2E_k - W} \right), \quad g^-(k) = -\frac{1}{(2\pi)^3} \left(\frac{k^2}{W} \right). \quad (2.89)$$

The equations (2.88) will be further reduced in the next section.

The partial wave expansion also simplifies the unitarity relation and the connection between the M matrix and the R matrix. The unitarity relations (2.68) for partial wave amplitudes become

$$\text{Im } M_{\lambda_1 \lambda'_1, \lambda_2 \lambda'_2}^{++J}(p, p'; P) = -\frac{k E_k}{(4\pi)^2} M_{\lambda_1 \bar{\lambda}_1, \lambda_2 \lambda'_2}^{++J*}(p, k; P) M_{\lambda \lambda'_1, \lambda' \lambda'_2}^{++J}(k, p'; P), \quad (2.90)$$

$$\text{Im } M_{\lambda_1 \lambda'_1, \lambda_2 \lambda'_2}^{-+J}(p, p'; P) = -\frac{k E_k}{(4\pi)^2} M_{\lambda_1 \bar{\lambda}_1, \lambda_2 \lambda'_2}^{-+J*}(p, k; P) M_{\lambda \lambda'_1, \lambda' \lambda'_2}^{-+J}(k, p'; P).$$

For *on-shell*, *uncoupled* amplitudes, the relations determine $M^{++J}(k)$

$$M^{++J}(k) = -\frac{(4\pi)^2}{k E_k} e^{i\delta_J} \sin \delta_J. \quad (2.91)$$

Applying this to *uncoupled* amplitudes with the initial state on shell gives

$$M^{++J}(p, k; P) = -|M^{++J}(p, k; P)| e^{i\delta_J}, \quad (2.92)$$

$$M^{-+J}(p, k; P) = -|M^{-+J}(p, k; P)| e^{i\delta_J}.$$

For coupled amplitudes the phases can also be determined by matrix inversion.

The relations for the R matrix also simplify. If the initial state is on-shell, the general relations are

$$\begin{aligned} M_{\lambda_1 \lambda'_1, \lambda_2 \lambda'_2}^{\rho+J}(p, k; P) \\ = R_{\lambda_1 \lambda'_1, \lambda_2 \lambda'_2}^{\rho+J}(p, k; P) \\ - i \frac{k E_k}{(4\pi)^2} R_{\lambda_1 \lambda, \lambda_2 \lambda'}^{\rho+J}(p, k; P) M_{\lambda \lambda'_1, \lambda' \lambda'_2}^{++J}(k). \end{aligned} \quad (2.93)$$

Again, if the amplitudes are *uncoupled* (2.93) has a simple solution

$$R^{\rho+J}(p, k; P) = \frac{M^{\rho+J}(p, k; P)}{1 + i e^{i\delta_J} \sin \delta_J} = - \left| \frac{M^{\rho+J}(p, k; P)}{\cos \delta_J} \right|. \quad (2.94)$$

In particular, for *uncoupled* channels,

$$R^{++J}(k) = -\frac{(4\pi)^2}{k E_k} \tan \delta_J. \quad (2.95)$$

I. Classification of states and block diagonalization of the equations

The equations (2.88) can be further reduced and simplified by identifying combinations of helicity amplitudes which have definite parity and interchange symmetry. In

Appendix A it is shown that the phases can be chosen so that the states $|JM\lambda_1\lambda_2\rangle$ transform under the parity operation \mathcal{P} as follows

$$\mathcal{P}|JM\lambda_1\lambda_2\rangle_{\pm} = \epsilon'(-1)^{J-1}|JM-\lambda_1-\lambda_2\rangle_{\pm} \quad (2.96)$$

where the subscript \pm refers to the $+$ channel (with two u spinors) or the $-$ channel (with one u and one v spinor). The extra phase on the RHS of (2.96), ϵ' , is a consequence of the odd parity of the v spinor, and is $+$ for $(+)$ channels and $-$ for $(-)$ channels. Similarly under interchange of the two particles, carried out by the exchange operator \mathcal{P}_{12} , the phases are chosen so that

$$\mathcal{P}_{12}|JM\lambda_1\bar{\lambda}_2\rangle_{\pm} = (-1)^{J-1}|JM\bar{\lambda}_2\lambda_1\rangle_{\pm} \quad (2.97)$$

where the bar over λ_2 is used to mean that the helicity of the particle is λ_2 , but that it is off-shell. Since the u spinors are the same for both on-shell and off-shell particles, this distinction is sometimes necessary only for $(-)$ channels, where the bar will locate the position of the v spinor. Hence, following Kubis, two combinations of $(-)$ channel states occur, referred to as even (e) and odd (o)

$$\begin{aligned} |\lambda_1\lambda_2\rangle_{e,o} &= \frac{1}{\sqrt{2}} [|\lambda_1\bar{\lambda}_2\rangle_{-} \pm |\bar{\lambda}_1\lambda_2\rangle_{-}] \\ &\sim \frac{1}{\sqrt{2}} [u_{\alpha}(\lambda_1)v_{\beta}(\lambda_2) \pm v_{\alpha}(\lambda_1)u_{\beta}(\lambda_2)]. \end{aligned} \quad (2.98)$$

Note in particular that the odd state is not zero, and that the phase of the interchange operation is the same for $(+)$ and $(-)$ channels.

It is convenient to view the two terms which compose \bar{V} in Eq. (2.13) as a direct and an exchange piece, as illustrated in Fig. 9. Then the interchange operation (2.97) can be used to express the helicity amplitudes in terms of the direct part only. Simplifying the notation for the partial wave helicity amplitudes introduced in (2.85),

$$V_{\lambda_1 \lambda'_1, \lambda_2 \lambda'_2}^J(p, k; P) = \langle \lambda_1 \lambda_2 | V^J | \lambda'_1 \lambda'_2 \rangle \quad (2.99)$$

it follows that

$$\begin{aligned} \langle \lambda_1 \lambda_2 | V^J | \lambda'_1 \lambda'_2 \rangle &= \frac{1}{2} \left[\langle \lambda_1 \bar{\lambda}_2 | V_{\text{direct}}^J | \lambda'_1 \lambda'_2 \rangle + (-1)^I \langle \lambda_1 \bar{\lambda}_2 | V_{\text{exchange}}^J | \lambda'_1 \lambda'_2 \rangle \right] \\ &= \frac{1}{2} \left[\langle \lambda_1 \bar{\lambda}_2 | V_{\text{direct}}^J | \lambda'_1 \lambda'_2 \rangle + (-1)^{J+I-1} \langle \bar{\lambda}_2 \lambda_1 | \hat{V}_{\text{direct}}^J | \lambda'_1 \lambda'_2 \rangle \right] \end{aligned} \quad (2.100)$$

where the notation \widehat{V}^J will be used to denote direct amplitudes in which particle 2 in the final state is on-shell. These are obtained from V by changing $p_o \rightarrow -p_o$. (The proof of this relation is given in Appendix A.) The exchange term with particle 1 on-shell has been expressed in terms of the direct term with particle 2 on-shell (referred to as “alternating” contributions), thus “uncrossing” the final nucleon lines, as illustrated in Fig. 10. The advantage of this operation is that all potentials may now be expressed in terms of the direct term only.

Next, the parity relations may be used to reduce the number of independent helicity amplitudes from 16 to 8. Since only the direct amplitudes are needed, these 8 amplitudes will be denoted

$$\begin{aligned} \phi_1 &= \langle ++ | V_{\text{direct}}^J | ++ \rangle = \epsilon \langle -- | V_{\text{direct}}^J | -- \rangle, \\ \phi_2 &= \langle ++ | V_{\text{direct}}^J | -- \rangle = \epsilon \langle -- | V_{\text{direct}}^J | ++ \rangle, \\ \phi_3 &= \langle +- | V_{\text{direct}}^J | +- \rangle = \epsilon \langle -+ | V_{\text{direct}}^J | -+ \rangle, \\ \phi_4 &= \langle +- | V_{\text{direct}}^J | -+ \rangle = \epsilon \langle -+ | V_{\text{direct}}^J | +- \rangle, \end{aligned} \quad (2.101)$$

$$\begin{aligned} \phi_5 &= \langle ++ | V_{\text{direct}}^J | +- \rangle = \epsilon \langle -- | V_{\text{direct}}^J | -+ \rangle, \\ \phi_6 &= \langle +- | V_{\text{direct}}^J | ++ \rangle = \epsilon \langle -+ | V_{\text{direct}}^J | -- \rangle, \\ \phi_7 &= \langle ++ | V_{\text{direct}}^J | -+ \rangle = \epsilon \langle -- | V_{\text{direct}}^J | +- \rangle, \\ \phi_8 &= \langle -+ | V_{\text{direct}}^J | ++ \rangle = \epsilon \langle +- | V_{\text{direct}}^J | -- \rangle, \end{aligned}$$

where ϵ is $+$ for V^{++} and V^{--} potentials, and $-$ for V^{+-} and V^{-+} potentials.

These parity relations, and the relations (2.100) obtained using the particle interchange operation, may be

$$\begin{aligned} v_i &= \frac{1}{2} \{ \langle \lambda_1 \bar{\lambda}_2 | V_{\text{direct}}^J | \lambda'_1 \lambda'_2 \rangle + \delta_1 \langle \lambda_1 \bar{\lambda}_2 | V_{\text{direct}}^J | -\lambda'_1 -\lambda'_2 \rangle \\ &\quad + \delta_2 (\langle \bar{\lambda}_1 \lambda_2 | \widehat{V}_{\text{direct}}^J | \lambda'_1 \lambda'_2 \rangle + \delta_1 \langle \bar{\lambda}_1 \lambda_2 | \widehat{V}_{\text{direct}}^J | -\lambda'_1 -\lambda'_2 \rangle) \}. \end{aligned} \quad (2.102)$$

If the *final state is a plus channel*, this expression shows that the phase under change of sign of p_o is δ_2 . In particular, if $\delta_2 = -1$, the amplitude will be zero on shell where $p_o = 0$. If the *final state is a minus channel*, the amplitude has no definite symmetry under $p_o \rightarrow -p_o$ because of (2.98), but when $p_o = 0$ it couples to only *one* of the two linear combinations $|\lambda_1 \lambda_2 \rangle_{e,o}$ depending on

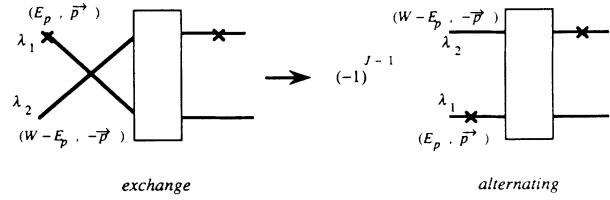


FIG. 10. Diagrammatic representation of how the exchange diagram with particle 1 on-shell is transformed into a direct diagram with particle 2 on-shell (referred to as an “alternating” diagram).

used to decouple the original equations into three distinct channels. Amplitudes in which particle one is on-shell in the final state will be denoted by ϕ_i as in Eq. (2.101), while those in which particle two in the final state is on-shell will be denoted by $\widehat{\phi}_i$, and are obtained from ϕ_i by letting $p_o \rightarrow -p_o$.

Instead of using linear combinations like (2.100), it was easier to program the 16 amplitudes given in Table VI. These amplitudes all have definite symmetries under parity and particle interchange, as shown in the Table, and these symmetries permit the recovery of the correct combination for each channel (to be described below). They also have certain properties on-shell, when the relative energy in the initial or final state is zero. These properties are summarized in Table VI and will be explained now.

The general form of any v_i in Table VI is

whether $\delta_2 = +1$ (e) or -1 (o). The combination which survives is given in Table VI; note that such amplitudes are not necessarily zero on-shell.

Determination of the behavior under interchange $k_o \rightarrow -k_o$ of the initial relative energy follows from the reflection symmetry given in Eq. (2.9), and in some cases, the use of parity. For amplitudes with $\lambda_1 = \lambda_2$, reflection

TABLE VI. The 16 independent amplitudes for which the final equations are constructed.

Amplitudes $v_i(p_o, k_o)$	Symmetries ($\eta = (-)^{J-1}$)															
	\mathcal{P}	V^{++}				\mathcal{P}	V^{+-}				\mathcal{P}	V^{--}				
		\mathcal{P}_{12}	p_o	k_o		\mathcal{P}_{12}	p_o	k_o		\mathcal{P}_{12}	p_o	k_o		\mathcal{P}_{12}	p_o	k_o
$v_1 = \frac{1}{2}(\phi_1 - \phi_2) \pm \frac{1}{2}(\widehat{\phi}_1 - \widehat{\phi}_2)$	$-\eta$	$\pm\eta$	\pm	\pm	$+\eta$	$\pm\eta$	\pm	e	$-\eta$	$\pm\eta$	e	\pm	$+\eta$	$\pm\eta$	e	e
$v_5 = \frac{1}{2}(\phi_3 - \phi_4) \pm \frac{1}{2}(\widehat{\phi}_3 - \widehat{\phi}_4)$	$-\eta$	$\mp\eta$	\pm	\pm	$+\eta$	$\pm\eta$	\pm	o	$-\eta$	$\pm\eta$	o	\mp	$+\eta$	$\mp\eta$	o	o
$v_2 = \frac{1}{2}(\phi_5 - \phi_7) \pm \frac{1}{2}(\widehat{\phi}_5 - \widehat{\phi}_7)$	$-\eta$	$\pm\eta$	\pm	\mp	$+\eta$	$\pm\eta$	\pm	o	$-\eta$	$\pm\eta$	o	\mp	$+\eta$	$\pm\eta$	o	o
$v_7 = \frac{1}{2}(\phi_6 - \phi_8) \pm \frac{1}{2}(\widehat{\phi}_6 - \widehat{\phi}_8)$	$-\eta$	$\mp\eta$	\pm	\mp	$-\eta$	$\mp\eta$	\pm	o	$+\eta$	$\mp\eta$	o	\mp	$+\eta$	$\mp\eta$	o	o
$v_3 = \frac{1}{2}(\phi_1 + \phi_2) \pm \frac{1}{2}(\widehat{\phi}_1 + \widehat{\phi}_2)$	$+\eta$	$\pm\eta$	\pm	\pm	$-\eta$	$\pm\eta$	\pm	e	$+\eta$	$\pm\eta$	e	\pm	$-\eta$	$\pm\eta$	e	e
$v_6 = \frac{1}{2}(\phi_3 + \phi_4) \pm \frac{1}{2}(\widehat{\phi}_3 + \widehat{\phi}_4)$	$+\eta$	$\pm\eta$	\pm	\pm	$-\eta$	$\mp\eta$	\pm	o	$+\eta$	$\mp\eta$	o	\mp	$-\eta$	$\pm\eta$	o	o
$v_4 = \frac{1}{2}(\phi_5 + \phi_7) \pm \frac{1}{2}(\widehat{\phi}_5 + \widehat{\phi}_7)$	$+\eta$	$\pm\eta$	\pm	\mp	$-\eta$	$\pm\eta$	\pm	o	$+\eta$	$\pm\eta$	o	\pm	$-\eta$	$\pm\eta$	o	o
$v_8 = \frac{1}{2}(\phi_6 + \phi_8) \pm \frac{1}{2}(\widehat{\phi}_6 + \widehat{\phi}_8)$	$+\eta$	$\pm\eta$	\pm	\mp	$+\eta$	$\pm\eta$	\pm	o	$-\eta$	$\pm\eta$	o	\pm	$-\eta$	$\pm\eta$	o	o

symmetry is sufficient, giving the phase δ_2 if $\lambda'_1 = \lambda'_2$, and $\delta_2 \delta_1$, if $\lambda'_1 \neq \lambda'_2$. In the former case, which applies to v_1, v_5, v_9 , and v_{13} , the p_o and k_o symmetries are identical. In the latter, which applies to v_3, v_7, v_{11} , and v_{15} , the symmetry is identical for v_{11} and v_{15} , and opposite for v_3 and v_7 . Finally, if $\lambda_1 \neq \lambda_2$, reflection symmetry and parity are both needed, giving the phase $\delta_1 \delta_2 \varepsilon$ if $\lambda'_1 = \lambda'_2$ and $\delta_2 \varepsilon$ if $\lambda'_1 \neq \lambda'_2$. In the former, which applies to v_4, v_8, v_{12} , and v_{16} , the phase is opposite for v_4 and v_8 , and the same for v_{12} and v_{16} . In the latter which applies to v_2, v_6, v_{10} , and v_{14} , the phase is the same for v^{++} and v^{--} potentials ($\varepsilon = 1$) and the opposite for v^{+-} and v^{-+} potentials ($\varepsilon = -1$).

Examination of Table VI shows that the potentials divide into four groups, depending on their parity and interchange symmetry. These are

$$\begin{aligned} \text{singlet (S)} : \quad \mathcal{P} &= (-1)^J = -\eta, \quad \mathcal{P}_{12} = (-1)^{J-1} = \eta, \\ \text{triplet (T)} : \quad \mathcal{P} &= (-1)^J = -\eta, \quad \mathcal{P}_{12} = (-1)^J = -\eta, \\ \text{coupled (C)} : \quad \mathcal{P} &= (-1)^{J-1} = \eta, \quad \mathcal{P}_{12} = (-1)^{J-1} = \eta, \\ \text{virtual (V)} : \quad \mathcal{P} &= (-1)^{J-1} = \eta, \quad \mathcal{P}_{12} = (-1)^J = -\eta. \end{aligned} \quad (2.103)$$

In the $(++)$ sector, with both the initial and final states on-shell, parity requires that states with the orbital angular momentum $L = J$ correspond to the usual uncoupled channels. The singlet states are those with an antisymmetric spin wave function, which requires $\mathcal{P}_{12} = -\mathcal{P}$, and the triplet states have $\mathcal{P}_{12} = \mathcal{P}$. The coupled channels, with $J = L \pm 1$, have parity η and are spin triplet states because $\mathcal{P}_{12} = \mathcal{P}$. Finally, the virtual states would have $J = L \pm 1$ and total spin zero, which is impossible on-shell. These amplitudes, $v_{13} - v_{16}$, therefore play no role in the $(++)$ sector, a fact which follows from their antisymmetry in p_o and k_o , as shown in Table VI.

Since parity and exchange symmetry are conserved by the equations, the potential matrices which contribute to each channel can be identified from Table VI and Eq. (2.103). The equations (2.88) can then be written, for each channel, in the matrix form

$$M^J = v^J - \int_0^\infty dk v^J \bar{g} M^J \quad (2.104)$$

where \bar{g} is the diagonal matrix

$$\bar{g} = \begin{pmatrix} g^+ & & & \\ & g^- & & \\ & & g^+ & \\ & & & g^- \end{pmatrix} \quad (2.105)$$

and the singlet potential matrix is

$$v^J = \begin{pmatrix} v_1^{++} & v_9^{+-} & | & v_3^{++} & v_{11}^{+-} \\ v_1^{-+} & v_9^{--} & | & v_3^{-+} & v_{11}^{--} \\ \hline v_4^{++} & v_4^{+-} & | & v_2^{++} & v_{14}^{+-} \\ v_{12}^{-+} & v_{12}^{--} & | & v_6^{-+} & v_{10}^{--} \end{pmatrix}, \quad (2.106)$$

the triplet matrix is

$$v^J = \begin{pmatrix} v_5^{++} & v_{13}^{+-} & | & v_7^{++} & v_{15}^{+-} \\ v_5^{-+} & v_{13}^{--} & | & v_7^{-+} & v_{15}^{--} \\ \hline v_8^{++} & v_8^{+-} & | & v_6^{++} & v_{10}^{+-} \\ v_{16}^{-+} & v_{16}^{--} & | & v_2^{-+} & v_{14}^{--} \end{pmatrix}, \quad (2.107)$$

and the coupled matrix is

$$v^J = \begin{pmatrix} v_9^{++} & v_1^{+-} & | & v_{11}^{++} & v_3^{+-} \\ v_9^{-+} & v_1^{--} & | & v_{11}^{-+} & v_3^{--} \\ \hline v_{12}^{++} & v_{12}^{+-} & | & v_{10}^{++} & v_6^{+-} \\ v_4^{-+} & v_4^{--} & | & v_{14}^{-+} & v_2^{--} \end{pmatrix}. \quad (2.108)$$

The equations (2.104) – (2.108) are the equations which are finally solved numerically.

While the construction of the equations presented in this section relied heavily on the use of the symmetry relations, they can, of course, be directly constructed by introducing the linear combinations of Table VI directly into (2.88).

The remaining task of showing how the relativistic potentials of Table VI are constructed from relativistic meson exchange diagrams will be taken up in Part III.

III. MESON-EXCHANGE MODEL

The development in Part II was very general, and holds for any choice of interaction kernel (or relativistic potential). In this part, potentials constructed from a sum of one-meson-exchange contributions are discussed in detail. The form of the meson-exchange contributions are given, and the choice of form factors (or self-energies) is described. Antisymmetrization of the potentials introduces undesirable singularities, and methods for removing them and treating them are described. Finally, the structure of the partial wave expansions of the potentials is developed.

A. Meson-exchange amplitudes in Dirac space

The equations permit one of the two nucleons to be off-shell, and this in turn allows a more general form of meson-nucleon coupling that is possible when both nucleons are on-shell. These additional degrees of freedom are described by additional mixing parameters, chosen so that the coupling to on-shell nucleons is independent of these parameters. Any dependence of the final results on these parameters is therefore a direct indication of the sensitivity of the dynamics to off-shell effects.

The most general form of the direct contribution to the one-meson-exchange kernel in Dirac space, the first term in Eq. (2.13), can be written

$$V_{\alpha\alpha',\beta\beta'} = \delta_i g_i^2 \left[\frac{\Lambda_{\alpha\alpha'}(p_1, p'_1) \otimes \Lambda_{\beta\beta'}(p_2, p'_2)}{\mu_i^2 - (p_1 - p'_1)^2} \right] \times F_i(p_1, p'_1) F_i(p_2, p'_2) \quad (3.1)$$

where g_i and μ_i are the meson-nucleon coupling constant and meson mass, respectively, of meson i , δ_i is a factor which depends on the isospin of the exchanged meson,

$$\delta_i = \tau_1 \cdot \tau_2 = \begin{cases} 1 & \text{for isovector mesons,} \\ -\frac{1}{3} & \text{for isoscalar mesons,} \end{cases} \quad (3.2)$$

$$\delta_i = 1 \quad \text{for isoscalar mesons}$$

and $F_i(p, p')$ is the meson nucleon-nucleon form factor, which will be discussed in Sec. III B below.

In this part, only the direct term need be considered; recall the discussion in Sec. III and Eq. (2.100). However, it will be necessary to consider both the direct and alternating amplitudes shown in Figs. 9 and 10. Note that the potential satisfies the reflection property (2.9), required for the proof of antisymmetrization given in Sec. II A.

The vertex functions Λ will have the following forms for scalar, pseudoscalar, and vector mesons:

$$\begin{aligned} i\Lambda(p, p') &= 1 \quad (\text{scalar}), \\ \Lambda(p, p') &= \lambda_i \gamma^5 + (1 - \lambda_i) \frac{\not{p} - \not{p}'}{2m} \gamma^5 \quad (\text{pseudoscalar}), \end{aligned} \quad (3.3)$$

$$\begin{aligned} \Lambda^\mu(p, p') &= [1 + \kappa_i(1 - \lambda_i)] \gamma^\mu + \frac{\lambda_i \kappa_i}{2m} i\sigma^{\mu\nu} (p - p')_\nu \\ &\quad - (1 - \lambda_i) \kappa_i \frac{(p + p')^\mu}{2m} \quad (\text{vector}), \end{aligned}$$

where, for vector mesons, the product in (3.1) includes the vector meson propagator

$$\Lambda_1 \otimes \Lambda_2 \rightarrow \Lambda_1^\mu \Lambda_2^\nu \left[g_{\mu\nu} - \frac{(p - p')_\mu (p - p')_\nu}{\mu_i^2} \right]. \quad (3.4)$$

Note that if both the initial and final nucleons are on-shell, the pseudoscalar and vector couplings are *independent* of the mixing parameters λ_i . For the vector case, this follows from the familiar Gordon decomposition

$$\bar{u}(p) \frac{i\sigma^{\mu\nu}}{2m} q_\nu u(p') = \bar{u}(p) \left[\gamma^\mu - \frac{(p + p')^\mu}{2m} \right] u(p') \quad (3.5)$$

which holds *only* on-shell. For pseudoscalar mesons, $\lambda_i = 1$ gives pure γ^5 coupling, which couples strongly to "pair" terms, and for this choice the V^{+-} potentials will be large. It was less clear before this work began what effect the vector mixing parameters would have (note that they have no effect if $\kappa_i = 0$), and the sensitivity of the results to these parameters came as a surprise, particularly in view of the size of the vector meson masses.

B. Form factors

As discussed in Part I, the meson exchange model is based on the assumption that the physics of low energy nucleon-nucleon scattering is well described by proper treatment of the long range or peripheral exchanges, and that it is insensitive to the short range behavior, as long as sufficient convergence is provided so that the equation has solutions. The role of the form factors is to provide this convergence in a relativistically invariant fashion, and to parametrize the nonperipheral, short range part of the interaction. If the assumptions are correct, the overall results should be insensitive to the details of how the form factors are chosen, and it is consistent with the basic philosophy adopted here to treat them phenomenologically in the simplest possible way. Accordingly, the form factors will be taken to be scalar functions which depend on three scalar variables.

It turns out that convergence of the equations requires damping in all three of these scalar variables. Anticipating the applications of these calculations to electromagnetic interactions, where it is convenient to interpret the form factors as self-energies, the form factors will be written in a factorized form

$$F_i(p, p') = f_i(q^2) h(p^2) h(p'^2). \quad (3.6)$$

Furthermore, note that the function h , which describes the dependence of the form factor F_i on the off-shell nucleon mass, is a *universal* function, a choice dictated by the desire to be able to interpret this function in terms of modifications of the nucleon self-energy.

The connection between form factors and self-energies follows from the relations

$$\frac{f_i^2(q^2)}{\mu_i^2 - q^2} = \frac{1}{\mu_i^2 - q^2 + \text{H}_i(q^2)}, \quad (3.7)$$

$$\frac{h^2(p^2)}{m - \not{p}} = \frac{1}{m - \not{p} + \Sigma(p)}$$

which give

$$\Pi_i(q^2) = (\mu_i^2 - q^2) \left[\frac{1}{f_i^2(q^2)} - 1 \right], \quad (3.8)$$

$$\Sigma(p) = (m - \not{p}) \left[\frac{1}{h^2(p^2)} - 1 \right].$$

This interpretation suggests that the f_i and h should satisfy the following requirements.

- (i) f_i should be only a function of q^2 , and h a function only of p^2 . [This condition is what lead to the factorization assumption(3.6).]
- (ii) f_i should decrease at most like a power of q^2 as $q^2 \rightarrow \infty$, and have no zeros, so that Π_i can be regarded as satisfying a multiply subtracted dispersion relation with no infinities on the real axis. Similar conditions should hold for h .
- (iii) $f_i(\mu_i^2)=1$, and $h(m^2)=1$, so that the residue of the propagator at its pole is unity, and the coupling constants are fully renormalized.

A simple form which satisfies these conditions is

$$f_i(q^2) = \left[\frac{(A_i^2 - \mu_i^2)^2 + A_i}{(A_i^2 - q^2)^2 + A_i} \right]^n \quad (3.9)$$

where $n=1$ was chosen. The parameter A_i is fixed by the requirement that the logarithmic derivative of $f_i(q^2)$ at $q^2=0$ be the same as the logarithmic derivative of the pure multipole

$$f_i^0(q^2) = \left(\frac{A_i^2 - \mu_i^2}{A_i^2 - q^2} \right)^n. \quad (3.10)$$

This gives $A_i = A_i^4$, giving a relativistically invariant form factor depending on a single parameter. This parameter was chosen to be A_m , a universal number for all mesons. The final meson form factors are therefore

$$\begin{aligned} f_i(q^2) &= \frac{(A_m^2 - \mu_i^2)^2 + A_m^4}{(A_m^2 - q^2)^2 + A_m^4} \\ &= \frac{2A_m^2(A_m^2 - \mu_i^2) + \mu_i^4}{2A_m^2(A_m^2 - q^2) + q^4}. \end{aligned} \quad (3.11)$$

The second form for f_i shows that in the nonrelativistic region, when $-q^2 \simeq \mathbf{q}^2 \ll A_m^2$ (and assuming $\mu_i^2 \ll A_m^2$) the form factor (3.11) approximates the monopole form factor commonly employed in nonrelativistic calculations. When q^2 is large, the monopole form (3.11) goes like q^{-4} . However, since the relativistic form of q^2 goes only like a single power of momentum at very high momentum the form (3.11) also falls off like the nonrelativistic monopole at large q^2 . Hence the form (3.11) behaves in many ways like its nonrelativistic counterpart

$$f_i^{NR} = \frac{A^2 - \mu_i^2}{A^2 + \mathbf{q}^2} \quad (3.12)$$

which facilitates comparisons with nonrelativistic treatments.

For the nucleon form factor h the same considerations apply, except that A is chosen to reproduce the derivative of a pure monopole at $p^2 = m^2$. This gives

$$\begin{aligned} h(p^2) &= \frac{2(A_N^2 - m^2)^2}{(A_N^2 - p^2)^2 + (A_N^2 - m^2)^2} \\ &= \frac{2(A_N^2 - m^2)^2}{2(A_N^2 - m^2)[A_N^2 - p^2] + (m^2 - p^2)^2} \end{aligned} \quad (3.13)$$

which again shows that, in the nonrelativistic limit when $m^2 - p^2 \ll m^2$, h behaves like a pure monopole, but that at large p^2 it falls like p^{-4} , providing additional needed convergence.

C. Singularities and their removal

Unfortunately, the alternating diagram, Fig. 10, corresponding to amplitudes where particle 2 in the final state is on-shell, has singularities in the physical region. One of these is natural and expected; it is due to the possibility for physical meson production and occurs only when $W > 2m + \mu_i$. However, the other is spurious, and arises from the process of separating out terms in which alternate nucleons are on shell. In this section the origin of this singularity will be described, and methods for its removal explained.

In the c.m. system, the denominator of the meson propagator corresponding to the alternating term is

$$\begin{aligned} \hat{D}(z) &= \mu^2 + (\mathbf{p} + \mathbf{k})^2 - (W - E_p - E_k)^2 \\ &= \mu^2 - 2m^2 + 2E_p E_k - 2pkz \\ &\quad - (W - 2E_p)(W - 2E_k) \\ &= D(-z) - (W - 2E_p)(W - 2E_k) \end{aligned} \quad (3.14)$$

where z is the cosine of the angle between the two momenta \mathbf{p} and \mathbf{k} , and $D(z)$ is the denominator of the direct term. The alternating term differs from the direct term in that the sign of the relative energy of the final state is changed, which produces the additional energy dependent term $(W - 2E_p)(W - 2E_k)$. It is this energy dependent term which produces the singularities, and it follows that these singularities are absent unless *both* the initial and final states are off-shell ($W \neq 2E_p$ and $W \neq 2E_k$).

The singularities occur at the zeros of \hat{D} , which are at

$$W = E_p + E_k \pm \omega_{p-k} \quad (3.15)$$

where ω_{p-k} is the on-shell energy of the meson. These singularities arise from the two time ordered contributions to meson exchange, shown in Fig. 11. The one in 11(a), corresponding to the plus sign in (3.15), is due to the possibility of real meson production. Specifically, when $W > 2M + \mu$, for any \mathbf{p} there exists a \mathbf{k} such that the exchanged meson can be physical, and integration over k in the integral equation will cross the pole at $\hat{D} = 0$, producing an imaginary contribution to \hat{V} which includes some of the imaginary terms needed to describe real meson production. While this singularity is physical and welcomed, it is not particularly helpful since other production mechanisms, such as those shown in Fig. 12, are needed to consistently describe inelastic processes.

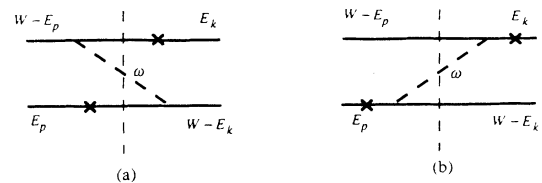


FIG. 11. Time ordered contributions to the alternating diagram shown in Fig. 10: (a) gives rise to real meson production, and (b) gives the spurious singularities discussed in the text.



FIG. 12. Self-energy contributions which also contribute to the real meson production singularities.

Hence this singularity will be eliminated in this work, but will be restored in the future when these equations are extended to treat inelasticities.

The second singularity, shown in Fig. 11(b), and corresponding to the minus sign in Eq. (3.15), is spurious. It is due to the fact that the off-shell nucleons can have energies less than m , and if their energies are sufficiently small there is the possibility that the physical on-shell nucleon could decay into a real meson and one of these low energy, off-shell nucleons. This vertex instability singularity, which also produces an imaginary contribution to \hat{V} , is however not really present in the full theory because it is cancelled by another unphysical process shown in Fig. 13. This is identical to Fig. 11(b), except that the meson is on-shell, and as $k = |\mathbf{k}|$ increases in the initial state, the energy of particle one, which is $W - E_p + \omega$, increases until it equals E_k , the on-shell energy of particle 1. At this point the pole in the propagator of particle 1 is

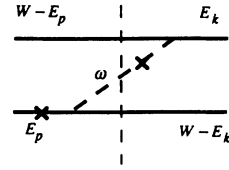


FIG. 13. Time ordered diagram which generates singularities which cancel the spurious singularities arising from Fig. 11(b).

encountered and there is a singularity, and a corresponding imaginary contribution to the integral equation. It can be shown that the two singularities from Fig. 11(b) and Fig. 13 cancel, but since mechanisms corresponding to Fig. 13 have not been included in the integral equation described in Part II, the cancellation cannot occur.

The solution to this problem is clearly to add additional contributions to the integral equation so that the unwanted singularities are cancelled. Before describing this, it will be demonstrated that the two singularities do indeed cancel. To see this, consider the box diagram shown in Fig. 14. Here the initial state is on-shell, for simplicity, so that $E_{p'} = W/2$, and the final state has particle 2 on shell. To see what happens, it is sufficient to treat scalar particles, in which case the box is

$$M_b = i \int \frac{d^4k}{(2\pi)^4} \frac{g^4}{[m^2 - (\frac{W}{2} + k)^2 - i\epsilon][m^2 - (\frac{W}{2} - k)^2 - i\epsilon](\mu^2 - q_1^2 - i\epsilon)(\mu^2 - q_2^2 - i\epsilon)}$$

Consider the k_o integration. There are 8 poles in the complex k_o plane, as shown in Fig. 15 for the case when $p' \simeq 0$, p and k are both small, but $p > k$, and $W < 2E_k$. The alternating contribution to the potential, arises when the k_o contour is closed in the lower half plane and the pole at $k_o = E_k - W/2$, which corresponds to particle 1 on-shell, is retained. (Remember that antisymmetrization requires that the nucleon pole contributions resulting from closing the contour in both the upper and lower half planes be retained—were it possible to keep those in the upper half plane only, there would be no spurious singularities.) Retaining this pole does give the leading contribution, but when $W > 2m + \mu$, the meson pole in the upper half plane can overtake the nucleon pole. This happens when

$$\omega_2 + E_p - \frac{1}{2}W = \frac{1}{2}W - E_k$$

which is the condition (3.15) with the plus sign, corresponding to real meson production. However, when both p and k are large, the meson pole in the lower half plane can also overlap the nucleon pole. This occurs at

$$\omega_2 + \frac{1}{2}W - E_p = E_k - \frac{1}{2}W$$

which is (3.15) with the minus sign. This is the spurious singularity, and it is clear that it will be eliminated if both the nucleon and meson poles in the lower half plane are retained. Alternatively, the two pole contributions correspond to the diagrams of Figs. 11(b) and 13, and

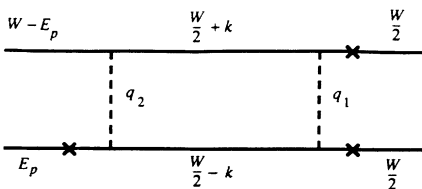


FIG. 14. Box diagram used to prove the cancellation of spurious singularities.

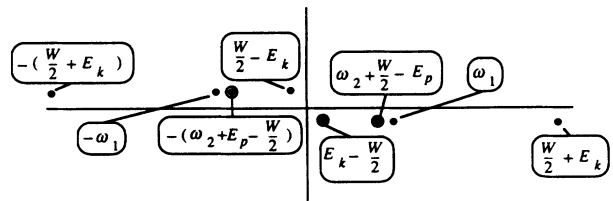


FIG. 15. Location of the singularities in the complex k_o plane of the box diagram shown in Fig. 14.

since they arise from singularities in the same half plane, they give canceling singularities when both are retained. Note that the same cannot be said of the production singularity, it pinches the nucleon pole and gives rise to the cut associated with meson production.

While it might be desirable to eliminate the spurious singularity by retaining the full meson pole contribution, this would complicate the equations by coupling to amplitudes in which both nucleons are off-shell. A simpler prescription is to subtract the most singular part, which occurs when both the meson and nucleon are on-shell. For spin zero mesons, this gives

$$\widehat{V} = \left(\frac{g^2}{\widehat{D}(z) - i\epsilon} - i\pi\delta(\widehat{D}(z)) \right) = \mathcal{P} \frac{g^2}{\widehat{D}(z)}. \quad (3.16)$$

Note that the direct term has no singularities, so the principle value has no effect on this term. For the alternating term, the delta function cancels the imaginary part of the meson propagator, leaving the real principal value. This does not eliminate the singularity entirely, but the resulting potential is real and the singularity is integrable, ensuring that the M matrix calculated from such an interaction is smooth. When calculating the two-meson-exchange potential, the δ function would be restored. The prescription (3.16) for removing the singularity is the principal value prescription referred to in Part I.

It is useful to test the numerical differences between alternative prescriptions for removing the singularity. To this end, and in order to produce a potential independent of the total energy W , use may be made of the fact that a sufficient condition for the Pauli principle to hold for the *half* off-shell *amplitude*, is that it hold for the *half* off-shell *potential*. This follows from the discussion given in Sec. II A, where it was shown that the final state was properly antisymmetrized provided only that the initial state was antisymmetrized, and that the potential satisfies the reflection property (2.9).

One prescription which meets these requirements is to choose

$$\widehat{D}(z) = D(z) \quad (\text{energy independent prescription}). \quad (3.17)$$

This choice completely eliminates all singularities and any energy dependence from the denominators of the meson propagator. It works because it holds if either the initial *or* final state is on-shell [recall Eq. (3.14)], and because it does not violate the reflection property (2.9). In the realistic case with spin, this prescription is applied only to the meson denominators in Eq. (3.1); the numerators are treated the same way in both cases.

A third possible prescription consists of a combination

of the principal value and energy independent prescriptions. Since the denominators for the direct and alternating terms are equivalent whenever the initial and/or final nucleon pairs are on the mass shell, the two previous prescriptions can be combined by using the principal value prescription for momenta below the on-shell point and the energy independent prescription for momenta above this point. The physical meson production singularities, which may occur at momenta below the on-shell point are thus treated as in the principal value prescription. The unphysical singularities, which always occur at momenta above the on-shell point are totally eliminated by using the energy independent prescription. This “mixed prescription” was used in the models labeled A, and previously reported in Ref. [10].

These three treatments of the Pauli principle give very similar numerical results, showing that the singularities in the “principal value” prescription are not numerically important. However, in applications the “principal value” prescription is preferred; it gives a realistic description of the mesons near their mass shell, which can be probed in electromagnetic interactions.

The fact that the singularities of the “principal value” prescription are not very large numerically follows from the observation that they only occur at relatively high momenta. If $p = k$, the singularities first occur at

$$p = \sqrt{\frac{(W + \mu_i)^2}{4} - m^2}. \quad (3.18)$$

For the worst case ($W=2m$, $\mu=\mu_\pi$) this happens at

$$p \simeq 367 \text{ MeV} \quad (3.19)$$

which is far off-shell in a region heavily damped by the wave function.

The numerical procedure for calculating the principle value of the potentials is explained in Appendix B.

D. Partial wave decomposition of the potentials

The final task is to construct the specific partial wave potentials given in Table VI from the amplitudes (3.1). This construction proceeds in three steps, which will be described in this section. More details can be found in Appendix C.

We first construct helicity amplitudes for both the direct and alternating versions of (3.1), then project out the J^{th} partial wave using the inverse of the expansion given in Eq. (2.85), and finally form the linear combinations given in Table VI.

The first step is carried out using the helicity spinors defined in Appendix A. The general form of the result is

$$V_{\lambda_1 \lambda'_1, \lambda_2 \lambda'_2}(p, k; P) = \frac{(E_p + m)(E_k + m)}{4E_p E_k} \sum_i \frac{g_i^2 \delta_i}{D_i} \bar{F}_i \left\{ \langle \lambda_1 \lambda_2 | \lambda'_1 \lambda'_2 \rangle > \left(I_i^{(1)} + z I_i^{(2)} \right) + \langle \lambda_1 \lambda_2 | \sigma_1 \cdot \sigma_2 | \lambda'_1 \lambda'_2 \rangle I_i^{(3)} \right\} \quad (3.20)$$

where the sum is over all mesons being exchanged, the factor $g_i^2 \delta_i$ was defined in Eq. (3.1), D_i is the denominator of the meson propagator [either the D or \widehat{D} defined in Eq. (3.14)], and \bar{F}_i is a shorthand notation for the product of form factors $F_i(p_1, k_1)F_i(p_2, k_2)$. The $\langle \rangle$'s are matrix elements of the two component nucleon spinors defined in Appendix C, and the $I_i^{(1)} - I_i^{(3)}$ are angle independent (but helicity dependent) terms characteristic of each meson. These terms, and the denominators D_i , are different for the direct and alternating contributions.

It is shown in Appendix C that

$$\langle \lambda_1 \lambda_2 | \sigma_1 \cdot \sigma_2 | \lambda'_1 \lambda'_2 \rangle = T \langle \lambda_1 \lambda_2 | \lambda'_1 \lambda'_2 \rangle \quad (3.21)$$

where T is either 1 or -3 and is independent of the angle θ . Hence the two terms in curly braces in (3.20) can be summed:

$$I_i^{(1)} + z I_i^{(2)} + T I_i^{(3)} = I_i. \quad (3.22)$$

It is convenient to expand the I_i (and \widehat{I}_i for the alternating potentials) in the following set of basis functions (which depend on λ_i and λ'_i):

$$\theta_i^\pm = 1 \pm \frac{4\lambda_i \lambda'_i p k}{(E_k + m)(E_p + m)}, \quad (3.23)$$

$$\phi_i^\pm = \frac{2\lambda_i p}{E_p + m} \pm \frac{2\lambda'_i h}{E_k + m}.$$

The form of the expansions depends on the ρ spin of the potentials. For the $++$ or $--$ potentials, the following expansion holds:

$$I = R_1 \theta_1^+ \theta_2^+ + R_2 \theta_1^- \theta_2^- + R_3 \theta_1^+ \theta_2^- + R_4 \theta_1^- \theta_2^+ + R_5 \phi_1^+ \phi_2^+ + R_6 \phi_1^- \phi_2^- + R_7 \phi_1^+ \phi_2^- + R_8 \phi_1^- \phi_2^+ \quad (3.24)$$

and for the V^{+-} and V^{-+} potentials, the expansion is

$$I = S_1 \theta_1^+ \phi_2^+ + S_2 \theta_1^+ \phi_2^- + S_3 \theta_1^- \phi_2^+ + S_4 \theta_1^- \phi_2^- + S_5 \phi_1^+ \theta_2^+ + S_6 \phi_1^+ \theta_2^- + S_7 \phi_1^- \theta_2^+ + S_8 \phi_1^- \theta_2^- \quad (3.25)$$

TABLE VII. The non-zero R 's and S 's for scalar mesons from which the I 's of Eqs. (3.24) and (3.25) are constructed, where $a = \frac{E_k - W/2}{m}$, $a' = \frac{E_p - W/2}{m}$, and $b = \frac{W}{2m}$.

0 ⁺ Mesons		
	Direct	Alternating
V^{++}	$R_2 = -1$	$\hat{R}_2 = -1$
V^{+-}	$S_3 = 1$	$\hat{S}_3 = 1$
V^{--}	$R_2 = 1$	$\hat{R}_5 = -1$
0 ⁻ Mesons		
	Direct	Alternating
V^{++}	$R_6 = 1$ $R_8 = -(1 - \lambda_i)(a - a')$	$\hat{R}_5 = -(1 - \lambda_i)^2 a a'$ $\hat{R}_6 = 1$ $\hat{R}_7 = (1 - \lambda_i) a'$ $\hat{R}_8 = -(1 - \lambda_i) a$
V^{+-}	$S_7 = -1$ $S_8 = (1 - \lambda_i) \frac{E_p}{m}$	$\hat{S}_5 = -(1 - \lambda_i) a'$ $\hat{S}_6 = (1 - \lambda_i)^2 b a'$ $S_7 = -1$ $\hat{S}_8 = (1 - \lambda_i) b$
V^{--}	$R_6 = 1$	$\hat{R}_1 = -1$ $\hat{R}_2 = -(1 - \lambda_i)^2 b^2$ $\hat{R}_3 = \hat{R}_4 = (1 - \lambda_i) b$

Tables VII and VIII give the R 's and S 's for the direct and alternating contribution from each meson. Note that these terms are mostly independent of $z = \cos \theta$; only the factor α which appears in some of the vector TT terms contains one power of z , which must be taken into account when carrying out the partial wave expansions. Note also that the off-shell dependence of the potentials is apparent in the parameters a, a', a_i, a'_i, b , and c . If both particles are on shell, all of the a 's are zero.

Next, the partial wave projections of (3.20) which are needed follow from Eq. (2.85)

$$V_{\lambda_1 \lambda'_1, \lambda_2 \lambda'_2}^J(p, k; P) = 2\pi \int dz d_{\lambda'_1 \lambda}^J(\theta) V_{\lambda_1 \lambda'_1, \lambda_2 \lambda'_2}(p, k; P). \quad (3.26)$$

These partial wave amplitudes are expanded in the form

$$V_{\lambda_1 \lambda'_1}^J(p, k; P) = \frac{m^2}{2E_p E_k} \int dz d_{\lambda'_1 \lambda}^J(\theta) \langle \lambda_1 \lambda'_1 | \lambda_2 \lambda'_2 \rangle \sum_i \frac{g_i^2 \delta_i \bar{F}_i}{D_i} \left\{ \tilde{I}_i(\lambda_1 \lambda_2, \lambda'_1 \lambda'_2) + z \tilde{I}_i^z(\lambda_1, \lambda_2, \lambda'_1 \lambda'_2) \right\} \quad (3.27)$$

where the \tilde{I}_i and \tilde{I}_i^z are independent of θ . Their explicit form can be found by combining Eqs. (3.20)–(3.25), and using Tables VII and VIII, but we will not record these intermediate results. Equation (3.27) shows that all of the partial waves can be expressed in terms of angular integrals of the form

$$A_j^i = 2\pi \int dz \frac{d_j}{D_i(z)} f_i^2(q^2) \quad (3.28)$$

where seven angular combinations A_j ($j = 1 - 7$) of the form

$$d_j = z^n \langle \lambda_1 \lambda_2 | \lambda'_1 \lambda'_2 \rangle d_{\lambda'_1 \lambda}^J(\theta), \quad (3.29)$$

with $n = 0$ or 1 , are required to evaluate all angular integrals involving the direct and exchange terms for each meson.

These angular combinations are listed in Table IX. Other integrals which may be required can be obtained using the relations

$$d_{\lambda\mu}^J = d_{-\mu, -\lambda}^J = (-1)^{\lambda-\mu} d_{\mu\lambda}^J \quad (3.30)$$

Finally, the linear combinations of potentials given in Table VI can be constructed from the expansions (3.27). The

TABLE VIII. The non-zero R 's and S 's for vector mesons from which the I 's of Eqs. (3.24) and (3.25) are constructed, where: $a = \frac{E_k - W/2}{m}$, $a' = \frac{E_p - W/2}{m}$, $b = \frac{W}{2m}$, $a_i = \frac{2E_k - W}{\mu_i}$, $a'_i = \frac{2E_p - W}{\mu_i}$, $b_i = \frac{W}{\mu_i}$, $c = \frac{E_p + E_k}{m}$, and $\alpha = \frac{(p+k)^2}{4m^2}$

	Direct	1^- Mesons Alternating
V_{VV}^{++}	$R_1 = 1$ $R_5 = -T$	$\hat{R}_1 = 1 - a_i a'_i$ $\hat{R}_5 = -T$
V_{VV}^{+-}	$S_2 = 1$ $S_6 = -T$	$\hat{S}_2 = 1 + b_1 a'_i$ $\hat{S}_6 = -T$
V_{VV}^{--}	$R_1 = 1$ $R_5 = T$	$\hat{R}_2 = -T$ $\hat{R}_6 = -1 + b_i^2$
V_{VT}^{++}	$R_2 = 2$ $R_3 = -c + (1 - \lambda_i)(a + a')$ $R_4 = -c$ $R_7 = \lambda_i T(a - a')$	$\hat{R}_1 = 2\lambda_i a_i a'_i$ $\hat{R}_2 = 2$ $\hat{R}_3 = -c + (1 - \lambda_i)(a + b a_i a'_i)$ $\hat{R}_4 = -c + (1 - \lambda_i)(a' + b a_i a'_i)$ $\hat{R}_7 = \lambda_i T a$ $\hat{R}_8 = -\lambda_i T a'$
V_{TT}^{++}	$R_2 = \frac{1}{4}c^2 + \alpha - \frac{1}{2}(1 - \lambda_i)c(a + a') - \frac{1}{2}\lambda_i(a - a')^2$	$\hat{R}_1 = -\lambda_i a_i a'_i$ $\hat{R}_2 = \frac{1}{4}c^2 + \alpha - \frac{1}{2}(1 - \lambda_i)c(a + a') - \frac{1}{2}\lambda_i(a - a')^2 + (1 - \lambda_i)^2[aa' - b^2 a_i a'_i]$ $\hat{R}_3 = \hat{R}_4 = -\lambda_i(1 - \lambda_i)b a_i a'_i$
V_{VT}^{+-}	$S_1 = \frac{E_p}{m} - (1 - \lambda_i)(a' - b)$ $S_3 = -2$ $S_4 = -\frac{E_p}{m}$ $S_5 = \lambda_i T \frac{E_p}{m}$	$\hat{S}_1 = \frac{E_p}{m} + (1 - \lambda_i)b(1 - a_i a'_i)$ $\hat{S}_2 = -2\lambda_i b_i a'_i$ $\hat{S}_3 = -2$ $\hat{S}_4 = -\frac{E_p}{m} + (1 - \lambda_i)a'[1 - b_i^2]$ $\hat{S}_5 = \lambda_i T b$ $\hat{S}_8 = -\lambda_i T a'$
V_{TT}^{+-}	$S_3 = \frac{1}{4}c(a + a') - \alpha - (\frac{1}{2} - \lambda_i)bc$	$\hat{S}_1 = \frac{1}{2}\lambda_i c a' + \lambda_i(1 - \lambda_i)b a_i a'_i$ $\hat{S}_2 = \lambda_i^2 b_i a'_i$ $\hat{S}_3 = \frac{1}{4}c(a - a') - \alpha - (\frac{1}{2} - \lambda_i)bc - \lambda_i a'$ $\quad - (1 - \lambda_i)^2 b(a' - b a_i a'_i) + \frac{1}{2}(1 - \lambda_i)(a' - a)a'$ $\hat{S}_4 = \lambda_i(1 - \lambda_i)b_i^2 a'$ $\hat{S}_7 = \lambda_i^2 T b a'$
V_{VT}^{--}	$R_2 = -2$ $R_3 = (1 - \lambda_i)b$	$\hat{R}_3 = \hat{R}_4 = \lambda_i T b$ $\hat{R}_5 = 2$ $\hat{R}_6 = -2\lambda_i b_i^2$ $\hat{R}_7 = (1 - \lambda_i)b[1 + b_i a'_i]$ $\hat{R}_8 = -(1 - \lambda_i)b[1 + b_i a_i]$
V_{TT}^{--}	$R_2 = \frac{1}{4}c^2 - \alpha - \frac{1}{2}(1 - \lambda_i)bc$	$\hat{R}_1 = -\lambda_i^2 T b^2$ $\hat{R}_5 = -\frac{1}{4}(a - a')^2 + \alpha - \lambda_i bc + (1 - \lambda_i)^2 b^2(1 - a_i a'_i)$ $\hat{R}_6 = \lambda_i^2 b_i^2$ $\hat{R}_7 = -\lambda_i(1 - \lambda_i)b_i^2 a'$ $\hat{R}_8 = \lambda_i(1 - \lambda_i)b_i^2 a$

TABLE IX. The combinations d_j , given in Eq. (3.29), needed for the angular integrals.

$d_j = z^n < \lambda_1 \lambda_2 \lambda'_1 \lambda'_2 > d_{\lambda' \lambda}(\theta)$		
d_1	$d_{00}^J = \frac{1}{2} [(1+z)d_{11}^J - (1-z)d_{1,-1}^J]$	$P_J(z)$
d_2	$z d_{00}^J$	$z P_J(z)$
d_3	$\frac{1}{2} [(1+z)d_{11}^J + (1-z)d_{1,-1}^J]$	$\frac{J}{2J+1} P_{J+1}(z) + \frac{J+1}{2J+1} P_{J-1}(z)$
d_4	$\sin \theta d_{10}^J = -\sin \theta d_{01}^J$	$\frac{\sqrt{J(J+1)}}{2J+1} [P_{J+1}(z) - P_{J-1}(z)]$
d_5	$z^2 d_{00}^J$	$z^2 P_J(z)$
d_6	$z \frac{1}{2} [(1+z)d_{11}^J + (1-z)d_{1,-1}^J]$	$z [\frac{J}{2J+1} P_{J+1}(z) + \frac{J+1}{2J+1} P_{J-1}(z)]$
d_7	$z \sin \theta d_{10}^J = -z \sin \theta d_{01}^J$	$z \frac{\sqrt{J(J+1)}}{2J+1} [P_{J+1}(z) - P_{J-1}(z)]$

final results can be written compactly in terms of the angular integrals (3.28):

$$v_k^J = \frac{m^2}{2E_p E_k} h(p_2^2) h(k_2^2) \sum_{i,j} g_i^2 \delta_i \frac{1}{2} [A_i^j B_{jk} \pm \hat{A}_i^j \hat{B}_{jk}] \tag{3.31}$$

where \hat{A} and \hat{B} refer to A and B evaluated for the alternating terms with $p_o \rightarrow -p_o$, as discussed in sections III and III C. The plus sign holds for those potentials even in p_o , $v_3, v_6, v_8 - v_{12}$, as shown in Table VI. The rest are odd in p_o and the minus sign in Eq. (3.31) is required. The nonzero elements B_{jk} are shown in Table X. They are sums of eight independent quantities B_i . For the ++ and -- potentials, these B_i 's can be expressed in terms of eight independent combinations of the R 's defined in Tables VII and VIII:

$$\begin{aligned} B_1 &= (R_1 + R_2)T^+ + (R_3 + R_4)T^- + (R_5 + R_6)U^+ + (R_7 + R_8)U^-, \\ B_3 &= (R_1 + R_2)T^+ + (R_3 + R_4)T^- - (R_5 + R_6)U^+ - (R_7 + R_8)U^-, \\ B_5 &= -(R_1 + R_2)T^- - (R_3 + R_4)T^+ - (R_5 + R_6)U^- - (R_7 + R_8)U^+, \\ B_7 &= -(R_1 + R_2)T^- - (R_3 + R_4)T^+ + (R_5 + R_6)U^- + (R_7 + R_8)U^+, \\ B_2 &= (R_1 - R_2 + R_5 - R_6)Y, \quad B_4 = (R_1 - R_2 - R_5 + R_6)Y, \\ B_6 &= (R_4 - R_3 + R_8 - R_7)Y, \quad B_8 = (R_4 - R_3 - R_8 + R_7)Y. \end{aligned} \tag{3.32}$$

Similarly, for the +- and -+ potentials, eight independent combinations of the S 's are required:

$$\begin{aligned} B_1 &= (S_1 + S_4 + S_5 + S_8)X_p^+ + (S_2 + S_3 + S_6 + S_7)X_p^-, \\ B_3 &= (-S_1 - S_4 + S_5 + S_8)X_p^+ + (-S_2 - S_3 + S_6 + S_7)X_p^-, \\ B_5 &= (-S_1 - S_4 - S_5 - S_8)X_p^- + (-S_2 - S_3 - S_6 - S_7)X_p^+, \\ B_8 &= (S_1 + S_4 - S_5 - S_8)X_p^- + (S_2 + S_3 - S_6 - S_7)X_p^+, \\ B_2 &= (S_1 - S_4 + S_5 - S_8)X_k^+ + (-S_2 + S_3 + S_6 - S_7)X_k^-, \\ B_4 &= (-S_1 + S_4 + S_5 - S_8)X_k^+ + (S_2 - S_3 + S_6 - S_7)X_k^-, \\ B_6 &= (S_1 - S_4 - S_5 + S_8)X_k^- + (-S_2 + S_3 - S_6 + S_7)X_k^+, \\ B_7 &= (-S_1 + S_4 - S_5 + S_8)X_k^- + (S_2 - S_3 - S_6 + S_7)X_k^+. \end{aligned} \tag{3.33}$$

TABLE X. The non-zero elements B_{jk} expressed in terms of the B_i 's defined in Eqs. (3.32) and (3.33). $T = -3$ for $B_{1,1}$ and $B_{1,5}, B_{1,9}$, and $B_{1,13}$. $T = 1$ for all other elements.

$k \setminus j$	1	2	3	4	5	6	7
$\frac{1}{5}$	B_1	$B_2 + B_{1z}$			B_{2z}		
$\frac{6}{2}$	B_3	B_{3z}	B_4			B_{4z}	
$\frac{3}{7}$				B_6			B_{6z}
$\frac{8}{4}$				B_8			B_{8z}
$\frac{9}{13}$	B_2	$B_1 + B_{2z}$			B_{1z}		
$\frac{10}{14}$	B_4	B_{4z}	B_3			B_{3z}	
$\frac{11}{15}$				B_5			B_{5z}
$\frac{12}{16}$				B_7			B_{7z}

These expansions are given in terms of the following functions:

$$\begin{aligned} T^+ &= \frac{E_p E_k}{m m} + 1, & T^- &= \frac{E_p + E_k}{m}, \\ U^+ &= \frac{E_p E_k}{m m} - 1, & U^- &= \frac{E_p - E_k}{m}, \\ X_k^+ &= \frac{k E_p}{m^2}, & X_k^- &= \frac{k}{m}, \\ X_p^+ &= \frac{p E_k}{m^2}, & X_p^- &= \frac{p}{m}, \\ Y &= \frac{k p}{m^2}. \end{aligned} \quad (3.34)$$

In Table X, the symbol B_i denotes the contributions to B_i independent of z , while B_{iz} denotes the contributions proportional to z , i.e., $B_i(z \text{ contribution}) = z B_{iz}$.

To summarize, partial wave amplitudes of the potentials of Table VI are given by Eq. (3.31) with the angular integrals defined in Eq. (3.28) and Table IX, and the B_{jk} expansion coefficients defined in Table X, Eqs. (3.32) and (3.33), and Tables VII and VIII.

ACKNOWLEDGMENTS

We are grateful to Dick Arndt for supplying the SAID program, error matrices, and helpful advice about data and the state of the phase shift analyses. We also acknowledge helpful conversations with D. Bugg, J. J. deSwart, R. Machleidt, and R. Wiringa. Support from the Department of Energy through CEBAF is gratefully acknowledged.

APPENDIX A: STATE DEFINITIONS AND SYMMETRIES

1. Definition of helicity states

Following the notation in Jacob and Wick [40], we define helicity spinors for particle 1 from rest spinors (quantized along the $+\hat{z}$ direction) by

$$u_1(\mathbf{p}, \lambda) \equiv u_1(p, \theta, \phi; \lambda) = H_p u_1(\mathbf{0}, \lambda) \quad (A1)$$

where $H_p = R_{\hat{p}} L_p$; L_p is a pure boost in the \hat{z} direction which carries the vector $(m, \mathbf{0})$ into $(E_p, 0, 0, p)$, and $R_{\hat{p}}$ is a pure rotation from the \hat{z} direction to the \hat{p} direction characterized by polar angles θ and ϕ . We use the convention

$$R_{\hat{p}} = R_{\phi, \theta, -\phi} = e^{-i\phi J_z} e^{-i\theta J_y} e^{i\phi J_z}. \quad (A2)$$

The rest spinor is

$$u_1(\mathbf{0}, \lambda) = \begin{pmatrix} 1 \\ 0 \end{pmatrix} |\lambda >_1 \quad (A3)$$

where

$$\left| \frac{1}{2} \right\rangle_1 = \begin{pmatrix} 1 \\ 0 \end{pmatrix}; \quad \left| -\frac{1}{2} \right\rangle_1 = \begin{pmatrix} 0 \\ 1 \end{pmatrix}. \quad (A4)$$

The helicity spinors for particle 2 (in the c.m. frame) are

obtained from those of particle 1 by first transforming $u_1(p, 0, 0, \lambda)$ into u_2 ,

$$u_2(p, 0, 0; \lambda) = (-1)^{\frac{1}{2}-\lambda} e^{-i\pi J_y} u_1(p, 0, 0; \lambda) \quad (A5)$$

and then performing the same rotation $R_{\hat{p}}$ used for particle 1. Hence, if $H_p^{(2)} = R_{\hat{p}} e^{-i\pi J_y} L_p$,

$$u_2(\mathbf{p}, \lambda) = (-1)^{1/2-\lambda} H_p^{(2)} u_1(\mathbf{0}, \lambda). \quad (A6)$$

The description of off-shell particles also requires negative energy v spinors, but with three momenta in the opposite direction, so that the v_2 spinor helicity states are obtained by charge conjugation from u_1 helicity spinors, and vice versa:

$$v_2(\mathbf{p}, \lambda) = \eta(\lambda) C \bar{u}_1^T(\mathbf{p}, \lambda), \quad (A7)$$

$$v_1(\mathbf{p}, \lambda) = \delta \eta(\lambda) C \bar{u}_2^T(\mathbf{p}, \lambda)$$

where δ and $\eta(\lambda)$ are phase factors. We will eventually fix these at

$$\eta(\lambda) = (-1)^{\frac{1}{2}-\lambda}, \quad \delta = -1. \quad (A8)$$

The reasons for these choices will be described below.

In the applications described in this paper, the scattering will be confined to the xz plane, with the initial state particles 1 and 2 moving in the $+\hat{z}$ and $-\hat{z}$ directions, respectively, and with the momentum components of particle 1 in the final state given by $\mathbf{p} = (p \sin \theta, 0, p \cos \theta)$. With these conventions, the actual spinors used in this calculation are

$$u_i(p, \lambda) = N \begin{pmatrix} 1 \\ 2\lambda \tilde{p} \end{pmatrix} |\lambda >_i, \quad (A9)$$

$$v_i(p, \lambda) = N \begin{pmatrix} -2\lambda \tilde{p} \\ 1 \end{pmatrix} |\lambda >_i$$

with $i=1$ or 2 , $\tilde{p} = \frac{p}{E_p+m}$, $N = \left(\frac{E_p+m}{2m} \right)^{\frac{1}{2}}$, and $|\lambda >_i$ are given in Table XI. This convention differs from that of Kubis by an overall factor of $(E_p/m)^{\frac{1}{2}}$

TABLE XI. The two component spinors of Eq. (A9).

	Initial state	
	$\lambda = \frac{1}{2}$	$\lambda = -\frac{1}{2}$
$ \lambda >_1$	$\begin{pmatrix} 1 \\ 0 \end{pmatrix}$	$\begin{pmatrix} 0 \\ 1 \end{pmatrix}$
$ \lambda >_2$	$\begin{pmatrix} 0 \\ 1 \end{pmatrix}$	$\begin{pmatrix} 1 \\ 0 \end{pmatrix}$
	Final state	
	$\lambda = \frac{1}{2}$	$\lambda = -\frac{1}{2}$
$ \lambda >_1$	$\begin{pmatrix} \cos \frac{1}{2}\theta \\ \sin \frac{1}{2}\theta \end{pmatrix}$	$\begin{pmatrix} -\sin \frac{1}{2}\theta \\ \cos \frac{1}{2}\theta \end{pmatrix}$
$ \lambda >_2$	$\begin{pmatrix} -\sin \frac{1}{2}\theta \\ \cos \frac{1}{2}\theta \end{pmatrix}$	$\begin{pmatrix} \cos \frac{1}{2}\theta \\ \sin \frac{1}{2}\theta \end{pmatrix}$

2. Parity transformations

First, consider the transformation

$$Y = e^{-i\pi J_y \mathcal{P}} \quad (\text{A10})$$

where \mathcal{P} is the parity operator. This transformation leaves the x - z plane invariant, but changes $\hat{y} \rightarrow -\hat{y}$, and hence is equivalent to changing ϕ to $2\pi - \phi$, and leaving θ unchanged. Since helicities are invariant under rotations, it also changes helicities λ to $-\lambda$. Explicit construction gives, on the Dirac space,

$$Y = -i\sigma_y \gamma^0 = \begin{pmatrix} -i\sigma_2 & \\ & i\sigma_2 \end{pmatrix} \quad (\text{A11})$$

and therefore

$$Y u_1(p, \theta, \phi; \lambda) = (-1)^{\frac{1}{2}-\lambda} u_1(p, \theta, 2\pi - \phi; -\lambda), \quad (\text{A12})$$

$$Y u_2(p, \theta, \phi; \lambda) = (-1)^{\frac{1}{2}+\lambda} u_2(p, \theta, 2\pi - \phi; -\lambda),$$

The Y parity transformation on the two-particle direct product space (α and β are Dirac indices)

$$|p, \theta, \phi; \lambda_1 \lambda_2 \rangle \equiv u_{1\alpha}(p, \theta, \phi; \lambda_1) \otimes u_{2\beta}(p, \theta, \phi; \lambda_2) \quad (\text{A13})$$

becomes

$$Y |p, \theta, \phi; \lambda_1 \lambda_2 \rangle = (-1)^{1-\lambda} |p, \theta, 2\pi - \phi; -\lambda_1 - \lambda_2 \rangle \quad (\text{A14})$$

where in a two-particle context $\lambda = \lambda_1 - \lambda_2$ (and should not be confused with the λ used previously to represent generic one-particle helicities).

For the negative energy spinors, the transformation laws (A12) become

$$Y v_1(p, \theta, \phi; \lambda) = \frac{\eta(\lambda)}{\eta(-\lambda)} (-1)^{\frac{1}{2}-\lambda} v_1(p, \theta, 2\pi - \phi; -\lambda) \quad (\text{A15})$$

and similarly for v_2 . With the choice of phase (A8), the ratio $\eta(\lambda)/\eta(-\lambda) = -1$, and the transformation laws of the v spinors under Y parity differ from (A12) only by the presence of an overall $-$ sign. When particle 2 is in a negative energy state, the direct product representation is

$$|p, \theta, \phi; \lambda_1 \bar{\lambda}_2 \rangle_- = u_{1\alpha}(p, \theta, \phi; \lambda_1) \otimes v_{2\beta}(p, \theta, \phi; \lambda_2) \quad (\text{A16})$$

where the $-$ subscript refers to the $-$ channel (with one u spinor and one v spinor) and the bar over λ_2 is used to mean that particle 2 is off-shell. Since the v spinor can only accompany an off-shell particle, the identification of the v spinor with particle 2 in Eq. (A16) is unique. The Y parity transformation on minus channels is similar to (A14), but with an extra minus sign

$$Y |p, \theta, \phi; \lambda_1 \bar{\lambda}_2 \rangle_- = -(-1)^{1-\lambda} |p, \theta, 2\pi - \phi; -\lambda_1 - \bar{\lambda}_2 \rangle_- \quad (\text{A17})$$

The presence of the additional minus sign in (A17), a consequence of our phase convention (A8), is a natural choice in view of the fact that the intrinsic parity of v spinors is opposite from that of u spinors.

The Y parity results can now be used to obtain Eq. (2.96) for the transformation of two-particle states under parity. First, following Jacob and Wick, we define states with good angular momentum by

$$|pJM \lambda_1 \lambda_2 \rangle_{\pm} = \sqrt{\frac{2J+1}{4\pi} \frac{1}{2\pi}} \int_0^\pi \sin \beta d\beta \int_0^{2\pi} d\alpha \int_0^{2\pi} d\gamma D_{M\lambda}^{*J}(\alpha, \beta, \gamma) R_{\alpha, \beta, \gamma} |p, 0, 0; \lambda_1 \lambda_2 \rangle_{\pm} \quad (\text{A18})$$

Operating by $\mathcal{P} = R_{0, \pi, 0}^{-1} Y$, and recalling that \mathcal{P} commutes with the rotations, gives

$$\mathcal{P} |pJM \lambda_1 \lambda_2 \rangle_{\pm} = \sqrt{\frac{2J+1}{4\pi}} \int dU D_{M\lambda}^{*J}(\alpha, \beta, \gamma) R_{\alpha, \beta, \gamma} R_{0, \pi, 0}^{-1} Y |p, 0, 0; \lambda_1 \lambda_2 \rangle_{\pm} \quad (\text{A19})$$

where dU is a shorthand notation for integration over the group elements α, β, γ . Next, introduce

$$R_{\alpha', \beta', \gamma'} = R_{\alpha, \beta, \gamma} R_{0, \pi, 0}^{-1} \quad (\text{A20})$$

and note that

$$D_{M\lambda}^J(\alpha, \beta, \gamma) = \sum_{\lambda'} D_{M\lambda'}^J(\alpha', \beta', \gamma') D_{\lambda'\lambda}^J(0, \pi, 0). \quad (\text{A21})$$

Hence, using

$$D_{\lambda'\lambda}^J(0, \pi, 0) = d_{\lambda'\lambda}^J(\pi) = (-1)^{J+\lambda'} \delta_{\lambda', -\lambda} \quad (\text{A22})$$

the relations (A14) and (A17), and the completeness of the group integration dU , gives finally

$$\begin{aligned} \mathcal{P} |pJM \lambda_1 \lambda_2 \rangle_{\pm} &= \epsilon' (-1)^{1-\lambda} \sqrt{\frac{2J+1}{4\pi}} \int dU' D_{M, -\lambda}^{J*}(\alpha', \beta', \gamma') (-1)^{J-\lambda} R_{\alpha', \beta', \gamma'} |p, 0, 0; -\lambda_1 - \lambda_2 \rangle_{\pm} \\ &= \epsilon' (-1)^{J-1} |pJM - \lambda_1 - \lambda_2 \rangle_{\pm} \end{aligned} \quad (\text{A23})$$

where $\epsilon' = +1$ for + states and -1 for - states. This completes the proof.

Finally, if the potential is invariant under parity, then

$$\mathcal{P}^{-1} V \mathcal{P} = V \quad . \quad (\text{A24})$$

Taking matrix elements of this potential in the angular momentum representation, and using (A23), gives immediately

$$\langle \lambda_1 \lambda_2 | V^J | \lambda'_1 \lambda'_2 \rangle = \epsilon'_f \epsilon'_i \langle -\lambda_1 - \lambda_2 | V^J | -\lambda'_1 - \lambda'_2 \rangle \quad (\text{A25})$$

where ϵ'_f and ϵ'_i are final (f) and initial (i) state phases from Eq. (A23). Hence, as in Eq. (2.101), $\epsilon = \epsilon'_f \epsilon'_i$ is + for V^{++} and V^{--} potentials, and - for V^{+-} and V^{-+} potentials.

3. Particle interchange

The particle interchange operator interchanges the momentum (all 4 components) and spin of the two particles. In Sec. III this was accomplished by changing the sign of the relative momentum, p , and interchanging Dirac indices, α and β . On the direct product space of nucleon spinors, the interchange is accomplished by interchanging the Dirac indices only, since this operation automatically interchanges the momentum and helicity of the two particle state. Hence for the + channel

$$\mathcal{P}_{12} |p, 0, 0; \lambda_1 \lambda_2 \rangle = u_{2\alpha}(p, 0, 0; \lambda_2) \otimes u_{1\beta}(p, 0, 0; \lambda_1). \quad (\text{A26})$$

Recalling the relation between u_1 and u_2 , Eq. (A5),

$$\begin{aligned} \mathcal{P}_{12} |p, 0, 0; \lambda_1 \lambda_2 \rangle &= \left[(-1)^{\frac{1}{2}-\lambda_2} e^{-i\pi J_y^\alpha} u_{1\alpha}(p, 0, 0; \lambda_2) \right] \otimes u_{1\beta}(p, 0, 0; \lambda_1) \\ &= (-1)^{\lambda_1-\lambda_2} e^{i\pi(J_y^\alpha + J_y^\beta)} \left[e^{-2i\pi J_y^\alpha} u_{1\alpha}(p, 0, 0; \lambda_2) \right] \otimes \left[(-1)^{\frac{1}{2}-\lambda_1} e^{-i\pi J_y^\beta} u_{1\beta}(p, 0, 0; \lambda_1) \right] \\ &= (-1)^{1+\lambda_1-\lambda_2} e^{i\pi J_y} |p, 0, 0; \lambda_2 \lambda_1 \rangle \end{aligned} \quad (\text{A27})$$

where J_y^α implies that J_y operates only on the Dirac space with index α and $J_y = J_y^\alpha + J_y^\beta$. In the last step, use was made of the relation

$$e^{-2i\pi J_y^\alpha} = -1 \quad (\text{A28})$$

which holds for states with half-integral spin.

For channels with a v spinor, a similar argument gives

$$\mathcal{P}_{12} |p, 0, 0; \lambda_1 \bar{\lambda}_2 \rangle_- = v_{2\alpha}(p, 0, 0; \lambda_2) \otimes u_{1\beta}(p, 0, 0; \lambda_1). \quad (\text{A29})$$

This is to be expressed in terms of the state

$$|p, 0, 0, \bar{\lambda}_2 \lambda_1 \rangle_- = v_{1\alpha}(p, 0, 0; \lambda_2) \otimes u_{2\beta}(p, 0, 0; \lambda_1). \quad (\text{A30})$$

Hence we need the relation between v_1 and v_2 . Using the definitions (A7) gives

$$\begin{aligned} v_2(p, 0, 0; \lambda_2) &= \eta(\lambda) C \gamma^\circ u_1(p, 0, 0; \lambda_2) \\ &= \eta(\lambda) C \gamma^\circ (-1)^{\frac{1}{2}-\lambda_2} e^{i\pi J_y} u_2(p, 0, 0; \lambda_2) \\ &= \eta(\lambda) (-1)^{\frac{1}{2}-\lambda_2} e^{i\pi J_y} C \gamma^\circ u_2(p, 0, 0; \lambda_2) \\ &= \delta (-1)^{\frac{1}{2}-\lambda_2} e^{i\pi J_y} v_1(p, 0, 0; \lambda_2). \end{aligned} \quad (\text{A31})$$

Hence the interchange gives

$$\mathcal{P}_{12} |p, 0, 0; \lambda_1 \bar{\lambda}_2 \rangle_- = \delta (-1)^{\lambda_1-\lambda_2} e^{i\pi J_y} |p, 0, 0; \bar{\lambda}_2 \lambda_1 \rangle_- .$$

The choice $\delta = -1$, Eq. (A8), insures that the + and - channels both behave in the same way under particle interchange.

Finally, using the definition (A18) of the good angular momentum states, and the relations (A20)–(A22), we obtain immediately Eq. (2.97):

$$\mathcal{P}_{12} |pJM \lambda_1 \bar{\lambda}_2 \rangle_{\pm} = (-1)^{J-1} |pJM \bar{\lambda}_2 \lambda_1 \rangle_{\pm} . \quad (\text{A32})$$

The particle interchange operation was used in Sec. III, Eq. (2.100), to express the exchange potentials in terms of direct potentials. In the notation of Eq. (2.100), the Dirac amplitudes for the direct and exchange potentials are, from Sec. II A

$$V_{\text{direct}}^J = V_{\alpha\alpha', \beta\beta'}^J(p_o, k_o), \quad (\text{A33})$$

$$V_{\text{exchange}}^J = V_{\beta\alpha', \alpha\beta'}^J(-p_o, k_o)$$

where all unnecessary variables are suppressed. Hence, if we let the operation \mathcal{P}_{12} denote interchange of Dirac indices only (to avoid confusion)

$$V_{\text{exchange}}^J = \mathcal{P}_{12} V_{\text{direct}}(-p_o, k_o) = \mathcal{P}_{12} \hat{V}_{\text{direct}} . \quad (\text{A34})$$

Hence, from (A32) we obtain immediately

$$\begin{aligned} \langle \lambda_1 \bar{\lambda}_2 | V_{\text{exchange}}^J | \lambda'_1 \lambda'_2 \rangle &= \langle \lambda_1 \bar{\lambda}_2 | \mathcal{P}_{12} \hat{V}_{\text{direct}} | \lambda'_1 \lambda'_2 \rangle \\ &= (-1)^{J-1} \langle \bar{\lambda}_2 \lambda_1 | \hat{V}_{\text{direct}} | \lambda'_1 \lambda'_2 \rangle . \end{aligned} \quad (\text{A35})$$

This justifies the results in Eq. (2.100).

4. Time reversal

Time reversal invariance can be used to prove that the scattering matrix is symmetric. For this purpose it is convenient to work with the operator $Z = e^{i\pi J_y} T$, where T is the Dirac time reversal operator

$$T = C\gamma^5 K = \begin{pmatrix} -i\sigma_2 & \\ & -i\sigma_2 \end{pmatrix} K \quad (\text{A36})$$

where K is the operation of complex conjugation. Hence, on the Dirac space

$$Z = K \quad (\text{A37})$$

and

$$Z|p, \theta, \phi; \lambda_1 \lambda_2 \rangle_{\pm} = |p, \theta, 2\pi - \phi; \lambda_1 \lambda_2 \rangle_{\pm}. \quad (\text{A38})$$

Hence, on the angular momentum states

$$\begin{aligned} Z|pJM\lambda_1\lambda_2 \rangle_{\pm} &= \sqrt{\frac{2J+1}{4\pi}} \int_0^\pi \sin\theta d\theta \int_0^{2\pi} d\phi D_{M\lambda}^J(\phi, \theta, -\phi) |p, \theta, 2\pi - \phi; \lambda_1 \lambda_2 \rangle_{\pm} \\ &= \sqrt{\frac{2J+1}{4\pi}} \int_0^\pi \sin\theta d\theta \int_0^{2\pi} d\phi D_{M\lambda}^J(-\phi, \theta, \phi) |p, \theta, \phi; \lambda_1 \lambda_2 \rangle_{\pm} \\ &= \sqrt{\frac{2JM}{4\pi}} \int_0^\pi \sin\theta d\theta \int_0^{2\pi} d\phi D_{M\lambda}^{J*}(\phi, \theta, -\phi) |p, \theta, \phi; \lambda_1 \lambda_2 \rangle_{\pm} \\ &= |pJM\lambda_1\lambda_2 \rangle_{\pm} \end{aligned} \quad (\text{A39})$$

where we use the fact that M and λ are integers. Now since Z is antiunitary, if the M matrix is invariant under T , then suppressing p , J , and M ,

$$\begin{aligned} \langle \lambda'_1 \lambda'_2 | M | \lambda_1 \lambda_2 \rangle &= \langle \lambda'_1 \lambda'_2 | Z M Z^{-1} | \lambda_1 \lambda_2 \rangle \\ &= \langle \lambda_1 \lambda_2 | M | \lambda'_1 \lambda'_2 \rangle. \end{aligned} \quad (\text{A40})$$

APPENDIX B: PRINCIPAL VALUE INTEGRATION

As shown in Table IX and Eq. (3.28), the partial wave decomposition of the exchange contribution to the potential can be expressed in terms of integrals of the form

$$I_\ell^n = P \int_{-1}^1 \frac{dz z^n P_\ell(z) f_i^2(q^2(z))}{\widehat{D}(z)}. \quad (\text{B1})$$

Defining z_0 such that $\widehat{D}(z) = 0$ or

$$2pkz_0 = \mu^2 - 2m + 2E_p E_k - (W - 2E_p)(W - 2E_k) \quad (\text{B2})$$

then the integral becomes

$$I_\ell^n = \frac{1}{2pk} P \int_{-1}^1 \frac{dz z^n P_\ell(z) f_i^2(q^2(z))}{z_0 - z}. \quad (\text{B3})$$

If the form factor mass is much larger than the mass of the exchanged meson (as is the case in the solutions presented in this paper), then $f_i^2(q^2(z))$ is slowly varying in the neighborhood of the singularity at $z = z_0$ ($q^2(z_0) = \mu^2$). Note, however, that $z^n P_\ell(z)$ may be rapidly varying near z_0 , particularly when z_0 is near the boundaries of the integration region.

The numerical evaluation of I_ℓ^n can be simplified by using a standard subtraction technique to rewrite I_ℓ^n as

$$\begin{aligned} I_\ell^n &= \frac{1}{2pk} \int_{-1}^1 \frac{dz z^n P_\ell(z) [f_i^2(q^2(z)) - f_i(\mu^2)]}{z_0 - z} \\ &\quad + \frac{f_i^2(\mu^2)}{2pk} P \int_{-1}^1 \frac{dz z^n P_\ell(z)}{z_0 - z}. \end{aligned} \quad (\text{B4})$$

The first term of (B4) is now a smooth function of z with a removable singularity at z_0 . The second term is singular but can be evaluated analytically.

In order to evaluate the second term of (B4), it is convenient to express z^n in terms of a sum of Legendre polynomials. This can be accomplished by using the identity

$$z^n P_\ell(z) = \sum_{\ell'=0}^n C_{\ell'}^{n,\ell} P_{\ell+n-2\ell'}(z) \quad (\text{B5})$$

where $C_{\ell'}^{n,\ell} = 0$ for $\ell+n-2\ell' < 0$. Recursion relations for the coefficients of this expansion can be derived from the recursion relations for the Legendre polynomials. The recursion relations for these coefficients are

$$C_0^{n,\ell} = \frac{n+\ell}{2(n+\ell)-1} C_0^{n-1,\ell}, \quad (\text{B6})$$

$$\begin{aligned} C_{\ell'}^{n,\ell} &= \frac{n+\ell-2\ell'}{2(n+\ell-2\ell')-1} C_{\ell'}^{n-1,\ell} \\ &\quad + \frac{n+\ell-2\ell'+1}{2(n+\ell-2\ell')+3} C_{\ell'-1}^{n-1,\ell}, \quad \ell' > 0. \end{aligned}$$

The starting points for the evaluation of these recursion relations are

$$C_0^{o,\ell} = 1 \quad \text{for all } \ell, \quad (\text{B7})$$

$$C_{\ell'}^{o,m} = 0 \quad \text{for all } \ell' > 0.$$

Using the expansion (B5), the integral

$$\begin{aligned} S_\ell^n(z_0^-) &\equiv P \int_{-1}^1 \frac{dz z^n P_\ell(z)}{z_0 - z} \\ &= \sum_{\ell'=0}^n C_{\ell'}^{n,\ell} P \int_{-1}^1 \frac{P_{\ell'}(z)}{z_0 - z} \\ &= 2 \sum_{\ell'=0}^n C_{\ell'}^{n,\ell} Q_{\ell'}(z_0) \end{aligned} \quad (\text{B8})$$

where Q_ℓ is the Legendre function of the second kind.

The use of Q_ℓ in numerical calculations involves some difficulties. The first of these is that the Legendre function Q_ℓ has logarithmic singularities at $z = \pm 1$. These singularities are integrable, but since they are present in the kernel of an integral equation and cannot be integrated analytically, it is necessary to require that the singularities do not introduce convergence problems in the solution of the integral equation. This can be done by "smoothing" the Legendre function. This is done by defining a "smoothed" Legendre function of the second kind as

$$Q_{\ell,\epsilon}(x) = \frac{1}{2} \operatorname{Re} \int_{-1}^1 \frac{dz P_\ell(z)}{x - z + i\epsilon} = \frac{1}{2} \int_{-1}^1 \frac{dz(x-z)P_\ell(z)}{(x-z)^2 + \epsilon^2}. \quad (\text{B9})$$

The recursion relations for the P_ℓ can be used to obtain recursion relations for $Q_{\ell,\epsilon}(x)$. These recursion relations appear as a coupled set

$$Q_{\ell,\epsilon}(x) = \frac{2\ell-1}{\ell} x Q_{\ell-1,\epsilon}(x) - \frac{\ell-1}{\ell} Q_{\ell-2,\epsilon}(x) + \frac{2\ell-1}{\ell} \epsilon^2 A_{\ell-1,\epsilon}(x), \quad (\text{B10})$$

$$A_{\ell,\epsilon}(x) = \frac{2\ell-1}{\ell} x A_{\ell-1,\epsilon}(x) - \frac{\ell-1}{\ell} A_{\ell-2,\epsilon}(x) - \frac{2\ell-1}{\ell} A_{\ell-1,\epsilon}(x)$$

where

$$A_{\ell,\epsilon}(x) = \frac{1}{2} \int_{-1}^1 \frac{dz P_{\ell-1}(z)}{(x-z)^2 + \epsilon^2}. \quad (\text{B11})$$

The functions $Q_{\ell,\epsilon}(x)$ and $A_{\ell,\epsilon}(x)$ can be calculated for $\ell = 0, 1$ directly from (B9) and (B11) to give

$$\begin{aligned} Q_{0,\epsilon}(x) &= \frac{1}{4} \ln \left[\frac{\epsilon^2 + (x+1)^2}{\epsilon^2 + (x-1)^2} \right], \\ A_{0,\epsilon}(x) &= \frac{1}{2\epsilon} \left[\tan^{-1} \frac{x+1}{\epsilon} - \tan^{-1} \frac{x-1}{\epsilon} \right], \\ Q_{1,\epsilon}(x) &= x Q_{0,\epsilon}(x) - 1 + \epsilon^2 A_{0,\epsilon}(x), \\ A_{1,\epsilon}(x) &= x A_{0,\epsilon}(x) - Q_{0,\epsilon}(x). \end{aligned}$$

From the numerical standpoint, one further problem remains. Although $Q_\ell(x)$ can be easily evaluated from either explicit analytic forms or recursion relations near the interval $-1 \leq x \leq 1$ for the range of ℓ 's needed here, these methods become unstable for arguments of larger magnitude. However, a series expansion of $Q_\ell(x)$ can be constructed for $|x| > 1$. Noting that we can expand the denominator in (B9) as

$$\frac{1}{x-z+i\epsilon} = \sum_{n=0}^{\infty} \frac{z^n}{(x+i\epsilon)^{n+1}}, \quad \text{for } \left| \frac{z}{x+i\epsilon} \right| < 1,$$

the smoothed Legendre function becomes

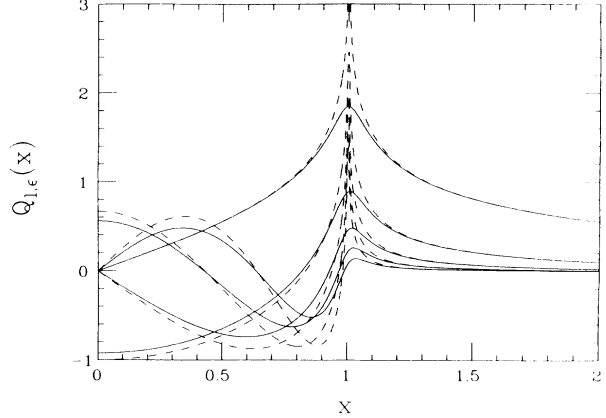


FIG. 16. Comparison of the smoothed Legendre function $Q_{\ell,\epsilon}(x)$ (solid) with the normal Legendre functions $Q_\ell(x)$ (dashes) for $0 \leq d \leq 4$.

$$Q_{\ell,\epsilon}(x) = \frac{1}{2} \sum_{n=0}^{\infty} \operatorname{Re} \frac{1}{(x+i\epsilon)^{n+1}} \int_{-1}^1 dz z^n P_\ell(z).$$

It is convenient to rewrite the integral as

$$\begin{aligned} \int_{-1}^1 dz z^n P_\ell(z) &= \int_{-1}^1 dz z^n P_0(z) P_\ell(z) \\ &= \sum_{\ell'=0}^n C_{\ell'}^{n,0} \int_{-1}^1 dz P_{n-2\ell'}(z) P_\ell(z) \\ &= \frac{1}{2\ell+1} \sum_{\ell'=0}^n C_{\ell'}^{n,0} \delta_{n-2\ell',\ell} \quad (\text{B12}) \end{aligned}$$

where the orthogonality relation for the Legendre polynomials has been used in the last step. Using

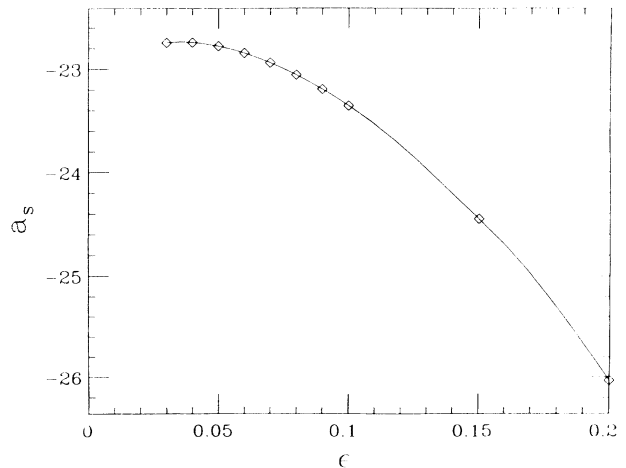


FIG. 17. The scalar scattering length a_s as a function of the smoothing parameter, ϵ . For small ϵ , all phase parameters are independent of ϵ , and the figure shows that $\epsilon \approx 0.05$ is sufficiently small for convergence.

$$\operatorname{Re} \frac{1}{(x + i\epsilon)^n} = \frac{\cos(n\phi)}{(x^2 + \epsilon^2)^{\frac{n}{2}}},$$

where

$$\phi = \tan^{-1} \frac{\epsilon}{x},$$

the series expansion for $Q_{\ell,\epsilon}(x)$ becomes

$$Q_{\ell,\epsilon}(x) = \frac{1}{2\ell + 1} \frac{1}{(x^2 + \epsilon^2)^{\frac{\ell+1}{2}}} \times \sum_{\ell'=0}^{\infty} C_{\ell'}^{2\ell'+\ell,0} \frac{\cos[(2\ell' + \ell + 1)\phi]}{(x^2 + \epsilon^2)^{\ell'}}.$$

Figure 16 shows a comparison between the smoothed Legendre function $Q_{\ell,\epsilon}(x)$ (solid line) and the Legendre function $Q_{\ell}(x)$ (dashed line) for $0 \leq \ell \leq 4$ and $\epsilon = 0.05$. This clearly displays the smoothing of the logarithmic singularity at $x = 1$. The oscillatory part of the function for $-1 < x < 1$ is also modified by the smoothing, however. In principle, the phase shift and bound state calculations are now functions of the parameter ϵ . This functional dependence is displayed in Fig. 17, where the scalar scattering length a_s is plotted as a function of ϵ . This scattering length, which is extremely sensitive to the parameters of the model, is clearly becoming independent of the value of ϵ for small values of ϵ . The calculations shown in this paper are performed with $\epsilon = 0.05$ which is chosen to provide a good compromise between conver-

gence in ϵ and convergence as a function of the number of grid points used in the solution of the integral equations.

APPENDIX C: PARTIAL WAVE DETAILS

In Section III D, the major steps in the calculation of the partial wave decomposition of the relativistic potentials were recorded. This appendix gives a few of the details.

The first step in calculating the partial wave potentials is to construct the helicity amplitudes. Examination of the couplings given in (3.1) shows that this requires computing the matrix elements of the following Dirac operators: $1, \gamma^5, \not{q}\gamma^5, \gamma^\mu$, and $\sigma^{\mu\nu} q_\nu$. The resulting matrix elements can all be easily expressed in terms of the θ_i^\pm and ϕ_i^\pm introduced in Eq. (3.23), and will not be given here. Combining these results with the proper factors and mixing parameters, λ_i , gives the results summarized in Tables VII and VIII.

In this calculation the matrix elements

$$\begin{aligned} < \lambda_1 \lambda_2 | \lambda'_1 \lambda'_2 > = < \lambda_1 | \lambda'_1 >_1 < \lambda_2 | \lambda'_2 >_2, \\ < \lambda_1 \lambda_2 | \sigma_2 \cdot \sigma_2 | \lambda'_1 \lambda'_2 > = < \lambda_1 | \sigma^i | \lambda'_1 >_1 < \lambda_2 | \sigma^i | \lambda'_2 >_2 \end{aligned} \quad (C1)$$

are encountered. Here the λ_i are the two component spinors summarized in Table XI. The first matrix element has already been given by Erkelenz [41], and can be written

$$< \lambda_1 \lambda_2 | \lambda'_1 \lambda'_2 > = \left(|\lambda_1 + \lambda'_1| \cos \frac{1}{2}\theta + (\lambda_1 - \lambda'_1) \sin \frac{1}{2}\theta \right) \left(|\lambda_2 + \lambda'_2| \cos \frac{1}{2}\theta - (\lambda_2 - \lambda'_2) \sin \frac{1}{2}\theta \right). \quad (C2)$$

The second matrix element is clearly related to the total spin S of the state, but because the λ 's are helicities, and not projections of the spin in a fixed direction, care must be taken. Note that

$$\sigma_1 \cdot \sigma_2 | \lambda - \lambda > = | \lambda - \lambda > \quad (C3)$$

but that

$$\sigma_1 \cdot \sigma_2 | \lambda \lambda > = -| \lambda \lambda > + 2 | - \lambda - \lambda >. \quad (C4)$$

Hence the only amplitudes for which T , as defined in Eq. (3.21), is not automatically 1, are those involving linear combinations of the form $< \lambda \lambda | \sigma_1 \cdot \sigma_2 | \lambda' \lambda' >$. Examination of Table VI and Eq. (2.101) shows that the only amplitudes so affected are v_1, v_5, v_9 , and v_{13} . Furthermore, in these amplitudes the combinations which occur are

$$C_{\pm} = \left\{ \left\langle \frac{1}{2} \frac{1}{2} \middle| \sigma_1 \cdot \sigma_2 \middle| \frac{1}{2} \frac{1}{2} \right\rangle C_1 \pm \left\langle \frac{1}{2} \frac{1}{2} \middle| \sigma_1 \cdot \sigma_2 \middle| -\frac{1}{2} -\frac{1}{2} \right\rangle C_2 \right\} d_{00}(\theta) \quad (C5)$$

where C_+ appears in v_9, v_{13} and C_- appears in v_1, v_5 . Explicit evaluation gives

$$\begin{aligned} C_{\pm} &= \left\{ \left\langle \frac{1}{2} \frac{1}{2} \middle| \frac{1}{2} \frac{1}{2} \right\rangle \left(-C_1 \pm 2C_2 \right) + \left\langle \frac{1}{2} \frac{1}{2} \middle| -\frac{1}{2} -\frac{1}{2} \right\rangle \left(2C_1 \mp C_2 \right) \right\} d_{00}(\theta) \\ &= \left\{ \frac{1}{2}(1+z) \left(-C_1 \pm 2C_2 \right) - \frac{1}{2}(1-z) \left(2C_1 \mp C_2 \right) \right\} d_{00}(\theta) \\ &= \left\{ (-3)\frac{1}{2} \left(C_1 \mp C_2 \right) + \frac{1}{2}z \left(C_1 \pm C_2 \right) \right\} d_{00}(\theta). \end{aligned} \quad (C6)$$

This shows that $T = -3$ for the term which multiplies the angular integral d_1 , and $T = 1$ for the term which multiplies d_2 . Furthermore, no additional terms involving $z = \hat{p} \cdot \hat{k}$ occur together with $\sigma_1 \cdot \sigma_2$. This explains why in Table X, only the terms $B_{1,1}, B_{1,5}, B_{1,9}$, and $B_{1,13}$ have $T = -3$.

- [1] See F. Coester, in *Nuclear and Particle Physics on the Light Cone*, edited by M. Johnson and L. S. Kisslinger (World Scientific), p. 421; B. D. Keister and W. N. Polyzou, University of Iowa report.
- [2] P. L. Chung, F. Coester, B. D. Keister, and W. N. Polyzou, *Phys. Rev. C* **37**, 2000 (1988).
- [3] See J. Fleischer and J. A. Tjon, *Nucl. Phys.* **B84**, 375 (1975); *Phys. Rev. D* **15**, 2537 (1977); **21**, 87 (1980). M. J. Zuilhof and J. A. Tjon, *Phys. Rev. C* **22**, 2369 (1980); **24**, 736 (1981); E. van Faassen and J. A. Tjon, *ibid.* **28**, 2354 (1983); **30**, 285 (1984); **33**, 2105 (1986).
- [4] E. E. Salpeter and H. A. Bethe, *Phys. Rev.* **84**, 1232 (1951).
- [5] R. Blankenbecler and R. Sugar, *Phys. Rev.* **142**, 1051 (1966).
- [6] For a recent overview, see F. Gross, *Czech. J. Phys.* **B 39**, 871 (1989).
- [7] F. Gross, *Phys. Rev.* **186**, 1448 (1969).
- [8] F. Gross, *Phys. Rev. D* **10**, 223 (1974).
- [9] F. Gross, *Phys. Rev. C* **26**, 2203 (1982).
- [10] F. Gross, J. W. VanOrden, and K. Holinde, *Phys. Rev. C* **41**, R1909 (1990).
- [11] F. Gross and D. O. Riska, *Phys. Rev. C* **36**, 1928 (1987).
- [12] F. Gross and K. M. Maung, *Phys. Lett. B* **229**, 188 (1989); K. M. Maung and F. Gross, *Phys. Rev. C* **42**, 1681 (1990).
- [13] F. Gross, K. M. Maung, J. A. Tjon, L. W. Townsend, and S. J. Wallace, *Phys. Rev. C* **40**, R10 (1989); K. M. Maung, F. Gross, J. A. Tjon, L. W. Townsend, and S. J. Wallace, *ibid.* **43**, 1378 (1991).
- [14] R. J. Yaes, *Phys. Rev. D* **3**, 3086 (1971).
- [15] G. E. Brown and A. D. Jackson, *The Nucleon-Nucleon Interaction* (North-Holland, Amsterdam, 1976).
- [16] F. Gross, *Phys. Rev. C* **26**, 2226 (1982).
- [17] J. M. Namyslowski, contribution III-11 to the 9th International Conference on Few Body Problems, Eugene, Oregon, 1980 (unpublished).
- [18] F. Gross, *Phys. Rev.* **140**, 410B (1965).
- [19] R. Reid, *Ann. Phys. (N.Y.)* **50**, 411 (1968).
- [20] W. W. Buck and F. Gross, *Phys. Rev. D* **20**, 2361 (1979).
- [21] M. J. Zuilhof and J. A. Tjon, *Phys. Rev. C* **24**, 736 (1981).
- [22] R. Machleidt, K. Holinde, and Ch. Elster, *Phys. Rep.* **149**, 1 (1987).
- [23] R. A. Arndt and L. D. Roper, Scattering Analysis and Interactive Dial-in (SAID) program, Virginia Polytechnic Institute and State University.
- [24] D. Bugg (private communication).
- [25] J. J. de Swart, R. A. M. Klomp, T. A. Rijken, and V. G. J. Stoks, invited talk given at the XIII European Conference of Few Body Problems, Elba, Italy, 1991 (unpublished).
- [26] R. Wiringa, R. Smith, and T. Ainsworth, *Phys. Rev. C* **29**, 1207 (1984).
- [27] R. Koch and E. Pietarinen, *Nucl. Phys.* **A336**, 331 (1980).
- [28] J. R. Bergervoet, P. C. vanCampen, T. A. Rijken, and J. J. de Swart, *Phys. Rev. Lett.* **59**, 2255 (1987); J. R. Bergervoet, *et al.*, *Phys. Rev. C* **41**, 1435 (1990); R. G. E. Timmermans, T. A. Rijken, and J. J. de Swart, *Phys. Rev. Lett.* **67**, 1074 (1991).
- [29] R. A. Arndt, Z. Li, L. D. Roper, and R. L. Workman, *Phys. Rev. Lett.* **65**, 157 (1990); R. A. Arndt and R. L. Workman, *Phys. Rev. C* **43**, 2436 (1991).
- [30] R. Machleidt and F. Sammarruca, *Phys. Rev. Lett.* **66**, 564 (1991).
- [31] M. M. Nagels, T. A. Rijken, and J. J. de Swart, *Phys. Rev. D* **17**, 768 (1978).
- [32] R. A. Arndt (private communication). The numbers shown in Table IV come from the recent solution VL40.
- [33] N. L. Rodning and L.D. Knutson, *Phys. Rev. Lett.* **57**, 2248 (1986).
- [34] J. L. Friar, in *Mesons in Nuclei*, edited by M. Rho and D. Wilkinson (North-Holland, Amsterdam, 1979), Vol. II, p. 595.
- [35] R. E. Arnold, C. E. Carlson, and F. Gross, *Phys. Rev. C* **21**, 2361 (1980); see also, F. Gross, in the *Proceedings of the 6th International Conference on Few Body Problems*, Quebec City, edited by R. J. Slobodrian *et al.* (University of Laval Press, Sainte-Foy, Quebec, 1975), p. 782; F. Gross, in *Modern Topics in Electron Scattering*, edited by B. Frois and I. Sick (World Scientific, Singapore, 1991).
- [36] E. Hummel and J. A. Tjon, *Phys. Rev. Lett.* **63**, 1788 (1989).
- [37] R. A. Bryan and A. Gersten, *Phys. Rev. Lett.* **26**, 1000 (1971); J. J. de Swart and M. M. Nagels, *Fortschr. Phys.* **26**, 215 (1978).
- [38] Th. Hippchen and K. Holinde, *Phys. Rev. C* **37**, 239 (1988).
- [39] J. J. Kubis, *Phys. Rev. D* **6**, 547 (1972).
- [40] M. Jacob and G. C. Wick, *Ann. Phys. (N.Y.)* **7**, 404 (1959).
- [41] K. Erkelenz, *Phys. Rep. C* **13**, 191 (1974).